

DEVELOPMENT OF SELF-HUMIDIFYING NANO-COMPOSITE MEMBRANE  
FOR POLYMER ELECTROLYTE MEMBRANE FUEL CELL

A THESIS SUBMITTED TO  
THE GRADUATE SCHOOL OF NATURAL AND APPLIED SCIENCES  
OF  
MIDDLE EAST TECHNICAL UNIVERSITY

BY

UMUT BAKİ ÇAÇAN

IN PARTIAL FULFILLMENT OF THE REQUIREMENTS  
FOR  
THE DEGREE OF MASTER OF SCIENCE  
IN  
POLYMER SCIENCE AND TECHNOLOGY

SEPTEMBER 2015



Approval of the thesis:

**DEVELOPMENT OF SELF-HUMIDIFYING NANO-COMPOSITE  
MEMBRANE FOR POLYMER ELECTROLYTE MEMBRANE FUEL CELL**

Submitted by **UMUT BAKİ ÇAÇAN** in partial fulfillment of the requirements for  
the degree of **Master of Science in Polymer Science and Technology Department,**  
**Middle East Technical University** by,

Prof. Dr. Gülbin Dural Ünver  
Dean, Graduate School of **Natural and Applied Sciences**

Prof. Dr. Necati Özkan  
Head of Department, **Polymer Science and Technology**

Prof. Dr. Necati Özkan  
Supervisor, **Polymer Science and Technology Dept., METU**

Asst. Prof. Dr. Yılser Devrim  
Co-Supervisor, **Energy System Eng. Dept., Atılım Uni.**

**Examining Committee Members:**

Prof. Dr. İnci Eroğlu  
Chemical Engineering Dept., METU

Prof. Dr. Necati Özkan  
Polymer Science and Technology Dept., METU

Asst. Prof. Dr. Yılser Devrim  
Energy System Engineering Dept., Atılım University

Asst. Prof. Dr. Serkan Kıncaç  
Chemical Engineering Dept., METU

Asst. Prof. Dr. Harun Koku  
Chemical Engineering Dept., METU

**Date:** 11.09.2015

**I hereby declare that all information in this document has been obtained and presented in accordance with academic rules and ethical conduct. I also declare that, as required by these rules and conduct, I have fully cited and referenced all material and results that are not original to this work.**

Name, Last name: UMUT B. ÇAÇAN  
Signature:

## **ABSTRACT**

### **DEVELOPMENT OF SELF-HUMIDIFYING NANO-COMPOSITE MEMBRANE FOR POLYMER ELECTROLYTE MEMBRANE FUEL CELL**

Çaçan, Umut Baki

M.S., Department of Polymer Science and Technology

Supervisor: Prof. Dr. Necati Özkan

Co-Supervisor: Asst. Prof. Dr. Yılser Devrim

September 2015, 130 pages

Low humidity self-humidifying nano-composite membrane electrode assemblies (MEA) were developed for Polymer Electrolyte Membrane Fuel Cell (PEMFC) working at elevated temperatures. The nano-composite membranes were prepared by adding nano-sized silica particles ( $\text{SiO}_2$ ) or inorganic fillers with a size of approximately 20 nm to a polymeric material which is commercially named as Nafion (Perfluoro Sulfonic Acid/PFSA). The particle content of the nano-composite membranes were between 2.5 – 10 wt. %. In this manner, highly specific interaction surfaces were obtained between the polymer and added  $\text{SiO}_2$  particles, so that dehydration in the assemblies can be prevented at elevated temperatures due to the chemically available water in the polymeric membrane. The composite membranes were prepared using both an ultrasonic probe and an ultrasonic bath, and the prepared composite membranes were characterized using thermal gravimetric analysis (TGA), x-ray diffraction technique (XRD), scanning electron microscopy (SEM), proton conductivity, water uptake, and mechanical testing measurements.

Pluronic L64<sup>®</sup> and PEG were used as the surface compatibility (dispersing) agents, and they were incorporated into the polymer matrix containing 3 wt. % SiO<sub>2</sub> to prevent uneven distribution of the nanosized SiO<sub>2</sub> particles. Additionally, the same inorganic filler (SiO<sub>2</sub> – 0.3 wt. % of catalyst solution) was also applied into the anode side catalyst layer, which was combined with the SiO<sub>2</sub> based composite membranes, and five layers MEAs were attained.

Performances of the PEMFC composite membranes having 5 cm<sup>2</sup> active electrode areas were determined using a single PEMFC test station using pure hydrogen gas and compressed dry air in order to determine the influence of working temperatures ranging from 65 to 80°C. The polarization curves of the membranes showed that the performance of the self-humidifying composite membranes containing SiO<sub>2</sub> at the anode side catalyst layer was better.

**Keywords:** Self-humidifying MEA, Nano-composite Membrane, PEM Fuel Cell, Nano-sized Powder SiO<sub>2</sub>, Dispersing Agent (Pluronic L64<sup>®</sup>, PEG)

## ÖZ

### **KENDİLİĞİNDEN NEMLİ NANO-KOMPOZİT MEMBRANIN POLİMER ELEKTROLİT MEMBRAN YAKIT HÜCRELERİ-PEMYH İÇİN GELİŞTİRİLMESİ**

Çaçan, Umut Baki

Yüksek Lisans, Polimer Bilim ve Teknoloji Bölümü

Tez Yöneticisi: Prof. Dr. Necati Özkan

Ortak Tez Yöneticisi: Yar. Doç. Dr. Yılser Devrim

Eylül 2015, 130 sayfa

Bu çalışmada, yüksek sıcaklıklarda ve düşük nemlilikte çalışabilen kendiliğinden nemlenebilen nano-kompozit membran elektrot bileşkesinin (MEB) Polimer Elektrolit Membran Yakıt Hücresi (PEMYH) için geliştirilmesi hedeflenmiştir. Nano-kompozit membranlar, nano boyutta toz haldeki silika ( $\text{SiO}_2$ ) parçacıklarının ( $\sim 20$  nm) ticari ismi Nafion (Perfluoro Sulfonic Acid/PFSA) olarak adlandırılan polimere eklenmesiyle hazırlanmıştır. Bu şekilde polimer ve  $\text{SiO}_2$  parçacıkları arasında yüksek özellikli etkileşim yüzeyi elde edilmiştir öyle ki kimyasal olarak polimer membranın içinde bulunan suyun dehidrasyonu yüksek sıcaklıklarda engellenebilmiştir. İki farklı hazırlama tekniğinin (ultra-sonik banyo ve prob) yardımıyla, membranların karakterizasyonu TGA, XRD, SEM analizleri, proton iletkenlik ölçümleri, su tutma ve mekanik çekme testleri ile yapılmıştır.

Nano-boyutta SiO<sub>2</sub> partiküllerin düzensiz dağılımının önüne geçmek için yüzey uyum (dispersiyon) ajanları da (Pluronic L64<sup>®</sup> ve PG – eklenen SiO<sub>2</sub>'nin % 3 ağırlığı kadar) polimer matriksine dâhil edilmiştir. Ek olarak, aynı inorganik dolgu (SiO<sub>2</sub>), anot tarafında katalizör tabakasına muamele edilmiştir öyle ki SiO<sub>2</sub> bazlı kompozit membranlarda bir araya getirilmiş ve 5 tabakalı MEB'ler elde edilmiştir.

Aktif elektrot alanı 5 cm<sup>2</sup> olan MEB'lerin performansları, tek hücreli PEMFC test istasyonunda 65-80°C çalışma sıcaklıklarında karşılaştırmalı olarak saf hidrojen gazı ve sıkıştırılmış kuru hava kullanılarak belirlenmiştir. Anot katalizör tabakasında SiO<sub>2</sub> eklenmiş kendiliğinden nemli kompozit membranların polarizasyon eğrileri, göreceli olarak iyi performans göstermiştir.

**Anahtar Kelimeler:** Kendiliğinden-nemli MEA, Nano-kompozit Membran, PEM Yakıt Hücresi, Nano-boyutlu Toz Silika, Yüzey Uyumluluk Ajanı (Pluronic L64<sup>®</sup>, PEG)

*To the parents who nurtured us.  
To the teachers who inspired us.*

## ACKNOWLEDGEMENTS

I would like to express my sincere gratitude to my supervisor Prof. Dr. Necati Özkan for the guidance he showed me in the extent of my thesis studies and for his help at the times of my frustration. His encouragement has enabled me to sustain my motivation throughout my thesis studies.

I would like to offer my sincere thanks to my co-supervisor Asst. Prof. Dr. Yilser Devrim for her endless support and the times she shared with me all of her academic and personal life experiences during the time we spend together.

Furthermore, I appreciate the contributions and welfare provided by Prof. Dr. İnci Eroğlu, Asst. Prof. Dr. Serkan Kınca, and Dr. Berker Fıçıcılar their support both morally and technically during my whole education and working period in the department.

I would like to express my special thanks to TEKSIS and AYES group companies' employees for their support and endless sharing of their knowledge and experience with me and their grateful friendship.

I would like to thank METU Chemical Engineering Department Fuel Cell Laboratory research group and METU Central Laboratory for their positive manner and support during this study.

METU Scientific Research Coordination and The Scientific and Technological Research Council of Turkey (TÜBİTAK) are acknowledged for the financial support with the research fund BAP-07-02-2014-006 and 113M205 respectively.

## TABLE OF CONTENTS

ABSTRACT .....	v
ÖZ.....	vii
ACKNOWLEDGEMENTS .....	x
TABLE OF CONTENTS .....	xi
LIST OF FIGURES .....	xiv
LIST OF TABLES .....	xix
NOMENCLATURE .....	xxi
CHAPTERS .....	xxiii
1. INTRODUCTION .....	1
1.1. Overview of Fuel Cell Technology .....	2
1.2. Types of Fuel Cells .....	5
1.2.1. Alkaline Fuel Cell –AFC .....	6
1.2.2. Phosphoric Acid Fuel Cell –PAFC .....	7
1.2.3. Molten Carbonate Fuel Cell –PAFC .....	8
1.2.4. Solid Oxide Fuel Cell –SOFC .....	9
1.2.5. Direct Methanol Fuel Cell –DMFC .....	10
1.2.6. Proton Exchange Membrane Fuel Cell –PEMFC .....	10
1.3. Components and properties of PEMFCs .....	11
1.3.2. Gas Diffusion Layer .....	13
1.3.3. Catalyst Layer .....	14
1.3.4. Membrane Layer .....	14
1.4. Working Principle of PEM Fuel Cell .....	17
1.4.1. Basic Thermodynamic Concepts of a PEMFC .....	17
1.4.2. Polarizations at a single Fuel Cell .....	24
1.4.3. Efficiency of a PEMFC .....	28

2.	MEMBRANES USED FOR FUEL CELL .....	29
2.1.	Types of Polymer Membranes .....	32
2.1.1.	Perfluorinated Membranes .....	33
2.1.2.	Hydrocarbon Membranes .....	33
2.1.3.	Aromatic Membranes .....	34
2.1.4.	Acid–Base Complexes .....	35
2.1.5.	Supported Composite Membranes .....	38
2.2.	Required Specifications for Membrane .....	39
2.2.1.	Proton Conductivity .....	40
2.2.2.	Water Uptake (Hydration Level).....	42
2.2.3.	Thickness.....	42
2.2.4.	Chemical and Mechanical Stability.....	43
3.	MATERIALS AND METHODS.....	45
3.1.	Preparation of Composite Membranes .....	45
3.2.	Preparation of Membrane Electrode Assemblies (MEAs) .....	48
3.3.	Objective of Study .....	51
4.	CHARACTERIZATION OF COMPOSITE MEMBRANES .....	53
4.1.	Water Uptake Capacity – WU Testing .....	53
4.2.	Scanning Electron Microscopy – SEM Testing.....	54
4.3.	Thermogravimetric Analysis .....	54
4.4.	Tensile Mechanical Testing.....	54
4.5.	Electro-Impedance Spectroscopy –EIS Testing .....	57
4.5.1.	Calculation of Proton Conductivity.....	57
4.6.	PEMFC Testing .....	60
5.	EXPERIMENTAL RESULTS AND DISCUSSIONS .....	63
5.1.	Water Uptake Capacity Results .....	64
5.2.	Tensile Mechanical Testing Results .....	66
5.2.1.	Recasting Nafion .....	67
5.2.2.	M1: Pluronic L-64 .....	68
5.2.3.	M4: Only SiO <sub>2</sub> (Ultrasonic Bath) .....	69
5.3.	Thermo-Gravimetric Analyses-TGA Results .....	71

5.4.	SEM & EDXS Results .....	72
5.5.	Particle Size Test Results .....	79
5.5.1.	Optimization of Adding Organic Additive – Pluronic L 64 .....	80
5.6.	Electro Impedance Spectrometry – EIS Results .....	83
5.7.	PEMFC Testing Results and SEM Analyses .....	86
5.7.1.	With External Humidification (at 100 % RH) .....	88
5.7.2.	With Self-Humidification (at 0 % RH) .....	100
6.	CONCLUSIONS .....	105
6.1.	Characterization of the films and membranes .....	105
6.2.	Overall Conclusions .....	109
	REFERENCES .....	111
	APPENDICES .....	115
A.	ADDITIONAL CHARACTERIZATION DATA .....	115
A.1.	SEM Pictures of Samples .....	115
A.2.	Mapping Pictures of Sample.....	116
A.3.	EDXS Pattern of Samples.....	117
B.	MATERIAL DATA SPECIFICATIONS .....	119
B1.	Production Specifications of Pluronic L64, PEG, SiO <sub>2</sub> , Nafion 1100.....	119
C.	TENSILE MECHANICAL TESTS .....	123
C.1.	M1: Pluronic L-64 prepared via Ultrasonic Probe (Testing at least two or three dog-bones for each membrane) .....	123
C.2.	M4: Only SiO <sub>2</sub> prepared via Ultrasonic Bath (Testing at least two or three dog-bones for each membrane) .....	127

## LIST OF FIGURES

### FIGURES

<b>Figure 1.</b> Schematic view of the components of a PEMFC [9]	12
<b>Figure 2.</b> Schematic view of a catalyst layer structure. GDL – gas diffusion layer; ACL – anode catalyst layer; CCL – cathode catalyst layer; PEM – proton exchange membrane [10]	12
<b>Figure 3.</b> 3-phase interface formation in catalyst layer [11]	14
<b>Figure 4.</b> Chemical formula of PFSA-Nafion [12]	15
<b>Figure 5.</b> Fuel cell OCVs as a function of temperature. Operating conditions: H <sub>2</sub> /air, 3,0 atm [8]	22
<b>Figure 6.</b> H <sub>2</sub> crossover current densities as a function of temperature at OCV with different MEAs. Operating conditions: 3, 0 atm backpressure, 100% RH [8]	23
<b>Figure 7.</b> Partial pressures of O <sub>2</sub> , H <sub>2</sub> , and H <sub>2</sub> O in fuel cell feed streams as a function of operating temperature. Operating conditions: 3,0 atm backpressure; 100% RH [8]	23
<b>Figure 8.</b> Polarization curves for a PEMFC [7]	24
<b>Figure 9.</b> Types of solid polymer membranes used for fuel cells [2]	32
<b>Figure 10.</b> Structure of grafted membranes: (a) FEP main; (b) sulfonated polystyrene side chain [2]	33
<b>Figure 11.</b> Chemical Structures of (a) SPSU, (b) SPEEK and (c) SPPBP [2]	34
<b>Figure 12.</b> Chemical structure of (a) tetraaminobiphenyl, (b) diphenylisophthalate and (c) poly [2,21-(m-phenylene)-5,51 bibenzimidazole] [2]	35
<b>Figure 13.</b> The view of proton, electron, oxygen and water transfer through MEA [10]	40
<b>Figure 14.</b> Demonstration of (a) vehicle mechanism and (b) Grotthuss mechanism [22]	41
<b>Figure 15.</b> Nano-composite membrane preparation scheme	47

<b>Figure 16.</b> The molecule structure of Pluronic L64® (Mn: 2900 g/mole) [30]	47
<b>Figure 17.</b> The molecule structure of PEG (Mn: 2000 g/mole) [29]	48
<b>Figure 18.</b> Process steps for production of 5 layer MEAs	49
<b>Figure 19.</b> ExactaCoat system (by SonoTek) [34]	50
<b>Figure 20.</b> The view of agglomerate structure of Pt/C SiO <sub>2</sub> Nafion [36]	52
<b>Figure 21.</b> A representative apparatus for tensile test [41]	55
<b>Figure 22.</b> The mechanical tensile test of recasting Nafion	56
<b>Figure 23.</b> Typical structure of 3- dimension modeling of four-point probe technique (by Omer Demir, TEKSIS)	58
<b>Figure 24.</b> Schematic view of settlement of membrane onto Pt wires [8]	59
<b>Figure 25.</b> The experimental setup of Wonatech - Electrochemical Workstation ZIVE SP2 instrument	59
<b>Figure 26.</b> The view of single PEMFC (5 cm <sup>2</sup> active area) at METU Chemical Engineering Fuel Cell Laboratory	60
<b>Figure 27.</b> Water uptake capacity vs. SiO <sub>2</sub> content	64
<b>Figure 28.</b> Sample analysis of stress-strain curves on Nafion 115 [44]	68
<b>Figure 29.</b> The mechanical tensile tests of 2.5 wt. % SiO <sub>2</sub> of M1, M4 and recasting Nafion	70
<b>Figure 30.</b> TGA plot of 4 different samples and recasting Nafion	71
<b>Figure 31.</b> SEM image of M1 containing 2.5 wt. % SiO <sub>2</sub> and Plutonic L64 (3.0 wt. % of added SiO <sub>2</sub> ) prepared via ultrasonic probe	72
<b>Figure 32.</b> EDXS pattern for M1: 2, 5 wt. % of SiO <sub>2</sub> + Pluronic L64 prepared via ultrasonic probe, (A); EDXS pattern of non-agglomerate SiO <sub>2</sub> region, (B): EDXS pattern of agglomerate SiO <sub>2</sub> region	73
<b>Figure 33.</b> SEM image of M2 containing 2.5 wt. % SiO <sub>2</sub> + PEG prepared via ultrasonic probe	73
<b>Figure 34.</b> EDXS pattern for M2: 2, 5 wt. % of SiO <sub>2</sub> + PEG prepared via ultrasonic probe, (A); EDXS pattern of non-agglomerate SiO <sub>2</sub> region, (B): EDXS pattern of agglomerate SiO <sub>2</sub> region	74
<b>Figure 35.</b> SEM image of M3 containing only 2.5 wt. % SiO <sub>2</sub> prepared via ultrasonic probe	75

<b>Figure 36.</b> EDXS pattern for M3: 2, 5 wt. % of SiO <sub>2</sub> + PEG prepared via ultrasonic probe M3, (A); EDXS pattern of non-agglomerate SiO <sub>2</sub> region, (B): EDXS pattern of agglomerate SiO <sub>2</sub> region	75
<b>Figure 37.</b> SEM image of M4 containing only 2.5 wt. % SiO <sub>2</sub> prepared via ultrasonic bath	76
<b>Figure 38.</b> EDXS pattern for M4: 2, 5 wt. % of SiO <sub>2</sub> + PEG prepared via ultrasonic probe M4, (A); EDXS pattern of non-agglomerate SiO <sub>2</sub> region, (B): EDXS pattern of agglomerate SiO <sub>2</sub> region	76
<b>Figure 39.</b> SEM images for MEA1: 2, 5 % Only SiO <sub>2</sub> (Ultrasonic Probe) Non-tested: 1.000 x magnified picture (A), 1.000 x magnified picture (B)	77
<b>Figure 40.</b> SEM images for MEA4: 2, 5 % Only SiO <sub>2</sub> (Ultrasonic Bath) Non-tested: 2.000 x magnified picture (A), 50.000 x magnified picture (B)	78
<b>Figure 41.</b> Recasting Nafion (Ultrasonic Probe) Non-tested MEA0: 1.000 x magnified picture (A), 100x magnified picture (B)	79
<b>Figure 42.</b> The sedimentation time of the suspensions containing various amount of Pluronic L64 (1 wt. %- 10 wt. % of the added silica)	80
<b>Figure 43.</b> The particle size analysis of the suspension containing 2.5 wt. % of SiO <sub>2</sub> and 3.0 wt. % of Pluronic L64 based on the SiO <sub>2</sub> content	81
<b>Figure 44.</b> Representative view of proton transport in SiO <sub>2</sub> composite membrane	83
<b>Figure 45.</b> A representative Nyquist plot of recasting Nafion at 80°C	85
<b>Figure 46.</b> Pristine Nafion (A) and Nafion + SiO <sub>2</sub> composite ion cluster (B) [46]	86
<b>Figure 47.</b> A representative PEMFC performance of M1 (2.5 wt. %) at 100 % RH of test station interface at METU Chemical Engineering Fuel Cell Laboratory (Anode: 0.1 slpm H <sub>2</sub> @ 100 % RH, Cathode: 0.42 slpm Compressed Dry Air @ 100 % RH)	87
<b>Figure 48.</b> The PEMFC performance tests of recasting Nafion: MEA0, at 65°C, 70°C, 75°C, 80°C, Anode: 0,1 slpm, H <sub>2</sub> @ 100 % RH; Cathode: 0,42 slpm, Compressed Dry Air @ 100 % RH	88
<b>Figure 49.</b> The PEMFC performance tests of 2,5 wt. % SiO <sub>2</sub> + Pluronic L64 via ultrasonic probe: MEA1, at 65°C, 70°C, 75°C, 80°C, Anode: 0,1 slpm, H <sub>2</sub> @ 100 % RH; Cathode: 0,42 slpm, Compressed Dry Air @ 100 % RH	91

<b>Figure 50.</b> The PEMFC performance tests of 2,5 wt. % SiO <sub>2</sub> + PEG via ultrasonic probe: MEA2, at 65°C, 70°C, 75°C, 80°C, Anode: 0,1 slpm, H <sub>2</sub> @ 100 % RH; Cathode: 0,42 slpm, Compressed Dry Air @ 100 % RH	93
<b>Figure 51.</b> The PEMFC performance tests of only 2,5 wt. % SiO <sub>2</sub> via ultrasonic probe: MEA3, at 65°C, 70°C, 75°C, 80°C, Anode: 0,1 slpm, H <sub>2</sub> @ 100 % RH; Cathode: 0,42 slpm, Compressed Dry Air @ 100 % RH	95
<b>Figure 52.</b> The PEMFC performance tests of only 2,5 wt. % SiO <sub>2</sub> via ultrasonic bath: MEA4, at 65°C, 70°C, 75°C, 80°C, Anode: 0,1 slpm, H <sub>2</sub> @ 100 % RH; Cathode: 0,42 slpm, Compressed Dry Air @ 100 % RH	97
<b>Figure 53.</b> The comparison tests between MEA1, MEA4 and MEA0, at 65°C, 70°C, 75°C, 80°C, Anode: 0,1 slpm, H <sub>2</sub> @ 100 % RH; Cathode: 0,42 slpm, Compressed Dry Air @ 100 % RH	99
<b>Figure 54.</b> The comparison tests between MEA1, MEA4 at dry condition, at 70°C, Anode: 0,1 slpm, H <sub>2</sub> @ 0 % RH; Cathode: 0,42 slpm, Compressed Dry Air @ 0 % RH	100
<b>Figure 55.</b> SEM pictures for MEA1 2, 5 % SiO <sub>2</sub> + Pluronic L64 Tested: 1000x magnified picture (A), 100x magnified picture (B)	102
<b>Figure 56.</b> SEM images for MEA4 2, 5 % Only SiO <sub>2</sub> (Ultrasonic Bath) Tested: 2.000 x magnified picture (A), 100 x magnified picture (B)	103
<b>Figure 57.</b> SEM images for Recasting Nafion MEA0 (Ultrasonic Probe) Tested: 1.000 x magnified picture (A), 100 x magnified picture (B)	103
<b>Figure 58.</b> The SEM pictures of M1 (A), M2 (B), M3(C), and M4 (D) at 20.000 x magnified	115
<b>Figure 59.</b> The SEM pictures of M1 (A), M2 (B), M3(C), and M4 (D) at 10.000 x magnified	116
<b>Figure 60.</b> Mapping pictures of M1(A), M2 (B), M3 (C) and M4 (D) with adding 2,5 wt. % of SiO <sub>2</sub>	116
<b>Figure 61.</b> The production specification of Poly (ethylene glycol) methyl ether – average Mn ~ 2,000 g/mole, flakes	119
<b>Figure 62.</b> The production specification of SiO <sub>2</sub> –nano powder, 10-20 nm particle size (BET), 99.5 % trace metals basis	120

<b>Figure 63.</b> The production specification of Poly (ethylene glycol) – block – poly (propylene glycol) – block – poly (ethylene glycol) – average Mn ~ 2,000 g/mole	120
<b>Figure 64.</b> Physical properties of Nafion – 1100 with the concentration of both 15 and 5 % weights (by LIQUION)	121
<b>Figure 65.</b> The mechanical tensile tests of (M1): Pluronic L64 2.5 wt. % SiO <sub>2</sub>	123
<b>Figure 66.</b> The mechanical tensile tests of (M1): Pluronic L64 5.0 wt. % SiO <sub>2</sub>	124
<b>Figure 67.</b> The mechanical tensile tests of (M1): Pluronic L64 7.5 wt. % SiO <sub>2</sub>	125
<b>Figure 68.</b> The mechanical tensile tests of (M1): Pluronic L64 10.0 wt. % SiO <sub>2</sub>	126
<b>Figure 69.</b> The mechanical tensile tests of (M4): only 2.5 wt. % SiO <sub>2</sub> with ultrasonic bath	127
<b>Figure 70.</b> The mechanical tensile tests of (M4): only 5.0 wt. % SiO <sub>2</sub> with ultrasonic bath	128
<b>Figure 71.</b> The mechanical tensile tests of (M4): only 7.5 wt. % SiO <sub>2</sub> with ultrasonic bath	129
<b>Figure 72.</b> The mechanical tensile tests of (M4): only 10.0 wt. % SiO <sub>2</sub> with ultrasonic bath	130

## LIST OF TABLES

### TABLES

<b>Table 1.</b> Brief information about types of fuel cells [6].....	5
<b>Table 2.</b> Comparison of properties between commercial membranes [2].....	30
<b>Table 3.</b> The comparison between acid–base blends [2].....	36
<b>Table 4.</b> Overall comparison between solid membranes [2].....	37
<b>Table 5.</b> Type of compounds and composite membranes [18]-[21].....	38
<b>Table 6.</b> The weight % of different content of SiO <sub>2</sub> and dispersing agents (PEG and Pluronic L64) in Nafion membranes.....	46
<b>Table 7.</b> Nomenclature of composite membranes .....	48
<b>Table 8.</b> Nomenclature of MEAs - 3 wt. % SiO <sub>2</sub> incorporated with anode catalyst layer .....	50
<b>Table 9.</b> The thickness of the prepared samples.....	66
<b>Table 10.</b> The mechanical properties of membranes.....	67
<b>Table 11.</b> The particle size analysis results from the DLS technique for the suspension (M1) containing 2.5 wt. % of SiO <sub>2</sub> and 3.0 wt. % of Pluronic L64 based on the SiO <sub>2</sub> content.....	82
<b>Table 12.</b> Z-Average particle size of SiO <sub>2</sub> suspensions (M2, M3, and M4).....	82
<b>Table 13.</b> Comparison of proton conductivity values of samples with only humid air (95 % RH) .....	84
<b>Table 14.</b> The proton conductivity of the samples –totally immersed in DI water ...	85
<b>Table 15.</b> Comparison of OCV and maximum power density values for recasting Nafion – MEA0.....	89
<b>Table 16.</b> Comparison of OCV and maximum power density values for MEA1 at 100 % RH.....	92

<b>Table 17.</b> Comparison of OCV and maximum power density values for MEA2 at 100 % RH.....	94
<b>Table 18.</b> Comparison of OCV and maximum power density values for MEA3 at 100 % RH.....	96
<b>Table 19.</b> Comparison of OCV and maximum power density values for MEA4 at 100 % RH.....	98
<b>Table 20.</b> Overall comparison of OCV and maximum power density values for MEA0, MEA1 and MEA4 at 100% RH condition.....	99
<b>Table 21.</b> Overall comparison of OCV and maximum power density values for MEA1 and MEA4 at 0 % RH condition .....	101
<b>Table 22.</b> EDXS pattern for M1: 2.5 wt. % of SiO <sub>2</sub> + Pluronic L64 prepared via ultrasonic probe, (A); EDXS pattern of non-agglomerate SiO <sub>2</sub> region, (B): EDXS pattern of agglomerate SiO <sub>2</sub> region .....	117
<b>Table 23.</b> EDXS pattern for M2: 2.5 wt. % of SiO <sub>2</sub> + PEG prepared via ultrasonic probe, (A); EDXS pattern of non-agglomerate SiO <sub>2</sub> region, (B): EDXS pattern of agglomerate SiO <sub>2</sub> region.....	117
<b>Table 24.</b> EDXS pattern for M3: 2.5 wt. % of SiO <sub>2</sub> + PEG prepared via ultrasonic probe M3, (A); EDXS pattern of non-agglomerate SiO <sub>2</sub> region, (B): EDXS pattern of agglomerate SiO <sub>2</sub> region.....	118
<b>Table 25.</b> EDXS pattern for M4: only 2.5 wt. % of SiO <sub>2</sub> prepared via ultrasonic bath, (A); EDXS pattern of non-agglomerate SiO <sub>2</sub> region, (B): EDXS pattern of agglomerate SiO <sub>2</sub> region.....	118

## NOMENCLATURE

Ag	: Silver
AFC	: Alkaline Fuel Cell
ASTM	: American Society for Testing and Materials
CCL	: Cathode Catalyst Layer
CF <sub>2</sub>	: Difluorocarbene
DLS	: Dynamic Light Scattering
DMAc	: Dimethylacetamide
DMF	: Dimethylformamide
DMFC	: Direct Methanol Fuel Cell
EODC	: Electro-Osmotic Drag Coefficient
FEP	: Poly (tetrafluoroethylene-co-hexafluoropropylene)
EDXS	: Energy-Dispersive X-Ray Spectroscopy
GDL	: Gas Diffusion Layer
HHV	: Higher Heating Value
H <sub>3</sub> O <sup>+</sup>	: Hydronium Ion
H <sub>3</sub> PO <sub>4</sub>	: Phosphoric Acid
IEC	: Ion Exchange Capacity
KOH	: Potassium Hydroxide
K <sub>2</sub> CO <sub>3</sub>	: Potassium Carbonate

LaMnO <sub>3</sub>	: Lanthanum Manganite
LiAlO <sub>2</sub>	: Lithium Aluminate
LHV	: Lower Heating Value
MCFC	: Molten Carbonate Fuel Cell
Ni	: Nickel
OCV	: Open Circuit Voltage (V)
PBI	: Polybenzimidazole
PAFC	: Phosphoric Acid Fuel Cell
PFSA	: Perfluoro-Sulfonic Acid
PEMFC	: Proton Exchange Membrane Fuel Cell
PTFE	: Poly Tetra-Fluoroethylene
RH	: Relative Humidity (%)
SOFC	: Solid Oxide Fuel Cell
SO <sub>3</sub> H	: Sulphonic Groups
SPSU	: Sulfonated Polysulfone
SPEEK	: Sulfonated Poly ether ether ketone
SPPBP	: Sulfonated Poly (4-phenoxybenzoyl-1,4-phenylene)
Pt/C	: Platinum/carbon
$\Delta H_f$	: Formation Enthalpy (kJ/mole)





## **CHAPTER 1**

### **INTRODUCTION**

In this chapter, historical background and working principles of fuel cells are presented with literature survey. Types of fuel cell and membranes are reviewed emphasizing the importance of Polymer Electrolyte Membrane (PEM). Fuel cells are one of the most important technologies for generating energy efficiently, economically, silently and environmentally friendly. When a fuel cell is used, the chemical energy in fuel gases are converted into electrical energy by means of an electrochemical process into electrical energy and this conversion can be done with less moving parts and can produce less air pollution. The polymer electrolyte membrane fuel cells (PEMFCs) are clean, renewable and used for sustainable energy applications that are supposed to cover world energy depletion. The PEMFCs are one of the most attractive fuel cell types owing to operating efficiently at low temperatures, working silently, and having nonhazardous wastes. In this sense, the polymeric membranes are most significant component of PEMFCs with having characteristics of proton transferring. Nowadays, Nafion is used extensively since it has good chemical and thermal stabilities, suitable mechanical properties, and high proton conductivity [1]. However, the utilization of the membrane has been limited at elevated temperatures and low humidity conditions due to performance losses. Above 80°C, proton conductivity decreases dramatically as dehydration occurs in the membrane. Besides, the mechanical and thermal stabilities of the membrane are weakened.

To be able to commercialize fuel cells, the limitations of the fuel cells should be prevented. In other words, for the commercialization of the PEMFCs, the water management is one of problem needs to be solved.

In order to provide proton transfer and obtain high performance, an external humidifier is usually used to humidify reactant gases for traditional PEMFCs. Nevertheless, the PEMFCs become more complex and their productivity is decreased. Therefore, the production of the self-humidifier or low-humid level membrane electrode assemblies (MEA) for the PEMFCs is considered as a key necessity with respect to water capacity management. In recent years, composite membranes have been notably used for the PEMFCs using the particles of inorganic materials ( $\text{SiO}_2$ , Zeolite, titania ( $\text{TiO}_2$ ), zirconia ( $\text{ZrO}_2$ )) in such a way that comparably high proton conductivity has been obtained at very low humidity levels [2].

### **1.1. Overview of Fuel Cell Technology**

Fuel cells transform chemical energy to electrical energy and heat with high efficiency. In the main structure of fuel cells, there is an electrolyte layer between two electrodes (an anode and a cathode). Normally in a fuel cell, fuels in gaseous formation are sent to the anode site which is known as the negative electrode meanwhile oxidant such as air or oxygen is forwarded to cathode site that is called as positive electrode. Electrochemical reactions take place at these electrodes to produce electrical current.

Advantages of fuel cells are as follows [3];

- **Efficiency:** Fuel cells have higher efficiency than piston or internal combustion engines. Another advantage of these devices is small sized systems work as efficient as large scale ones which is a considerable property for assembling of heat and power generation.
- **Simplicity:** The fundamentals of fuel cells are substantially simple. There is almost no moving part in the fuel providing long-term durable systems.

- Low Emission: Pure water is the only product for the overall reaction of fuel cell when hydrogen gas is used as a fuel suggesting that when the transportation vehicles powered with fuel cells are used zero emission of pollutants can be achieved. However, during the production of hydrogen, carbon dioxide emission should be taken into account.
- Working Silently: Even used for a commissioning device, fuel cells work silently.
- Lots of types of energy resources can be provided.
- Comparing with batteries, fuel cells can produce the energy immediately while batteries need to be charged from time to time, fuel cells produce electricity as long as fuels are introduced.

Disadvantages of fuel cells are the following;

- Economic limitations in terms of the transportation and storage of pure hydrogen
- Losing performance when other fuels are used due to deterioration of catalyst and electrolyte.

Electricity is generated by externally supplying fuels and oxidizing agents at anode and cathode, respectively. Fuel and oxidizing agents are interacted with the environment of electrolyte. During the operation of a fuel cell, the reaction gases (hydrogen and oxidant gases) enter the system and after the electrochemical reaction the products leave the system. In this sense, fuel cells can be operated continuously as long as the flows of reaction gases are provided. In fuel cells, although reacting materials are continuously depleted, electrical energy is stored as chemically in a closed volume. Besides, the electrodes remain catalytically stable during the production of electrical energy.

Working principle of fuel cells is based upon to catalysts' fundamentals where fuel is separated into electrons and protons. The electrons are carried by an external circuit so that electrical current is produced [4].

A wide range of materials are utilized in fuel cells. Generally, metals such as nickel or carbon nano-tubes covered with platinum are used as electrodes. Ferrous or palladium nano particles are used as catalysts. Also, bipolar plates are integrated in order to obtain higher efficiencies. Carbon paper separates the electrodes from electrolytes which is mostly made of ceramic or spurious membrane [5].

Fuel cells; having a commanding lead over conventional power generator systems due to the following reasons;

- Lower environmental contamination
- Higher energy production efficiency
- Working with different fuels (Natural gas, liquid petroleum gas-LPG etc.)
- Recovering waste heat
- Modular structure
- Short installation time
- Requiring less amount of cooling material
- Safer system
- Easy to applicability
- Potential for future growth
- No solid waste and noise issues

For a requested amount of energy, a fuel cell can be connected either as parallel or serial manner. Serial fuel cells provide higher voltage, whereas parallel ones referred to as stack structures enable to have higher currents. In addition, to draw higher currents, active fuel cell area can be increased.

## 1.2. Types of Fuel Cells

Generally, fuel cells are categorized into five types in terms of their electrolytes. However, different types of fuel cells have become evident recently. In Table (1), the types of fuel cells are summarized. Regarding some properties such as working condition, applicability, and high efficiency; a PEMFC is the most accentuated type of fuel cells.

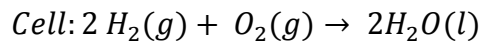
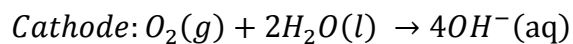
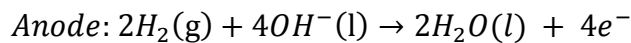
**Table 1.** Brief information about types of fuel cells [6]

Fuel Cell Types	Electrolyte	Operating Temperature °C	Electrochemical Reactions
Polymer Electrolyte Membrane (PEM)	Solid organic polymer (poly-perfluoro sulfonic acid)	60 – 100	$Anode: H_2 \rightarrow 2H^+ + 2e^-$ $Cathode: \frac{1}{2}O_2 + 2H^+ + 2e^- \rightarrow H_2O$ $Cell: H_2 + \frac{1}{2}O_2 \rightarrow H_2O$
Alkaline (AFC)	Aqueous solution of potassium hydroxide soaked in a matrix	90 – 100	$Anode: H_2 + 2(OH)^- \rightarrow 2H_2O + 2e^-$ $Cathode: \frac{1}{2}O_2 + H_2O + 2e^- \rightarrow 2(OH)^-$ $Cell: H_2 + \frac{1}{2}O_2 \rightarrow H_2O$
Phosphoric Acid (PAFC)	Liquid phosphoric acid soaked in a matrix	175 - 200	$Anode: H_2 \rightarrow 2H^+ + 2e^-$ $Cathode: \frac{1}{2}O_2 + 2H^+ + 2e^- \rightarrow H_2O$ $Cell: H_2 + \frac{1}{2}O_2 \rightarrow H_2O$
Molten Carbonate (MCFC)	Liquid solution of lithium, sodium and / or potassium carbonates, soaked in a matrix	600 - 1000	$Anode: H_2 + CO_3^{2-} \rightarrow H_2O + CO_2 + 2e^-$ $Cathode: \frac{1}{2}O_2 + CO_2 + 2e^- \rightarrow CO_3^{2-}$ $Cell: H_2 + \frac{1}{2}O_2 + CO_2 \rightarrow H_2O + CO_2$
Solid Oxide (SOFC)	Solid zirconium oxide to which a small amount of yttria is added. And other types of solid oxides	600 - 1000	$Anode: H_2 + O^{2-} \rightarrow H_2O + 2e^-$ $Cathode: \frac{1}{2}O_2 + 2e^- \rightarrow O^{2-}$ $Cell: H_2 + \frac{1}{2}O_2 \rightarrow H_2O$

### 1.2.1. Alkaline Fuel Cell –AFC

The electrolyte in this fuel cell is changed according to working temperatures: 85 wt. % of potassium hydroxide (KOH) is used at high operating temperatures (about 250 °C); however for low temperatures (below 120°C), 35-50 wt. % of KOH is utilized. The electrolyte is stored in asbestos structure and various type of electro-catalysts are used (e.g. Ag, Ni, metal oxide and noble metals). Fuel supply materials are restricted to only hydrogen and carbon monoxide (CO) which has a poisonous effect. The carbon dioxide (CO<sub>2</sub>) reacts with KOH and produce potassium carbonate (K<sub>2</sub>CO<sub>3</sub>) which deforms electrolyte. Even trace amount of CO<sub>2</sub> in air may anticipated as poisonous influence on alkaline fuel cells [6].

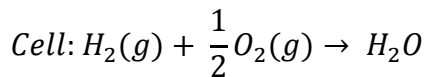
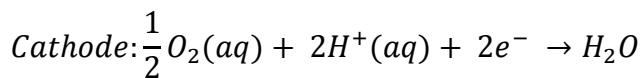
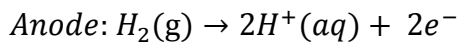
Comparing other fuel cells, the advantage of AFC is its excellent performance due to highly active oxygen kinetics and wide range of electro-catalyst utilization.



On the other hand, sensitivity of electrolyte to CO<sub>2</sub> and requirement of highly pure hydrogen are main disadvantages. Thus, more productive system – a reformer, is needed to be able to remove CO<sub>2</sub> and CO. In addition to that, once air used as oxidant agent, CO<sub>2</sub> should be distracted from air. Although it is not a technological challenge, this process negatively affects the size of system and cost.

### 1.2.2. Phosphoric Acid Fuel Cell –PAFC

100 % phosphoric acid ( $H_3PO_4$ ) is used as the electrolyte in PAFCs and it works at 150-200°C. At low temperature,  $H_3PO_4$  is a weak ionic conductor and toxicity of Pt owing to CO is dramatically increased. Comparing to other acids, the stability of concentrated phosphoric acid is high. Hence, PAFCs have capabilities to be operated at temperature between 100 and 200°C. Additionally, using of 100 %  $H_3PO_4$  minimize vapor pressure of water so that water management can be easier. The main structure to hold acid is mostly silicon carbide; moreover Pt is used for both anode and cathode as an electro-catalyst [6].



The main advantage of PAFC shows more tolerance to CO comparing to PEMFC and AFC. Working temperature is low enough to be able to use common materials for fuel cells.

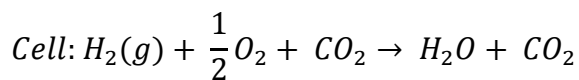
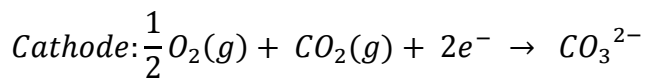
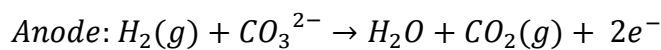
Disadvantages: the cathode site reduction reaction in this fuel cell is slower than that in the AFC and much more Pt catalyst is required. Despite having less complexity than PEMFC, intensive fuel is still needed for the process. Lastly, by reason of highly abrasiveness of phosphoric acid, more expensive materials are used for the construction of this type of fuel cell.

### 1.2.3. Molten Carbonate Fuel Cell –PAFC

Combination of alkaline and carbonate is generally used as electrolyte for this type of fuel cell which implicit into main lithium aluminate ( $\text{LiAlO}_2$ ) ceramic structure and works at temperatures between 600-700°C. In these operating temperatures, ceramics are notably conductive, and constitute a molten salt formation in order to provide conductivity of carbonate ions.

At these elevated temperatures, Ni (anode) and Nickel Oxide (cathode) are equivalently reactive. Nobel metals aren't necessity for the operation and lots of hydrocarbons are processed with reformers.

Having ability to work high temperature provides some advantages. To illustrate, utilization of expensive electrodes is no longer an issue since nickel electrodes demonstrates high activity. Furthermore, with help of special reformer plates, some dirty hydrocarbons are converted to hydrogen; thereby they can be used as fuels for MCFCs.



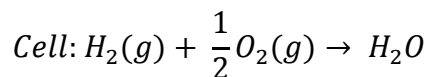
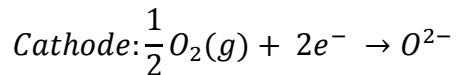
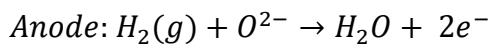
Nevertheless, the main disadvantage of MCFCs is using high endurance stainless steel and nickel in corrosive and mobile electrolyte cell structure. The difficulties come with high operating temperatures which reduces mechanical durability and cell life [6].

#### 1.2.4. Solid Oxide Fuel Cell –SOFC

In this type of fuel cell, a solid metal oxide (generally stabilized zirconium oxide -  $ZrO_2$ ) is the electrolyte. The SOFC works between 600-1000°C and in this region oxygen ions become a part of conductivity. Mostly, nickel (Ni) or cobalt (Co) -  $ZrO_2$  and lanthanum manganite ( $LaMnO_3$ ) doped with strontium (Sr) are used for anode and cathode site, respectively.

SOFC can be facilitated for different fuels such as hydrocarbons. Solid ceramic structure minimizes possible corrosion drawbacks. Moreover, solid structure provides a certain application for three phase restriction.

Electrolyte movement and pressing at electrodes are prevented as well. The cell is kinetically more reactive than others and carbon monoxide can be used as fuel directly.



The difficulties come with working at high temperatures in SOFC. Unequal expansions and sealing may take place between different materials used for in the cell.

### **1.2.5. Direct Methanol Fuel Cell –DMFC**

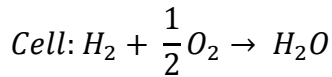
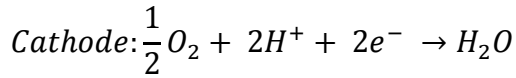
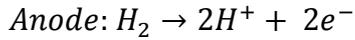
Direct methanol fuel cell is a type of PEMFC and methanol is turned into carbon-dioxide and hydrogen ions at the anode site. After this stage, hydrogen ions follow the same path as in a PEMFC and react with oxygen at the cathode site. The cell can be performed in the vicinity of 120°C that is higher operating temperature comparing with a PEMFC and efficiency is about 40 %. Unlike PEMFC, transforming methanol into CO<sub>2</sub> and hydrogen at low temperature is required much more catalyst which is one of the most prominent drawback for DMFCs due to increasing cost. However, facilitating liquid phase fuels and working without reformer units are major benefits [6].

### **1.2.6. Proton Exchange Membrane Fuel Cell –PEMFC**

Utilization of PEMFC is started with the invention by General Electric in 1960s. A polymeric membrane acting as an electrolyte is installed to separate an anode and cathode site. Owing to the reaction of hydrogen with catalyst, protons and electrons are formed in such a manner that they are transported by electrolyte and an external circuit, respectively. In the meantime, oxygen reacts with protons and electrons on the surface of catalyst surface and at the end electricity and water are produced [7].

PEMFC consists of a solid electrolyte which is commonly utilized by a perfluorinated sulfonic acid polymer providing proton conductivity. Operating temperature and pressure of PEMFC is at very low temperatures (50-80°C) and pressures (1-8 atm). The cell is needed a certain amount of humidity to be fed with hydrogen and oxygen. High power densities are obtained from the cell producing approximately 350 mWcm<sup>-2</sup>. PEMFCs have some capabilities such as quick start up, high power density and adoptable to different power output which allow using in transportation domain. Due to activation, component of cell, resistivity of inner connections and mass transportation losses as current increases voltage decreases.

Working principle of PEMFC is exactly reverse of water electrolysis and reactions take places at anode and cathode as follows [8];



The products of these reactions are electricity, heat and water. As the generated water is reused, total efficiency can be increased [6].

### **1.3. Components and properties of PEMFCs**

The components of PEMFC are seen in Figure (1). For a single cell from the bottom to top; a gas diffusion channel, catalyst layers for both anode and cathode sides and electrolyte are mainly established as a sandwich model. The components vary from cell to cell where a catalyst can be directly loaded onto membrane without using carbon cloth or paper. Covering electrodes with membrane and performing hot pressing forms the key component of the PEMFC that is called as MEA. The MEA, the heart of the cell, is the most significant component and determinant in terms of performance [9].

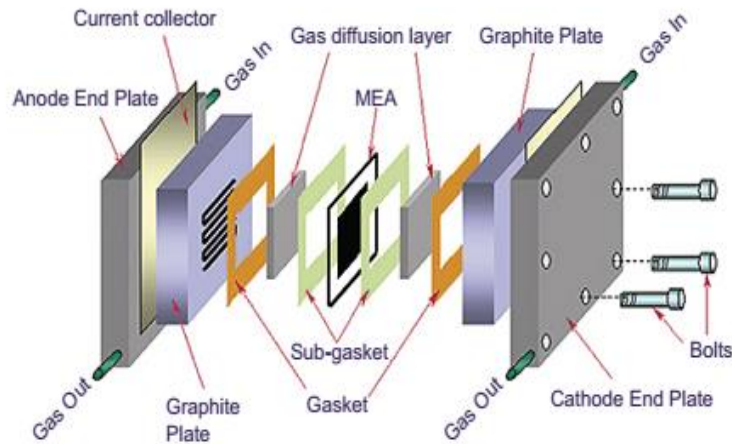


**Figure 1.** Schematic view of the components of a PEMFC [9]

### 1.3.1. Electrode

The electrodes comprise catalyst layers where reactions take place on both the surfaces, anode and cathode. Since gases, electrons, and protons are in different phases they can react anywhere in the catalyst surface where being able to achieve to find themselves. In order to grow the reaction zone, one may harden the surface of membrane, minimize the catalyst particle size, and add ionomer into catalyst layers [10].

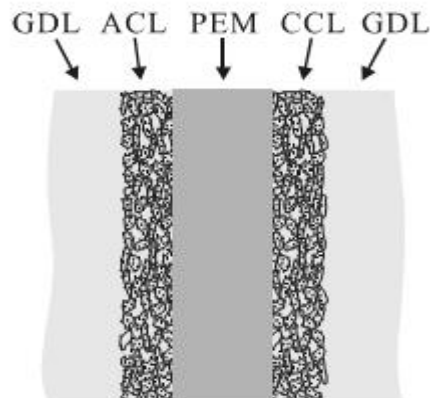


**Figure 2.** Schematic view of a catalyst layer structure. GDL – gas diffusion layer; ACL – anode catalyst layer; CCL – cathode catalyst layer; PEM – proton exchange membrane [10]

The fuels are transported through a porous electrode and reach the anode catalyst layer. Reactants arrive in the catalyst layer and separated into ions and electrons. Electrons are driven through an external circuit to generate power, whereas the ions go by way of electrolyte and achieve at the cathode site to produce water and heat which is shown in Figure (2). Without depending on the type of a fuel cell, catalyst layers should separate ions and electrons effectively, have high active surface area, and be cost efficient.

Besides, the catalyst layer should have the following properties;

- High porosity
- High electrical conductivity
- Easy to produce and abound in nature
- Good mechanical and chemical stability
- High physical, chemical, and thermal interactivity with reactants [11]

### **1.3.2. Gas Diffusion Layer**

Gas diffusion layer intervene between bipolar plates and catalyst layer and used for the management of hydrogen, oxygen and water flows in a proper manner [11]. Mostly carbon papers or clothes are materials for gas diffusion layers and they provide porous structure for reactants, products and electrons to have an efficient transportation. During fuel cell manufacturing, a catalyst layer can be established on the gas diffusion layer or the membrane directly. Fluorinated-polymer and black carbon are treated with gas diffusion material in order to enhance electron conductivity and water management. These materials are effective to increase diffusivity of reactants into the gas diffusion layer. In addition, the gas diffusion layer is served for a certain amount of humidity to contact with a MEA; in the meantime, it should compensate excess amount of water at the cathode site so that flooding is prevented.

### 1.3.3. Catalyst Layer

Platinum (Pt) is the best catalyst for both anode and cathode sites. Initially, about 28 mg/cm<sup>2</sup> Pt loading on the layer was a problem due to high cost of Pt. However, Pt loading is reduced to 0.1 mg/cm<sup>2</sup> when nanosized Pt catalyst particles are used on the surface of carbon powders.

Figure (3) shows that Pt is highly split up to groups and evenly distributed so that most of the surfaces enable to contact with reactants effectively [11].

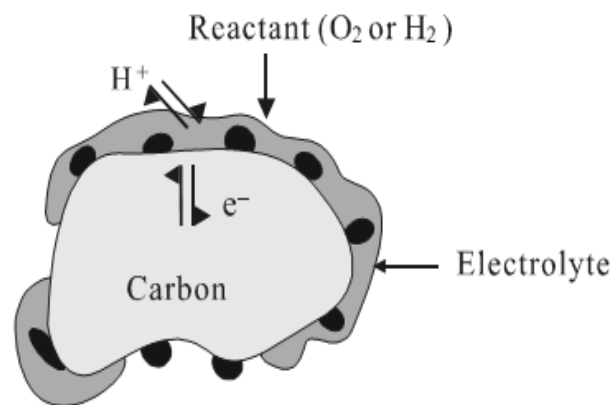


**Figure 3.** 3-phase interface formation in catalyst layer [11]

### 1.3.4. Membrane Layer

The membrane layer is made of a polymeric material in order to transport ions with supplying high conductivity; as a result these cells are referred to as PEMFCs where the membrane is a solid electrolyte. Nowadays, many types of polymers are used as electrolytes which have a common characteristic that is generally formed by sulfonated fluoro-polymers. From 1970s, Nafion has been used extensively which is a commercial name of perfluoro-sulfonic acid (PFSA) [12].

The backbone material of this electrolyte (Nafion) is synthetic polyethylene (PE) which is fluorinated later on and named as poly tetra-fluoroethylene (PTFE) and that is commercially known as Teflon.

Improvement of PTFE is substantially significant in terms of fuel cell performance that includes strong bonds between fluorine and carbon making the electrolyte solid resistant and chemically stable to external factors. Besides, the hydrophobicity of structure ensures easy to remove water and avoid flooding. However, one more step is required to obtain electrolyte that is treating PTFE with sulfonic acid.

This process enables adding hydrogen sulfite- $\text{HSO}_3^-$  as side chain to the polymer backbone hereby sulfite ion- $\text{SO}_3^-$  and chemically available hydrogen ion- $\text{H}^+$  have strong interactions which is shown in Figure (4). Side chain structures are tend to agglomeration and mainly have characteristic of hydrophilic property which means it enables to hold water.

Therefore, hydrophilic zones are formed onto hydrophobic structures. The hydrophilic regions created in the vicinity of sulfite ions assist to absorb tremendous amount of water somehow as much as half of total weight is increased which yield a diluted acidic environment and in this way different phases are formed in solid hydrophobic structure.

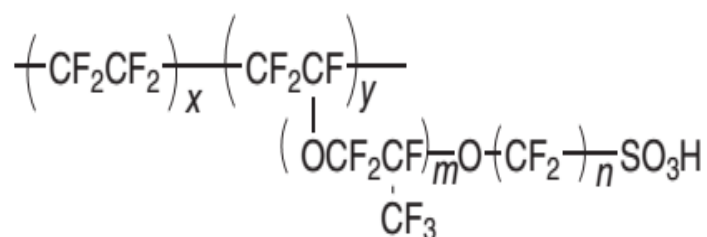


**Figure 4.** Chemical formula of PFSA-Nafion [12]

For low temperature PEMFCs, Nafion is widely used which is produced by DuPont and equivalent membranes such as Dow, Flemion, and Aciplex are manufactured as well. Nafion is one step ahead among mentioned electrolytes since it has the highest proton conductivity and good chemical and mechanical stabilities.

Drawbacks of PFSA can be itemized regarding necessity of having to work at low temperature and ensure a certain level of humidity. Other disadvantages for PFSA are high crossover effect and intense water management. To be able to work with PFSA at elevated temperatures and low humidity, many studies have been conducted in order to prevent crossover effect and improve water management. In this sense, some approaches are available such as changing water with low volatility liquid and/or phosphoric acid, acetic acid and ionic liquids.

Adding hygroscopic oxide particles (such as  $\text{SiO}_2$ ) to the polymer membrane matrix is another approach. In addition, using hetero poly-acids for decreasing humidity and zirconium phosphate - solid proton conductivity particles are other approaches. Moreover, modified PFSA can be operated at  $120^\circ\text{C}$  at 1 atm or  $150^\circ\text{C}$  from 3 to 5 atm. Various alternative aromatic based polymer membranes are expected to be used for PEMFCs due to their low cost and stabilities.

Modifications on the backbone of polymer or changing integrated groups are methods to increase proton conductivity. Poly esters, poly benzimidazole (PBI), poly imide, poly ether imide, poly phenylene sulfide, poly sulfones, poly (ether sulfones) (PES), poly ether ketone (PEK), poly ether ether ketone (PEEK) are some examples for possible candidates where can be even used as backbones in inorganic/organic composite membrane structures. In contrast to PFSA membranes, aromatic ones have less hydrophobic backbones and acidic and polar functional groups. Hence, the proton conductivity of aromatic ones is less dependent on the humidity level comparing to that of PFSA membranes.

Nevertheless, even at high humidity conditions, they have low proton conductivities. Acid-base polymer complexes are obtained by basic or acidic zones containing networks with adding inorganic acids or bases. PBI, poly ethylene oxide, poly (vinyl acetate) (PVA), poly acryl amide (PAM) can be shown as examples for these types of membranes.

The phosphoric acid, an inorganic acid, shows high proton conductivity and stability even at high temperature in anhydride form. Although containing high acidity level means high proton conductivity, it decreases mechanical stability at elevated temperatures. In order to obtain good mechanical strength, polymers are cross linked, inorganic fillers are added to the polymer matrix, or polymers with high glass temperature are chosen [13].

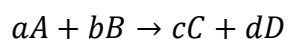
#### **1.4. Working Principle of PEM Fuel Cell**

The heart of a single PEMFC is composed of two electrodes: a negatively charged one (anode) and positively charged one (cathode). A membrane acting as an electrolyte is positioned in the middle of these electrodes. Hydrogen is oxidized at the anode and oxygen is reduced at the cathode sides through diffusion and/or convection. Protons are transported through the electrolyte; whereas, electrons are carried to cathode side by means of an external circuit. In the cathode side, oxygen is reacted with protons and electrons forming water and heat. Catalysts loaded in the electrodes play an essential role in order to accelerate the reactions.

##### **1.4.1. Basic Thermodynamic Concepts of a PEMFC**

Practically, it is easier to perform half reactions at constant temperature and pressure compared to constant temperature and volume conditions; therefore, change in Gibbs free energy ( $\Delta G$ ) is appropriate to determine electrical potential. In other words, the total reaction between hydrogen and oxygen occurs spontaneously which means reaction prior to proceed to product sides due to  $\Delta G$  of product is less than reactants'.

The  $\Delta G$  of a typical reaction can be expressed as the following which is shown in Equation (1);



$$\Delta G = d\mu_d + c\mu_c - (a\mu_a + b\mu_b) \quad (1)$$

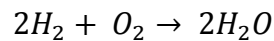
where;  $\mu$  is defined as the chemical potential as indicated in Equation (2)

$$\mu = \left( \frac{\partial G}{\partial n_i} \right)_{T,P,n_j} \quad (2)$$

where;  $j \neq i$

The measurement of the maximum nominal work,  $\Delta G$ , can be obtained from a chemical reaction. When the change in entropy ( $\Delta S$ ) is zero,  $\Delta G$  is equal to change in enthalpy ( $\Delta H$ ).

As can be comprehended, in a chemical reaction if the product is in gaseous form, and molar ratio of reactants are equal to each other, then change in entropy of this reaction is approximately zero. The reason of this phenomenon can be expressed as the number of gaseous molecules remains the same which means diverted entropy is equivalent to entropy change. The reaction at standard conditions takes place for the hydrogen and oxygen which are in gas form as the following;



$$\Delta G^{\circ}_{rxn} = -237.3 \frac{kJ}{mol}$$

$\Delta G^{\circ}_{rxn}$ : Gibbs free energy at standart conditions (25°C and 1 atm)

The measurement of  $\Delta G$  gives information about a reaction whether will it take place by itself or not. As long as the sign of  $\Delta G$  is negative, the reaction occurs spontaneously.

Change in enthalpy (Equation (3)) for a reaction can be expressed thermodynamically as follows at which  $\Delta E$  is defined as total energy;

$$\Delta H = \Delta E + P\Delta V = Q - W + P\Delta V \quad (3)$$

If a reaction happens in heat engine, then only work (W) is the work done by the system due to expansion at which change in enthalpy equals heat absorbed (Q) by the system which is expressed in Equation (4).

$$\Delta H = Q \quad (4)$$

If the reaction occurs electrochemically, then the work is not only because of expansion but also due to electrical work that is accumulated of proton transfer from anode to cathode site with an external circuit. Reversible potentials at anode and cathode are defined as  $E_{r,Anode}$  and  $E_{r,Cathode}$ , respectively.

Then, the maximum electrical work (neglecting internal resistance and over-voltage losses) in form of molar quantities resulting from a complete reaction inside a PEMFC can be calculated from the following Equation (5):

$$W_{el} = nF(E_{r,Cathode} - E_{r,Anode}) \quad (5)$$

where;  $n$ : number of electrons contributed into the reaction

$$F: \text{Faraday's Constant} = 96485 \text{ Cmol}^{-1}$$

Then reversible cell voltage is defined as in Equation (6);

$$E: \text{Reversible Cell Voltage} = E_{r,Cathode} - E_{r,Anode} \quad (6)$$

Summation of the electrical and expansion works can be expressed as follows (Equation (7)):

$$W = W_{el} + P\Delta V \quad (7)$$

Assuming reversible conditions;

$$Q = T\Delta S \quad (8)$$

$$\Delta H = T\Delta S - nF(E_{r,Cathode} - E_{r,Anode}) \quad (9)$$

Under the isothermal condition,

$$\Delta H = -nF(E_{r,Cathode} - E_{r,Anode}) \quad (10)$$

For standard conditions of reactants and products the Gibbs free energy can be described as the following Equation (11);

$$\Delta G^o = -nFE^o \quad (11)$$

The maximum electrical work depends upon the Gibbs free energy of reaction and presented as the theoretical cell voltage at 25°C and atmospheric pressure ( $E^o$ );

$$W_{el} = -\Delta G \quad (12)$$

$$E = -\frac{\Delta G}{nF} = \frac{237,34 \frac{J}{mol}}{2 \cdot (96485 \frac{C}{mol})} \cong 1.23 V \quad (13)$$

Taking account of all the Gibbs free energy which is converted into electrical energy, then maximum theoretical efficiency  $-\eta_{theo}$  is calculated as in Equation (14);

$$\eta_{theo} = \frac{\Delta G}{\Delta H} = \frac{237,34}{286,02} \cong 83 \% \quad (14)$$

Since the theoretical reversible cell voltage is dependent on temperature and pressure; it is also expressed as the following Equation (15);

$$E_{T,P} = -\left(\frac{\Delta H}{nF} - \frac{T\Delta S}{nF}\right) + \frac{RT}{nF} \ln\left(\frac{a_{H_2} \cdot a_{O_2}^{0.5}}{a_{H_2O}}\right) \quad (15)$$

The ‘‘ $a$ ’’ is defined as activity or ratio of partial pressure of reactants and products to atmospheric pressure (for liquid water,  $a_{H_2O} = 1$ ).

Irreversible over-potentials cause losses; therefore real performances are deviated from the theoretical values. The losses can be occurred due to lots of reasons which can be mainly ordered as kinetic losses of electrochemical reactions, internal and ionic resistances, transportation difficulties of reactants at reaction zone, internal currents, and cross-over effects [11].

To be able have a concrete expression on PEMFC performance, the Open Circuit Voltage (OCV) is explained in detail.

- Open Circuit Voltage | OCV

The OCV value is expressed as the voltage at zero current density which means that the circuit is open without any power output [8]. It is known that OCV in PEMFC is generally between, 0.95 and 1.05 voltage.

It is lower than the theoretical value, 1.23 V, due to three major parameters which are hydrogen crossover, temperature and mixed potentials meaning that side reactions including  $O_2$ ,  $H_2$ , the impurities  $CH_x$ , carbon support C, and Pt PEMFC cathode side at low current density [8]. In general, mixed potential is explained with formation of hydrogen peroxide ( $H_2O_2$ ) but it is negligibly small to take into account.

Among the factors, mixed potential on cathode side (especially Pt oxidation) is known as one of the major factor for OCV drop and partial pressure of oxygen is the function of it. According to the literature, Pt- $O_2$  reaction can cause up to 182 mV which proves that mixed potential is one of the major factor of OCV drop in which temperature is also strongly function of it. As temperature increases (from 23°C to 120°C), the voltage loss (from 182 to 96 mV) because of mixed potential decreases which is shown in Figure (5) [8].

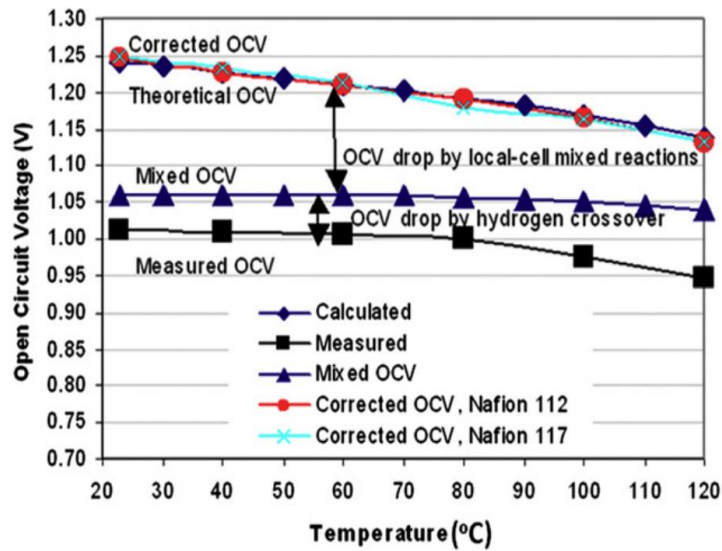


**Figure 5.** Fuel cell OCVs as a function of temperature. Operating conditions: H<sub>2</sub>/air, 3,0 atm [8]

The hydrogen crossover is a phenomenon that hydrogen crosses over from anode to cathode without separating into electron and proton. The hydrogen crossover has recessive character on OCV drop comparing with mixed potential factor and it is proportional with temperature which is shown in Figure (6).

More than that, the thickness of membrane is very critical function of hydrogen crossover. It is proven that as the thickness decreases higher gas permeability is occurred which causes larger hydrogen crossover current density and hence larger OCV drop.

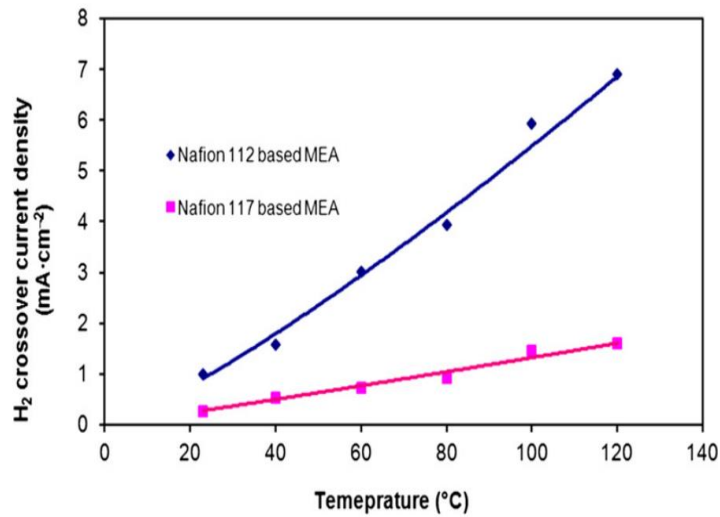


**Figure 6.** H<sub>2</sub> crossover current densities as a function of temperature at OCV with different MEAs. Operating conditions: 3, 0 atm backpressure, 100% RH [8]

Third and last factor, temperature, is effective on OCV drop because of changing partial pressure of fuel (H<sub>2</sub>, O<sub>2</sub>, and H<sub>2</sub>O) and oxidant gas streams. It is stated that especially after 80°C, temperature is strongly proportional with partial pressure of H<sub>2</sub>O; however, it is reverse proportional with H<sub>2</sub> and O<sub>2</sub>.

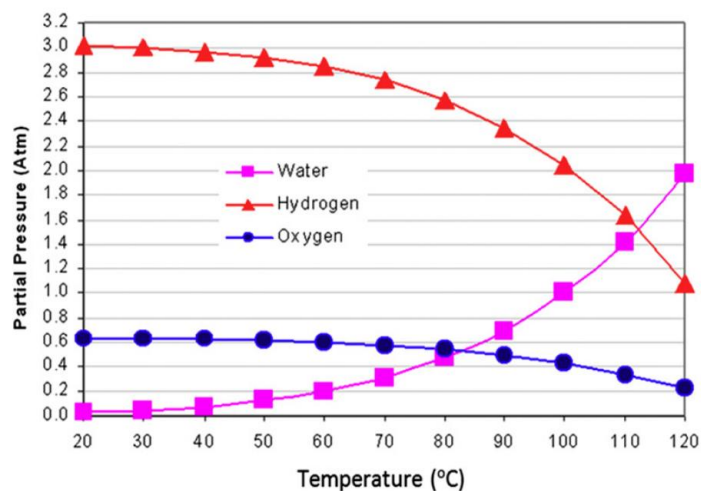


**Figure 7.** Partial pressures of O<sub>2</sub>, H<sub>2</sub>, and H<sub>2</sub>O in fuel cell feed streams as a function of operating temperature. Operating conditions: 3,0 atm backpressure; 100% RH [8]

$$E_{theory}^{OCV} = 1.229 - 0.000846 \times (T - 298.15) + 2.303 \frac{RT}{2F} \log \left( \frac{P_{H_2} P_{O_2}^{\frac{1}{2}}}{P_{H_2O}} \right) \quad (16)$$

According to Equation (16), as temperature increases, the theoretical OCV ( $E_{theory}^{OCV}$ ) of PEMFC decreases because of the relationship between temperature and partial pressure of  $H_2$ ,  $O_2$ , and  $H_2O$  which is shown in Figure (7) [8].

#### 1.4.2. Polarizations at a single Fuel Cell

Despite the fact that approximately 1,23 V is obtained in theory, due to irreversible losses which are named as over-potentials, smaller cell voltages are observed for a typical single cell which is demonstrated in Figure (8).

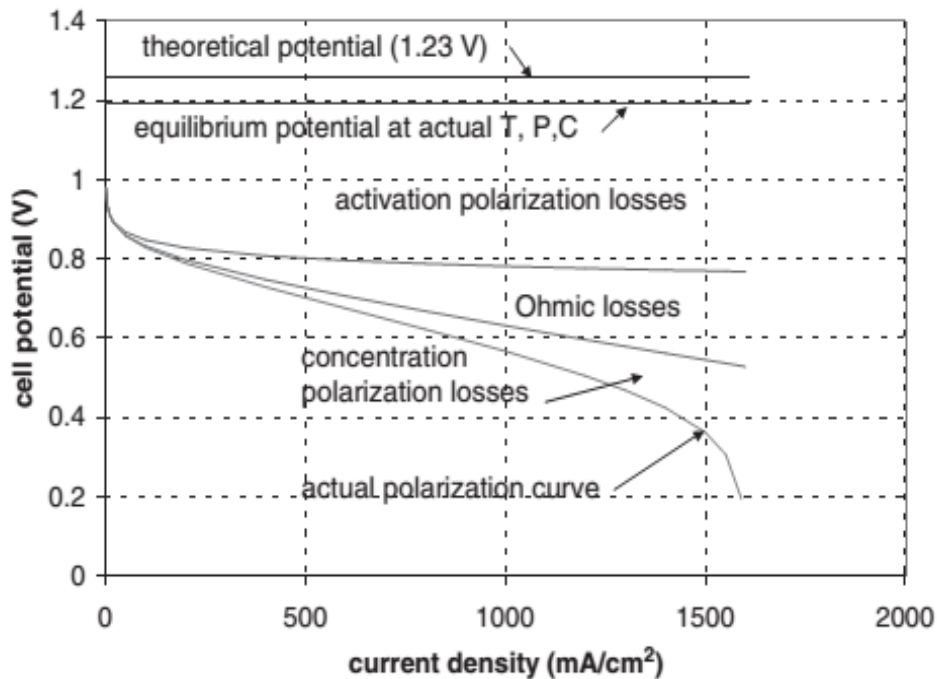


**Figure 8.** Polarization curves for a PEMFC [7]

Main types of losses are described in the following sections.

#### **1.4.2.1. Electrode Polarizations**

The losses early on named as polarization in galvanic units which contains current is determined with definitions of reaction kinetics, physical structure of cell, and type of electrolyte. These cases are affected by the structure of electrode and ion mobility and mass transfer in a porous media. Instead of using the polarization term, the usage of over-potential is preferred for the processes such as loading in electrochemical system, electrolysis, and coating.

Practically, over-potential is the difference voltage between open circuit voltage and limiting voltage. The over-potential is lower at discharging loading and limiting voltage is higher than open circuit voltage. Over potential can be described as measurement of currents that is occurred due to current in any direction as well [7].

#### **1.4.2.2. Voltage Losses**

The voltage in a single PEMFC is obtained under constant operating temperature, applied load, and fuel/oxidant flow rates. In a PEMFC, the main criterion for the performance can be obtained from a polarization curve which describes current density (Current / Area) against cell potential (Voltage) behavior [7].

Once current is discharged, acquired electrical energy and cell voltage is reduced due to various types of irreversible losses. The cell voltage is determined by subtracting irreversible potentials ( $V_{irreversible}$ ) from the reversible potential ( $V_{reversible}$ ).

The real open circuit voltage of PEMFC is less than theoretical value because of species transportation from one electrode to another electrode, internal currents.

The losses can be divided into three major categories that are activation, resistance, and concentration polarizations. The fuel cell voltage can be defines as the following;

$$V(i) = V_{reversible} - V_{activation,anode} - V_{activation,cathode} - V_{resistance} - V_{concentration,anode} - V_{concentration,cathode} \quad (17)$$

Equation (17) shows that activation and concentration are defined for both anode and cathode sides; whereas resistance stands for ohmic losses in the cell [7].

#### 1.4.2.2.1. Activation Polarization

An activation barrier is available for the molecules which react chemically or electrochemically. For the calculation of activation polarization, Tafel equation is used [7].

Usually empirical approaches are used to express Tafel equation. Over potential on the surface of electrode was observed to follow a likely path in lots of chemical reaction.

$$A = \frac{RT}{2aF} \quad (18)$$

In Equation (18),  $a$  is defined as charge transfer coefficient which is the ratio of applied electrical energy to obtained electrical energy due to change in rate of electrochemical reaction and  $A$  is defined as Tafel slope and its unit is voltage. The charge transfer coefficient depends on reaction and material of electrode. The value of the charge transfer coefficient changes from 0 to 1.0. It is nearly 0.5 at anode site, whereas at cathode site it is between 0.1 and 0.5. To be able to evaluate different over-potentials, the equation is mentioned above can be used.

$$i = i_o \cdot \exp\left(\frac{2aF\Delta V_{act}}{RT}\right) \quad (19)$$

The exchange current density ( $i_o$ ) is expected to be as much as possibly high which has crucial role for the performance of a cell. As the exchange current density increases, the surface of the electrode becomes much more active. Equation (19) is known as Butler-Volmer Equation which is mostly equivalent to Tafel equation.

#### 1.4.2.2.2. Resistance Polarization

Resistance polarizations occur due to crossing electrons and ions from electrodes and electrolyte, respectively. As the conductivity of ions is increased, the resistance polarization is decreased.

Since electrodes and electrolyte obey the Ohm law, the resistance polarization can be defined as the following;

$$\Delta V_{ohm} = iRi \quad (20)$$

$$Ri = Ri,i + Ri,e + Ri,c \quad (21)$$

In Equation (20),  $i$  is current density, and  $Ri$  is the total cell internal resistance that covers ionic, electronic, and contact resistance which have unit as  $U \text{ cm}^2$  which is indicated in Equation (21).

#### 1.4.2.2.3. Concentration Polarization

A reason for the concentration polarization taking place is consuming of the reactants which is a result of electrochemical reactions on the surface of electrode. In addition, the reactants cannot be delivered fast enough to the active area which causes concentration polarization as well. It can be expressed as the following equation which is known as Nernst Equation;

$$\sigma_{conc} = \frac{RT}{nF} \ln \left( 1 - \frac{i}{i_L} \right) \quad (22)$$

In Equation (22),  $C_B$  is bulk concentration of reactant,  $\text{mol} \cdot \text{cm}^3$   
 $C_S$  is concentration of reactant at the surface of the catalyst,  $\text{mol} \cdot \text{cm}^3$

The other considerations are;

- Low gas diffusivity in porous electrode structure
- Low mass transfer rate between solution and electrode surface
- Low diffusion rate between products and membrane

### 1.4.3. Efficiency of a PEMFC

The efficiency of the cell can be expressed as the ratio of electrical energy production for each mole fuel to  $\Delta H_f$ . Two types of enthalpies are available (LHV and HHV).

The water as the result of combustion reaction is in the vapor form in this case ( $\Delta H_f = -241,83 \text{ kJ/mole}$ ). Meanwhile, for the HHV, the water is in liquid form ( $\Delta H_f = -285,84 \text{ kJ/mole}$ ) [7].

The maximum acquirable electrical energy (in Equation (23)) by calculating HHV equals to Gibbs free energy and represented as the following;

$$\text{The Maximum Acquirable Electrical Energy} = \frac{-\Delta G_f}{-\Delta H_f} \times 100 \quad (23)$$

Working voltage of a cell can be associated with the efficiency. If the whole energy coming from combustion of hydrogen could be turned into electrical energy, then the cell (100 % efficiency) voltage would have 1,25 and 1,48 V for LHV and HHV, respectively as calculated using the following equation.

$$E = -\frac{\Delta H_f}{2F} \quad (24)$$

Considering LHV and HHV ( $\Delta H_f$ ) values, cell potential (E) can be changed which is expressed in Equation (24).

## CHAPTER 2

### MEMBRANES USED FOR FUEL CELL

This chapter covers particular information about expedient membranes for fuel cell applications.

PEMFCs are overemphasized due to its working environment, applicability, high efficiency. The key component of a PEMFC is a polymer membrane that provides proton conductivity [14].

The proton is formed by the help of a region where the platinum and active side of sulfonic acid groups on membrane are contacted each other. The functionality of polymer electrolyte membrane is the transportation of proton from anode to cathode site by help of available water molecules in the membrane which is weakly bonded with proton. In other words, while active sites on the membrane are responsible snatching protons away from hydrogen, water in the membrane is functionalized to transport them to cathode site.

Apart from membranes which are used for separation processes, the polymer electrolyte membranes are not desired to permit ions to passing through from one side to another. In PEMFCs, the electrolytes are demanded to separate ions of fuels to be able to produce electricity efficiently.

Having ionic groups in polymer electrolyte membranes make them different from others. The cation and anion exchange membranes are categorized in terms of having negative and positive active sites respectively. In this sense, membranes are asked to allow opposite charges to pass; however similar ones not that is only probable with possessing high ion exchange capacity and low resistivity.

During 1970s, DuPont has started to produce Nafion<sup>®</sup> which is called as perfluorosulfonic acids-PFSAs copolymer, and since then commonly used for PEMFCs. Other than DuPont, Asahi and Dow Chemical Companies worked separately on perfluorosulfonic acid membranes which have shorter side chains and a higher ratio of SO<sub>3</sub>H to CF<sub>2</sub> groups [15]. Brief information about cation-exchange membranes is given at Table (2).

**Table 2.** Comparison of properties between commercial membranes [2]

Membrane	Membrane Type	IEC (mequiv/g)	Thickness (mm)	Gel water (%)	Conductivity (S/cm) at 30°C and 100 % RH
Asahi Chemical Industry					
Company Ltd., Chiyoda-ku, Tokyo, Japan					
K101	Sulfonated Polyarylene	1.4	0.24	24	0.0114
Asahi Glass Company Ltd., Chiyoda-ku, Tokyo, Japan					
CMV	Sulfonated Polyarylene	2.4	0.15	25	0.0051
DMV	Sulfonated Polyarylene	-	0.15	-	0.0071
Flemion	Perfluorinated	-	0.15	-	-

Ionac Chemical Company, Sybron Corporation, USA					
MC 3470	-	1.5	0.6	35	0.0075
MC 3142	-	1.1	0.8	-	0.0114
Ionics Inc., Watertown, MA 02172, USA					
61AZL386	-	2.3	0.5	46	0.0081
61AZL389	-	2.6	1.2	48	-
61CZL386	-	2.7	0.6	40	0.0067
Du Pont Company, Wilmington, De 19898, USA					
N117	Perfluorinated	0.9	0.2	16	0.0133
N901	Perfluorinated	1.1	0.4	5	0.01053
Pall RAI Inc., Hauppauge, NY 11788, USA					
R-1010	Perfluorinated	1.2	0.1	20	0.0333

Nafion shows excellent chemical and physical properties such that its durability is between 10,000-100,000 hour [2]. However, there are some limitations such as low proton conductivity at high temperature and low humidity levels, high fuel crossover effects, and high cost that is why synthesis of alternative polymers becomes an attractive issue. Mainly, membranes used in fuel cells are categorized into three parts which are inorganic, organic and composites.

In this point, organic membranes provide some advantages such as easy to be processed and cheaper. However due to having weak thermal and mechanical stabilities, alternative ones were also developed. Comparing with other membranes, the inorganic membranes ensure long durability. They are stable under high mechanical pressures and chemical attacks from organic solvents. Porous size and distribution of inorganic membranes can be controlled easily. Nevertheless, inorganic membranes are not preferred because of brittle structure and high cost. On the other hand, composites possess both characteristic of organic and inorganic membranes and they can be functionalized to be able to make it work effectively with techniques such as sulfonation so that desired properties can be achieved in this manner.

## 2.1. Types of Polymer Membranes

In Figure (9), the solid polymer membranes are categorized into five parts which are named as perfluorinated, partially fluorinated, non-fluorinated, acid-base blends, and others which are given as follows;

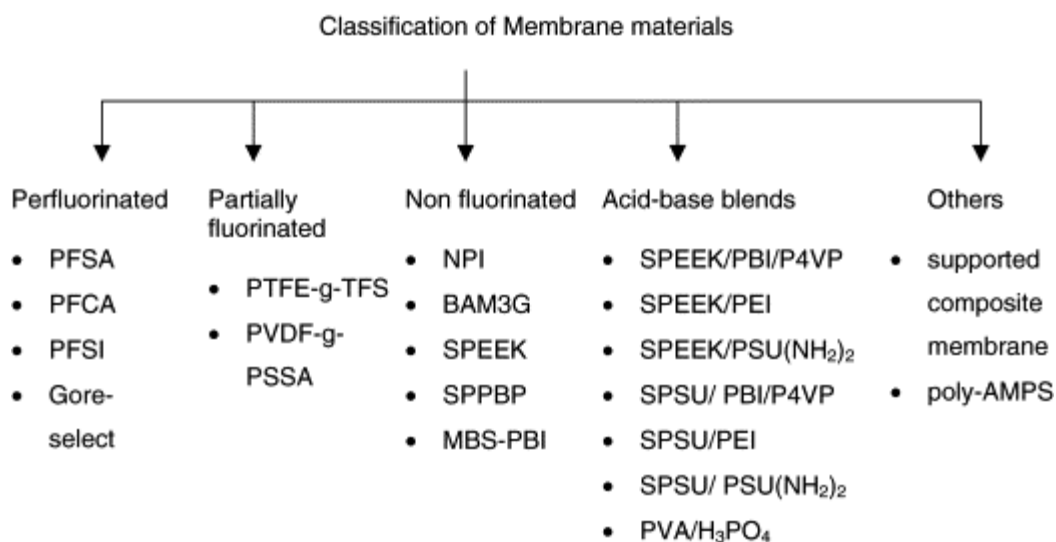


**Figure 9.** Types of solid polymer membranes used for fuel cells [2]

The perfluorinated ones have several properties which meet with the requirements as a suitable membrane [2].

### 2.1.1. Perfluorinated Membranes

The membranes possess a perfluorinated backbone and bonding with sulfonic acid groups. Perfluorinated membranes are mostly manufactured by DuPont and commercially available as Nafion<sup>®</sup>. In addition, identical membranes are also presented by Asahi Glass (Flemion<sup>®</sup>) and Asahi Chemical (Aciplex-S<sup>®</sup>) companies; however their products are less preferred due to Nafions' excellent proton conductivity, chemical stability, mechanical strength, and its durability about 60,000 h [16].

The proton conductivity of Nafion was 0.2 S/cm under humidified conditions. When a membrane with a thickness of 100 μm was used, the cell resistance was measured as 0.05 Ωcm<sup>2</sup> and the voltage loss and current density of this cell were obtained as 50 mV and 1 A/cm<sup>2</sup>, respectively.

### 2.1.2. Hydrocarbon Membranes

Comparing PFSA, hydrocarbon membranes have some advantages such as less cost, and commercial availability. Moreover, the structure is allowed to add polar sites that cause more water uptake capacity. The promising candidate which is expected to be interchanged with Nafion among 60 alternatives is given in Figure (10) [2];

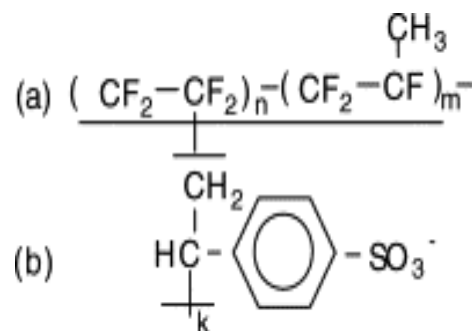


**Figure 10.** Structure of grafted membranes: (a) FEP main; (b) sulfonated polystyrene side chain [2]

### 2.1.3. Aromatic Membranes

There are two paths to be able to increase thermal stability at high temperatures. The first approach is introducing aromatic hydrocarbons to backbone of hydrocarbon polymers.

The second is making changes on backbone of polymers with bulky groups so that required proton conductivity is achieved. Since inflexible and bulky aromatic groups are available in polyarylenes, the glass transition temperature is above 200°C. In addition, polyesters are not preferred due to instability in acidic environment.

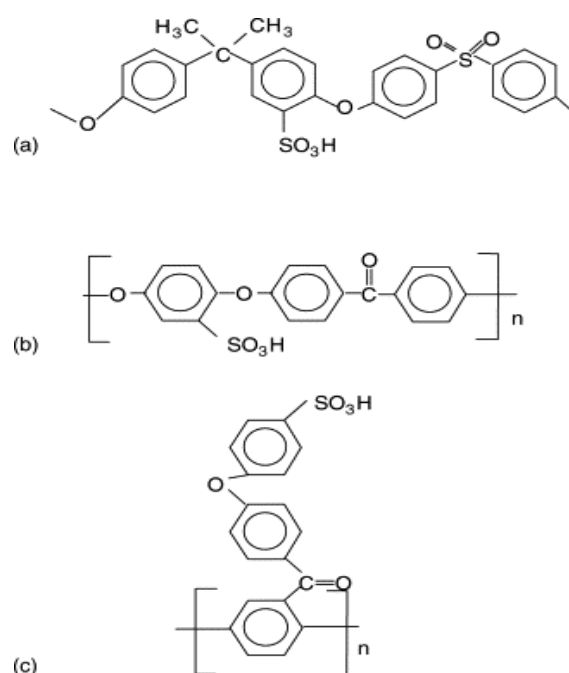


**Figure 11.** Chemical Structures of (a) SPSU, (b) SPEEK and (c) SPPBP [2]

However, polyaromatics are favored because they are thermally stable and seen as applicable for fuel cells. Being concerned about diminishing water swelling degree and fuel permeability (methanol-CH<sub>3</sub>OH), polyphosphazenes are offered in Figure (11) as potential candidate where their conductivity is near to 10<sup>-5</sup> S/cm at 120°C [2].

#### 2.1.4. Acid–Base Complexes

Having high proton conductivity renders acid-base complexes as a proper candidate even at high rate of water loss and elevated temperatures. Alkaline polymers are introduced with acid constituents in order to obtain good proton conductivity.

In Figure (12), to illustrate phosphoric acids are incorporated with poly (2, 2<sup>1</sup>-(m-phenylene)-5, 5<sup>1</sup>-bibenzimidazole) (PBI). Considering Nafion, the PBI has surpassing property. Its proton conductivity is not dependent on humidity level but doping level and temperature is. As an illustration, PBI doped with H<sub>3</sub>PO<sub>4</sub> membrane at 190°C and atmospheric pressure has outstanding performance generating power density around 0.55 W/cm<sup>2</sup> and around 1.2 A/cm<sup>2</sup> current density and poison allowance degree is diminished [2]. Additional superiority, electro osmotic drag coefficient (EODC) of PBI is zero which is directly linked with doping degree; whereas EODC of Nafion is 3.2. Grotthuss mechanism is offered to be responsible for proton conductivity in PBI where, as the doping increases, range through the clusters of acid regions is reduced in such a way that the anion segments provide the proton hopping among imidazole sites [17].

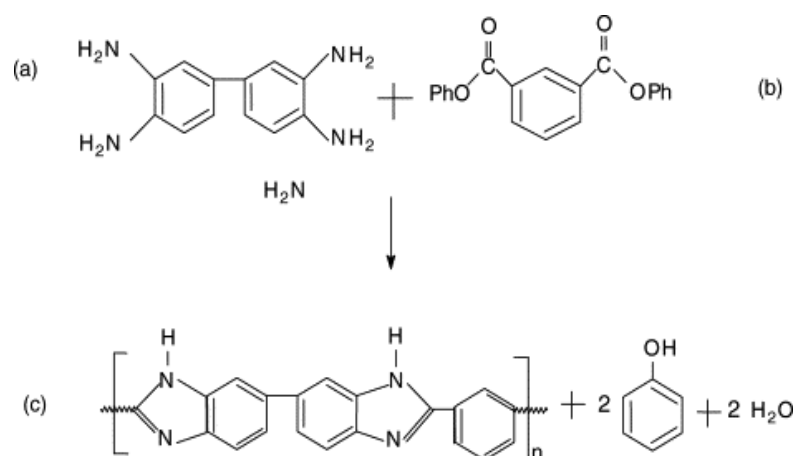


**Figure 12.** Chemical structure of (a) tetraaminobiphenyl, (b) diphenylisophthalate and (c) poly [2,21-(m-phenylene)-5,51 bibenzimidazole] [2]

As 500% doped PBI maximum outputs are attained where steady state conditions are available after 200 h operation especially minimum humidity degree at which the membrane can be accepted as the alternative one regarding Nafion.

**Table 3.** The comparison between acid–base blends [2]

<b>Types of Acid-Base Blend Membrane</b>	<b>Blend Ratio</b>	<b>Physical Properties</b>	<b>Observations</b>
SPEEK/PBI	90/10	High temperature tolerance at 350°C; thermally stable; good miscibility	Comparable performance to Nafion 112 at short-term tests (300h)
PVA/H <sub>3</sub> PO <sub>4</sub>	Highly doped	Good mechanical strength  Thermally stable up to 70°C	As acid concentration reducing ‘Grotthuss transport mechanism’ decreases  Works at low temperatures
PBI/H <sub>2</sub> SO <sub>4</sub>	500 % doping	Good mechanical strength; thermally stable	Potential candidate at moderate temperatures

The conductivity is developed if PBI is acidified with sulfuric, hydrochloric and phosphoric acid. Near term, PBI is expected to replace with Nafion because of lower methanol permeability at moderate temperature, especially for direct methanol fuel cells (DMFCs).

However, durability of PBI is still an issue to be testified. Apart from that acid and base blends are given in the Table (3) where good mechanical and thermal stabilities are obtained [2].

**Table 4.** Overall comparison between solid membranes [2]

<b>Types of Solid Polymer Membranes</b>	<b>Structure</b>	<b>Physical Properties</b>
Perfluorinated Membranes	<ul style="list-style-type: none"> <li>▪ Fluorinated backbone like PTFE</li> <li>▪ Fluorocarbon side chain</li> <li>▪ Ionic Clusters consisting of sulfonic acid ions attached to the side chains</li> </ul>	<ul style="list-style-type: none"> <li>▪ Membranes are strong and stable in both oxidative and reductive environments</li> </ul>
Partially Fluorinated Membranes	<ul style="list-style-type: none"> <li>▪ Fluorocarbon base</li> <li>▪ Hydrocarbon or aromatic side chain grafted onto the backbone, which can be modified</li> </ul>	<ul style="list-style-type: none"> <li>▪ Membranes possess good mechanical strength</li> <li>▪ Poor chemical and thermal stability</li> </ul>
Non Fluorinated Membranes	<ul style="list-style-type: none"> <li>▪ Aromatic base, typically modified with polar/sulfonic acid groups</li> </ul>	<ul style="list-style-type: none"> <li>▪ Good mechanical strength</li> <li>▪ Chemically and thermally stable even at high temperatures</li> </ul>
Acid-Base Blend Membranes	<ul style="list-style-type: none"> <li>▪ Incorporation of acid component into an alkaline polymer base</li> </ul>	<ul style="list-style-type: none"> <li>▪ Stable in oxidizing, reducing and acidic environments</li> <li>▪ High thermal stability</li> </ul>

In Table (4), physical properties and structures of the solid polymer membranes are given. Although the non-fluorinated membranes have better chemically and thermally stability, partially fluorinated membranes are very stable in oxidative and reductive environments.

### 2.1.5. Supported Composite Membranes

Table (5) demonstrates the type of compounds that could be incorporated with Nafion polymer and interpretations are also available.

**Table 5.** Type of compounds and composite membranes [18]-[21]

Type of Compounds	Interpretations
Zirconium phosphate-ZrP	In wide temperature range, fair proton conductivity as to Nafion
Sulfonated ZrP	Remarkable increment in conductivity compared to ZrP
Milled ZrP	Slight increment in proton conductivity compared to ZrP
Pillared ZrP	Great increment in conductivity compared to ZrP (doubtable stability)
Sulfonated TiP	Higher conductivities than comparable zirconium materials
Cesium Phosphate	Good conductivity above 140°C (needs further improvement)
Cesium Sulfate	Good conductivity above 140°C (doubtable stability)
Sol-gel P <sub>2</sub> O <sub>5</sub> -TiO <sub>2</sub> -SiO <sub>2</sub>	Conductivity of ca 10 <sup>-3</sup> S cm <sup>-1</sup> (low stability)
ZrO <sub>2</sub>	Less improved conductivity compared to ZrP
Sulfonated ZrO <sub>2</sub>	Conductivity of ca 0.05 S cm <sup>-1</sup> from 60 to 100°C at saturated conditions
Fullerenes	Fair results for dry conductivity till to 200°C
Fumed Silica/ZrP	Hydration dependent conductivities ca 1 order of magnitude below Nafion
<b>Composite Membranes</b>	
Nafion/ZrP	Having similar proton conductivity as Nafion, highly developed MEA and fuel crossover
Nafion/SiO <sub>2</sub>	Having similar proton conductivity as Nafion, highly developed fuel crossover
Nafion/HPA	Good developments on proton conductivity than Nafion
Nafion/Mordenite	Less developments on proton conductivity
Nafion/Imidazole	Better proton conductivity ( but poisoning Pt catalyst)
SPEEK/ZrP	No remarkable development considering SPEEK

SPEEK/ZrO <sub>2</sub>	Less than first order of magnitude reduction in methanol permeability and conductivity
SPEEK/ SiO <sub>2</sub>	Reduction in water permeability without an important decrease in conductivity
SPEEK/ZrP /ZrO <sub>2</sub>	Highly decreasing in methanol permeability without a large conductivity sacrifice
SPEEK/BPO <sub>4</sub>	Fair proton conductivity as to Nafion composites at 100–140°C

---

Based on Table (5), one could comprehend that '*Fullerenes*' could be a better candidate for types of compounds in case dry conditions are available. In addition, sulfonated/sulfated compounds are better than pristine compounds regarding conductivity. The composite membranes with SiO<sub>2</sub> fillers, they are almost same conductivity level with less water permeability and fuel crossover [18]–[21].

## 2.2. Required Specifications for Membrane

Membranes, which are the most important component of a PEMFC, should have the following properties in order to operate in a PEMFC system efficiently;

- High proton and zero electronic conductivity, low resistivity
- Good mechanical, chemical and electrochemical strength and stability
- Good moisture control in stack
- Extremely low fuel or oxygen permeability
- Low manufacturing cost

The significant parameters come into play from the point of membrane performance which is hydration level, membrane thickness, proton conductivity, chemical and mechanical stabilities.

### 2.2.1. Proton Conductivity

The proton conductivity has the most important effect on utilization of ion exchange membrane. The primary functionalities of proton conductivity are accounted as type and size of ions, and structure of membrane. The proton transferring through the membranes is handled by using hydrogen which is used as mobile ions in PEMFCs and water is used as carrier through the membrane. To that end, this is most suitable phenomenon to facilitate proton transferring.

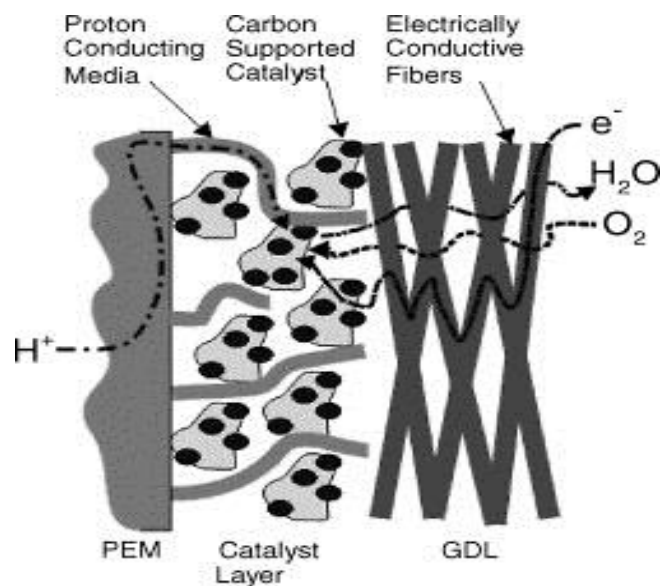


**Figure 13.** The view of proton, electron, oxygen and water transfer through MEA [10]

According to Figure (13), it is seen that by the help of carbon supported catalyst and electrically conductive fibers the proton and electron are combined together and water is drained out of the GDL.

### 2.2.1.1. Proton Transfer Mechanism

Fundamentally, two sort of proton transport mechanisms are available in Figure (14) which are called as ‘‘Grotthuss or proton hopping’’ and ‘‘vehicle’’ [22]. In case of Grotthuss, protons are transferred from one chain of water molecule to another in which  $\text{H}_3\text{O}^+$  are appeared and disappeared.

However, protons are relocated with the help of diffusion by way of the electrolyte that is known as vehicle mechanism. During this mechanism, water molecules are tied up with protons and generate  $\text{H}^+ [\text{H}_2\text{O}]_n$  and the process needs less driving force/power comparing Grotthuss.

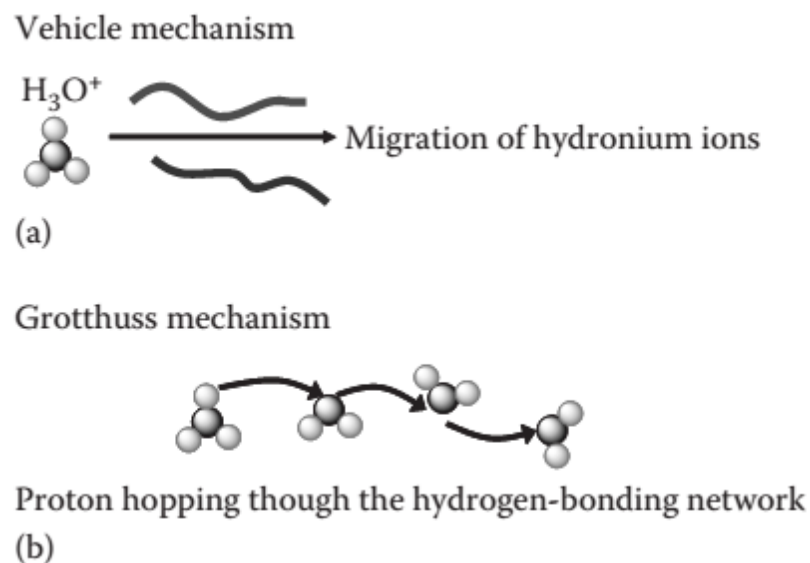


**Figure 14.** Demonstration of (a) vehicle mechanism and (b) Grotthuss mechanism [22]

Both mechanisms are available for Nafion. Vehicle mechanism is more dominantly supposed to happen in Nafion because of the fact that large diameter channels in the electrolyte lead to transfer hydrated protons easily at high temperature or lack of water. However, the Grotthuss mechanism is only valid in the opposite conditions of vehicle mechanism [23], [24].

### **2.2.2. Water Uptake (Hydration Level)**

Due to the fact that the hydration level is function of proton conductivity, as hydration level is increased, the PEMFC performance is enhanced. However, one should be aware of flooding at cathode site in case of high water content which is based on high electro-osmotic drag (EODC). In order to measure hydration level quantitatively, EODC is used to express the number of water molecules carried per protons which strongly depends on water level. However, it is independent of Nafion types [25]. The water in an electrolyte is diffused by the help of both electro-osmotic drag and concentration gradient at the anode and the cathode sites. It is known that the PEMFC performance decrease at which the regions in the membrane suffer from lack of water so that the resistivity of the membrane increases at these regions. The impact of dehydration level of the membrane is crucial on physical dimension, and electrolyte resistance which can be explained in terms of utilization of ion exchange membranes as electrolyte in fuel cells [26].

### **2.2.3. Thickness**

Decreasing membrane thickness has prominent influence on fuel cell performance to prevent water crossover issue and to lower resistivity so that performance is enhanced. Reducing the thickness is also in favor of cost and quick hydration but there is an optimum in terms of long life stability and fuel crossover. Optimally, the problem is overcome with enhancement of charge density or supervising acidic regions with help of thin film composite formation which can be facilitate by surface modification agent such as Pluronic L64 [2].

As the thickness is reduced, back diffusion of water is increased which allows enhancement of dehydration level at elevated temperatures that indeed induces to operate fuel cell at low humidity [2].

#### **2.2.4. Chemical and Mechanical Stability**

The limited information is available in the literature with regard to ion exchange membranes which are exposed to different chemical environments. The chemical stability of membrane plays a fundamental role since oxidation and reduction reactions happen on the surface of membrane which contacts with both anode and cathode electrodes.

The membranes loss its activity due to presence of carbon monoxide and carbon dioxide gases that are formed when different fuel gases are used instead of pure hydrogen. These gases make a fuel cell unusable.

On the other hand, the high concentration of active groups in a membrane, which provide proton conductivity, causes mechanical weakness that is why the membranes consisting of active groups should be strengthen [27]. The PEMFC membranes are asked to have some requirements. These requirements are, working stably at harsh chemical and electrochemical conditions, having sufficient mechanical strength at operational conditions, having low permeability to reactant gases, being cost effective and possessing high proton conductivity. Besides, certain drawbacks are still issue for development of novel membrane such as carbon monoxide poisoning on platinum (Pt) catalyst at low temperature, low thermal and water management, low chemical and mechanical endurances, and expensiveness. At elevated temperatures, the new tendencies are enhancing water retention capacity, and making proton conductivity independent from membrane humidity.

Up to 80°C, Nafion is mostly preferred due to its properties as mentioned above. For PEMFCs, an alternative membrane, which is able to operate under low humidity and high temperature conditions, has been investigated.



## CHAPTER 3

### MATERIALS AND METHODS

In Chapter 3, with further discussion on conditions of different synthesis, materials and methods for nano-composite membrane are expressed. In principle, within the scope of this study, '*solution recasting method*' is used in order to distribute powder nano-sized SiO<sub>2</sub> into Nafion polymer solution so that nano-composite membrane can be synthesized for PEMFCs. The prepared membranes are then characterized to measure their properties such as proton conductivity, thermal and mechanical stability, and water uptake capacity. Furthermore, the performances of nano-composite membranes which have 5 cm<sup>2</sup> active area are finally determined using a single PEMFC test station.

#### **3.1.Preparation of Composite Membranes**

The composite membranes containing inorganic additives are prepared in glass petri dishes by solution casting technique which uses Dimethyl formaldehyde (DMF) and/or Dimethyl acetamide (DMAc) solvents. Ultrasonic mixers are used to disperse the added silica particles in the polymer solution. The proportion of polymer (mg)/solvent (ml) is generally specified as 1/10. Ultra-sonication bath is accomplished for 1-3 hrs. and ultra-sonic probe at 20 Hz power for about 2 minutes; thereby at a particular amount of inorganic and dispersing (PEG and Pluronic L64) materials are added into the polymer solution [28].

Then the mixture is poured into glass petri dishes and solvent is gradually evaporated in a furnace 60 °C and 80°C for approximately 24 hrs.

With this slow evaporation process, crack formation in the membranes can be prevented. Nafion, SiO<sub>2</sub> powder (20 nm), solvent (DMAc) and copolymers were mixed with different concentrations summarized in Table (6).

**Table 6.** The weight % of different content of SiO<sub>2</sub> and dispersing agents (PEG and Pluronic L64) in Nafion membranes

<b>Wt.% SiO<sub>2</sub></b>	<b>SiO<sub>2</sub> [g]</b>	<b>PEG [g]</b>	<b>Pluronic L64 [g]</b>	<b>Nafion [ml]</b>
-	-	-	-	3.93
2.5	0.0125	0.000375	0.000375	3.25
5.0	0.0250	0.000750	0.000750	3.17
7.5	0.0375	0.001125	0.001125	3.08
10.0	0.0500	0.001500	0.001500	3

With the help of two different techniques (ultrasonic probe and bath), nano-composite membranes were prepared. The preparation of the films using the ultrasonic-probe technique lasts around 2 minutes.

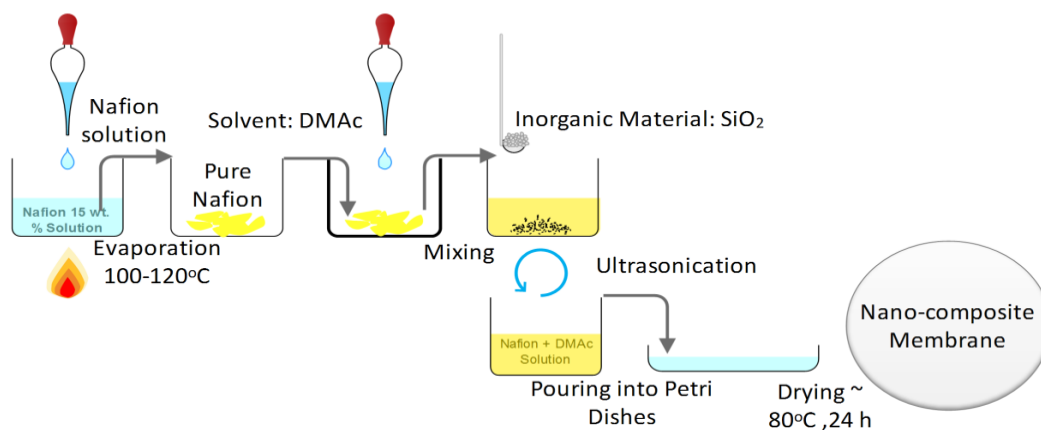


**Figure 15.** Nano-composite membrane preparation scheme

For both mixing processes, the content of SiO<sub>2</sub> particles was changed between 2.5 and 10 wt. %; therefore for each set, four membranes containing 2.5, 5.0, 7.5 and 10 wt. % of SiO<sub>2</sub> were prepared as shown in Figure (15).

Moreover, different dispersant were put into the solution with SiO<sub>2</sub> particles that are PEG [29] and Pluronic -L64 [30].

The content of the dispersing agents were fixed at 3 wt. % of added SiO<sub>2</sub> to be able to well distribute the SiO<sub>2</sub> particles without agglomeration in the polymer solution. The molecular structures of both dispersing agents are shown in Figure (16) and Figure (17).

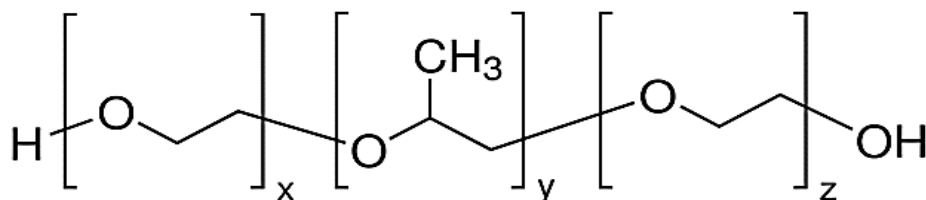


**Figure 16.** The molecule structure of Pluronic L64® (Mn: 2900 g/mole) [30]

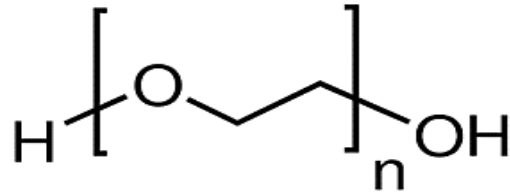


**Figure 17.** The molecule structure of PEG (Mn: 2000 g/mole) [29]

**Table 7.** Nomenclature of composite membranes

Samples	Co-polymers	Techniques	SiO <sub>2</sub> wt. %			
M1	Pluronic L64	Ultrasonic Probe	2.5	5	7.5	10
M2	PEG	Ultrasonic Probe	2.5	5	7.5	10
M3	-	Ultrasonic Probe	2.5	5	7.5	10
M4	-	Ultrasonic Bath	2.5	5	7.5	10
Recasting Nafion <sup>®</sup>	-	Ultrasonic Bath	-	-	-	-

To be able to clarify the different characteristics of membranes, each of them are named as M1, M2, M3, M4 and recasting Nafion which is shown in Table (7). So, one may keep the differences between the different composite membranes easily.

### 3.2. Preparation of Membrane Electrode Assemblies (MEAs)

In order to test the composite membranes in a PEMFC, both surfaces of the membranes should be coated with electrode layers; therefore MEAs need to be prepared. In this study, for the purpose of examining effect of inorganic material on catalyst layer, SiO<sub>2</sub> is also added to the anode electrode. The process flow diagram shows each process step of preparation of MEAs.

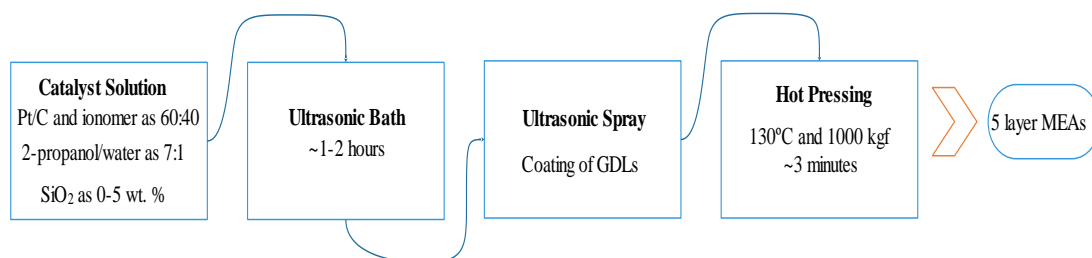


**Figure 18.** Process steps for production of 5 layer MEAs

In Figure (18), preparation stages of MEAs are composed of preparation of catalyst solution, implementation of catalyst solution onto gas diffusion layer; cleaning membrane and coating catalyst solution onto gas diffusion layer which is cut ( $5 \text{ cm}^2$ ) in desired active area so that electrode-membrane structure is formed. The catalyst solution is prepared in the percent of Pt/C (60 wt. % Pt on Carbon) and ionomer as 60:40, inorganic material ( $\text{SiO}_2$ ) as 3.0 wt. % which will be added to only anode catalyst layer [31]–[33], and in the ratio of 2-propanol/water as 7:1.

The solution is stirred in an ultrasonic bath about 1-2 hours to achieve a homogenous mixture. The catalyst solution is loaded till to have  $0.4 \text{ mg of Pt/cm}^2$  onto GDL. The loading process is very critical to be able to obtain an even distribution of ink onto GDL.

Therefore, ultra-sonication is used to have an even distribution of catalyst ink which is loaded then by coating process onto GDL. The coating process is done by a special machine which have effective nozzles.

As seen in Figure (19), ultrasonic spray (ExactaCoat system) is used for the coating of gas diffusion layers with the catalyst solution till achieving desired Pt and ionomer loading.



**Figure 19.** ExactaCoat system (by SonoTek) [34]

Once the requested loading ( $0.4 \text{ mg of Pt / cm}^2$ ) is achieved, the gas diffusion layers are hot pressed on the membrane from both sides which is carried at  $130^\circ\text{C}$  and 1000 kilogram force (kgf) for 3 minutes. In this fashion, five layer MEAs with an active surface area of  $5 \text{ cm}^2$  are obtained. The MEA types are tabulated in Table (8).

**Table 8.** Nomenclature of MEAs - 3 wt. %  $\text{SiO}_2$  incorporated with anode catalyst layer

Samples	Organic Additive	Techniques	$\text{SiO}_2$ wt. %
MEA1	Pluronic L64	Ultrasonic Probe	2.5
MEA2	PEG	Ultrasonic Probe	2.5
MEA3	-	Ultrasonic Probe	2.5
MEA4	-	Ultrasonic Bath	2.5
MEA0 (Recasting -Nafion <sup>®</sup> )	-	Ultrasonic Bath	-

### 3.3. Objective of Study

The self-humidifying PEMFCs attracts considerable attention since the cell is more stable in terms of reacting gases. Moreover, total cost is expected to reduce because external humidifier is unnecessary. In this sense, such inorganic filler materials are used in MEAs extensively to capable of certain level of water retention. Furthermore, the studies on the membranes which endure at elevated temperatures have gained enormous attraction among scientists, recently. Additionally, hydration level plays significant role in the membrane. In other words, the certain amount of water should be available in the electrolyte to be able to transport protons within the electrolyte.

However, at elevated temperatures, nearly at 80°C, the PEMFC loses its water that is already existed in the polymeric membrane. Thus, mechanical strength becomes weaker and fuel crossover increases in terms of hydrogen and oxygen gases thereby cell performance decreases dramatically due to high polarizations. Adding hygroscopic materials like SiO<sub>2</sub> into the polymer matrix at a certain concentration, the membrane gains more stability and durability even at low humidity and high temperature conditions because of water holding capacity of added SiO<sub>2</sub> [34]. Additionally, controlling water management in the composite membranes becomes easier compared to free SiO<sub>2</sub> polymer membrane. The water resulting from half reactions is entrapped in the composite membrane. In this fashion, the PEMFC can be operated at elevated temperatures without requiring any external humidification step.

More than that, the SiO<sub>2</sub> is also introduced to catalyst layer to prevent dehydration of MEAs. However, it is found that the size of the SiO<sub>2</sub> particles plays a crucial role so that as the size of the particles increases, electrical surface area and ohmic resistivity increases and performance of the cell decreases.

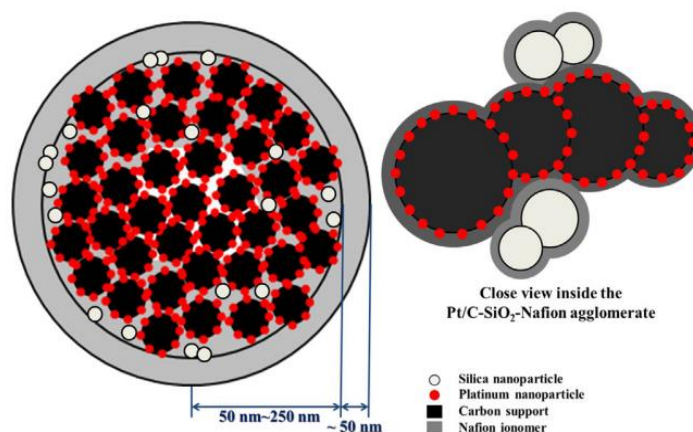


**Figure 20.** The view of agglomerate structure of Pt/C, SiO<sub>2</sub>, and Nafion [36]

It is also interesting that, adding hygroscopic agent into catalyst layer lead to ohmic resistance increment. So, it is found that, in long-time running of PEMFC, performance decreases because of using hydrophilic materials. Up to now, different hydrophilic materials were added into catalyst layer such as PVA, sulfated zirconia to preserve humidity in the MEAs. With this manner, it was aimed to have a long-time running period without any performance drop at PEMFC [35]. One of other study on self-humidifying MEA showed that better results were obtained in terms of water retention until 60°C. The cell performance increases by introducing PVA (3 wt. %) as polymer and SiO<sub>2</sub> (3 wt. %) as hydrophilic filler even at 15 % RH which is hypothetically shown in Figure (20) [36]. In this regard, SiO<sub>2</sub> particles are also added into anode electrode which act as a mini water reservoir. Recently and in the future, common applications of PEMFCs are seen as portable electronic devices which works as a power supply. However, available products of these utilization areas are small systems and have few components. In this study, with the help of improved MEAs, the usage of external humidification is expected to minimize so that proper systems for portable applications can be realized. It is also supposed to obtain data to enlighten future studies by analyzing commercial PEMFC operation conditions in terms of water management issue which is known as one of the most important obstacle to overcome.

## CHAPTER 4

### CHARACTERIZATION OF COMPOSITE MEMBRANES

Chapter 4 describes various characterization techniques which are used to determine structural and morphological of prepared materials. The most important parameters which are water uptake capacity and proton conductivity are tested gravimetrically and analyzed with Electro Impedance Spectroscopy-EIS technique, respectively. Thermal, mechanical, and morphological measurements are obtained by using thermogravimetric analysis (TGA), tensile testing, and scanning electron microscopy (SEM), respectively.

#### 4.1. Water Uptake Capacity – WU Testing

The water uptake or retention level is desired to be high for the membranes since humid membranes provide low resistance and high proton conductivity [37]. According to the method, the synthesized membranes are dried at 80°C to be able to get rid of moisture and then kept waiting in distilled water for 24 hours at 70°C. In this manner, the dried ( $w_{dry}$ ) and ( $w_{wet}$ ) membranes are weighted by using a sensitive weighing instrument and WU are calculated as in Equation (25).

$$\text{Water Uptake \%} = \frac{w_{wet} - w_{dry}}{w_{dry}} \times 100 \quad (25)$$

#### **4.2. Scanning Electron Microscopy – SEM Testing**

Under favor of beams of electrons which have high energy, an image of the substance is generated. The SEM image provides important information about morphology and composition of the sample. Due to the fact that the durability is an issue for PEMFCs, one may infer the degradation mechanism from cross-sectional surface of both composite membranes and MEAs [38]. Especially the difference between the SEM images of the performed and not performed MEAs can be examined easily. In this study, the SEM images were taken at 20.00 kV for both composite membranes and MEAs.

#### **4.3. Thermogravimetric Analysis**

In this analysis, the sample was subjected to a controlled temperature program. Therefore, as the weight is lost from the sample, the corresponding temperature can be read from the TGA plot. TGA was used for the composite membranes to determine contents of the various components such as moisture, organic, inorganic and solvent [37]. In this study, the composite membranes and pristine Nafion were heated from 30°C to 950°C at a heating rate of 20°C/min under nitrogen gas atmosphere.

#### **4.4. Tensile Mechanical Testing**

The tensile test was used to characterize mechanical strength of samples to obtain engineering stress and elongation at break. The tensile tests were carried out according to ASTM 638. The test can also be used to assess the aging performance so that mechanical durability of the substance can be estimated.

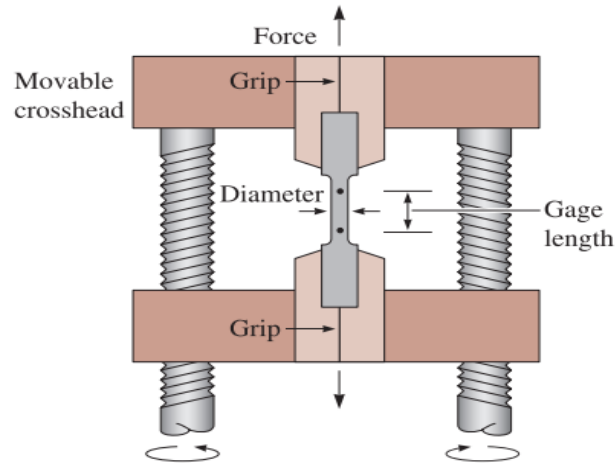


**Figure 21.** A representative apparatus for tensile test [41]

Dog-bone type samples were cut from the solvent casted films and they were tested using a universal test machine illustrated in Figure (21). Then, the load or force ( $F$ ) is applied. With the help of extensometer, the change in length of the specimen ( $\Delta l$ ) is measured considering original length ( $l_o$ ).

$$\text{Engineering Stress (MPa), } S = \frac{F}{A_o} \quad (26)$$

$$\text{Engineering Strain (\%), } e = \frac{\Delta l}{l_o} \quad (27)$$

where  $A_o$  is the original cross-sectional area of the specimen before the test begin.[39]

The engineering stress and strain are calculated by the Universal Mechanical Testing machine using Equations (26) and (27).

Typical stress-strain curves of Nafion which was recasted from recasting 15 wt. % of Nafion solution, is shown in Figure (22).

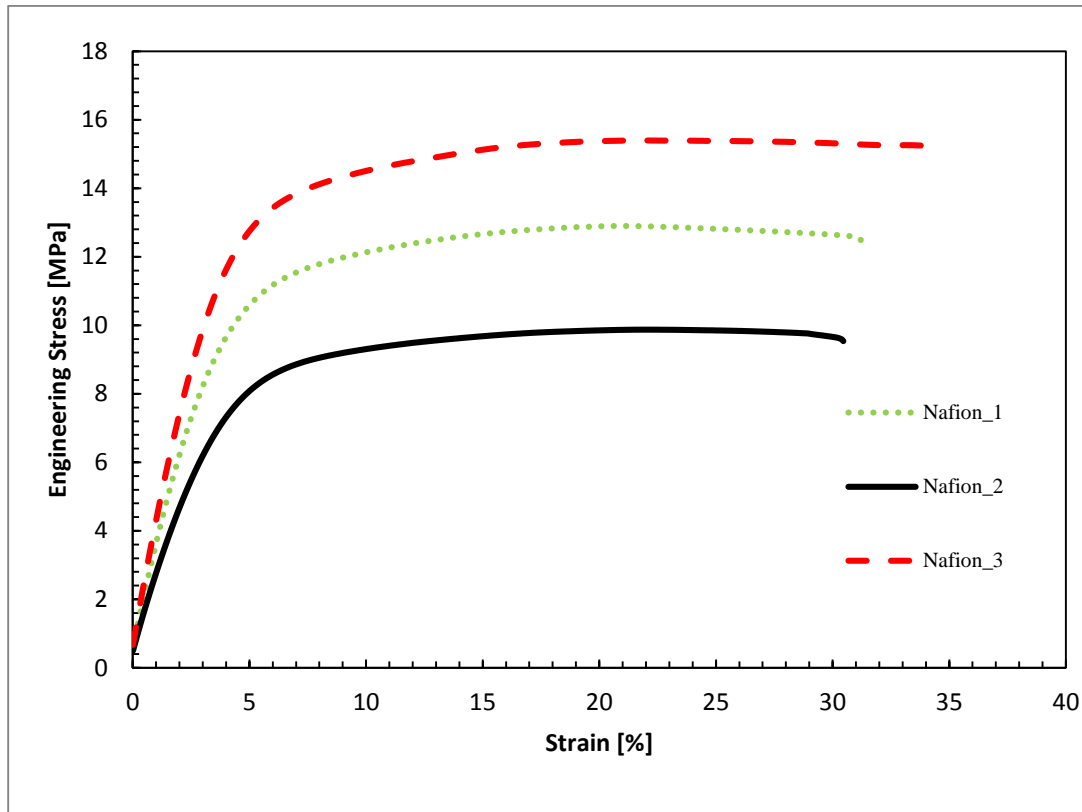


**Figure 22.** The mechanical tensile test of recasting Nafion

The three dog bone specimens of recasting Nafion (Nafion 1, Nafion 2, and Nafion 3) which were cut from different regions of the membrane, were repeated three times.

#### 4.5. Electro-Impedance Spectroscopy –EIS Testing

The EIS test is quite well known characterization technique to understand electrolyte and electrode interfaces and divided into two types which are called as ex-situ and in-situ. The in-situ measurement is used during operation condition in a fuel cell; whereas ex-situ is used to measure membrane, bi-polar plates and catalyst resistance outside of the cell. Therefore, in this study ex-situ measurement was used with the help of small AC amplitude signals. At the end of the measurement, Bode and Nyquist plots can be obtained. In this sense, the Nyquist plot gives the connection between real and imaginary impedances. However, the Bode plot provides correlation information between resistance and the phase angle regarding with frequency. In addition, two sort of control fashions are available in EIS measurement which are potentiostatic (voltage control) and galvanostatic (current control). Despite the fact that two fashions supply almost the same result, they are restricted in terms of potentiostat.

Due the fact that the membrane is heart of a PEMFC from the point of proton conductivity, it is important to measure it. The protons can be transferred into two directions which are crossing or through the membrane. Two types are theoretically deviates from each other in case the membrane is isotopic in direction of crossing and through the membrane [8].

##### 4.5.1. Calculation of Proton Conductivity

The ionic conductivity, distance between the reference electrodes, the resistance of the membrane, and the cross sectional area of the membrane are denoted as  $\sigma$  (S/cm), L (cm), R(k $\Omega$ ), and A (cm<sup>2</sup>) which is width multiply by thickness, respectively. The proton conductivity can be calculated as the following (Equation (28));

$$\sigma = \frac{L}{R \cdot A} \quad (28)$$

$\sigma$ : Proton conductivity [S $cm^{-1}$ ] L: Thickness of membrane [cm]

R: Membrane Resistivity [ $\Omega$ ] A: Area [cm<sup>2</sup>]

The most essential technical specification for a polymeric membrane is the proton conductivity which was performed by 4 probe technique (in Figure (23)). To be able to avoid interfacial impedance from conductivity measurements, the four-probe technique is more common to use. For that purpose, Wonatech - Electrochemical Workstation ZIVE SP2 instrument were used at which frequency interval was defined between 0.01 Hz and 300 kHz.

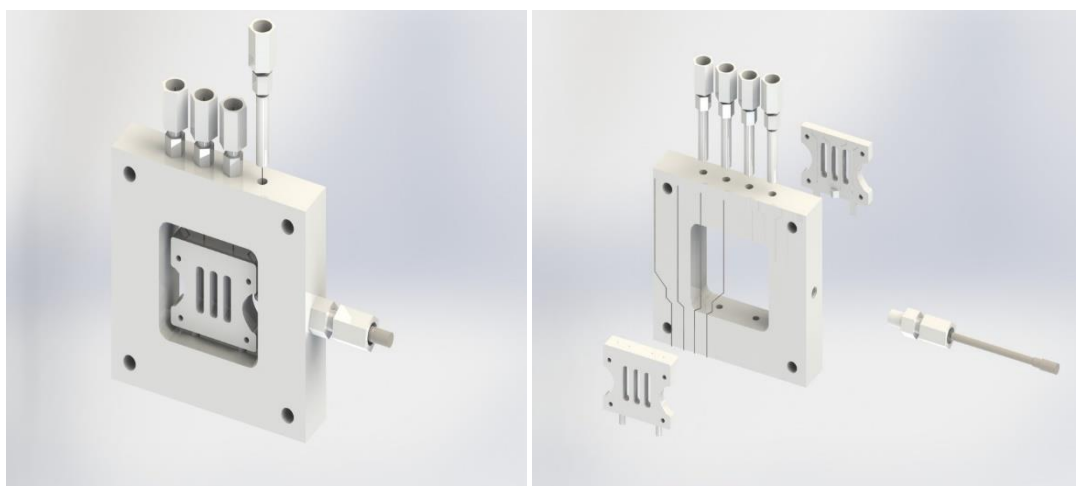


**Figure 23.** Typical structure of 3- dimension modeling of four-point probe technique (by Omer Demir, TEKSIS)

As can be seen from Figure (23), the distance between two reference electrodes is defined as  $L$ . The thickness of membrane is  $H$ , and the width is indicated as  $W$ . The membrane was cut as rectangle shape which have 5 cm length and 1 cm width. At the outer side, two electrodes (Working Electrode-WE and Counter Electrode-CE) are available to perform direct current where a potential gradient is originated through the membrane. Meanwhile, at inner side, reference electrodes-REs are responsible for quantifying potential difference of the membrane thereby detecting proton streams through the surface [8].

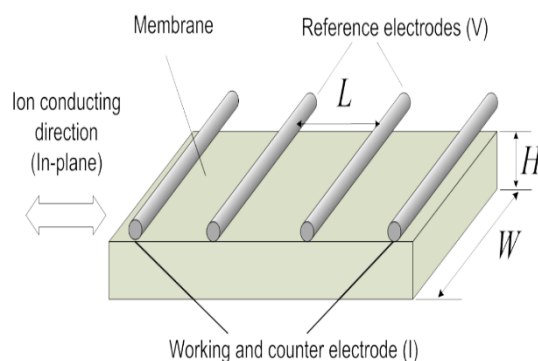


**Figure 24.** Schematic view of settlement of membrane onto Pt wires [8]

Moreover, a thermocouple is used to keep the temperature constant where a PID (proportional-integral-derivative) controller is incorporated within the system which is shown in Figure (25) [40].

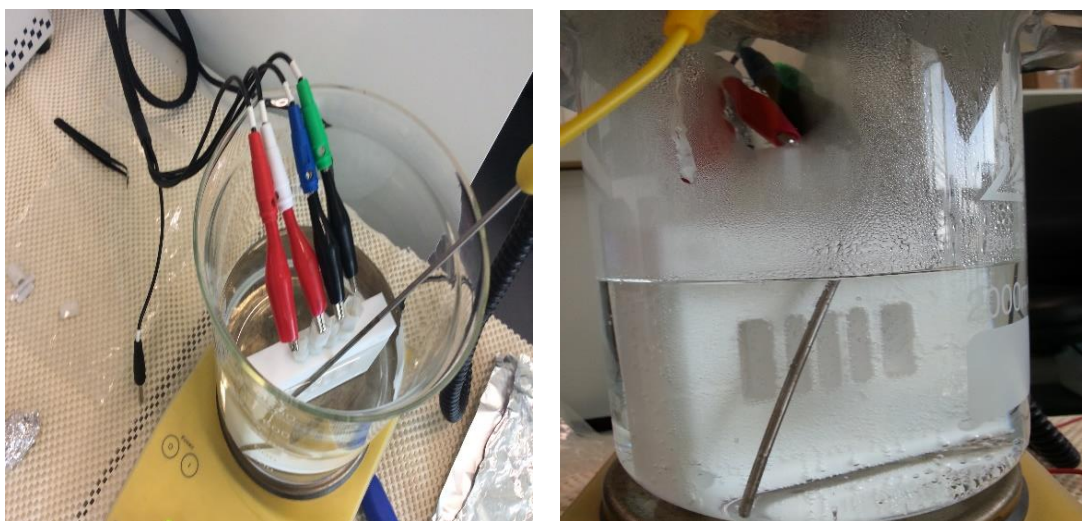


**Figure 25.** The experimental setup of Wonatech - Electrochemical Workstation ZIVE SP2 instrument

In this thesis, the thickness of membranes was measured using a micrometer from 5 different regions of the sample since the membrane swelled after immersion into DI water. Therefore, this procedure was followed in order to get accurate results because of dimensional instabilities.

#### 4.6. PEMFC Testing

The best way to attain the performance of the PEMFC is the performance tests which provides information about the current, voltage and hence power. In Figure (26), PEMFC testing is shown for the single cell which have 5 cm<sup>2</sup> active area. One may see how they correlate with each other. Therefore, three ways are available in order to measure the performance of PEMFC, which are called as current, voltage and power controls. Among these, power control is the uncommon way. In case of current control, the currents are controlled at specific values and corresponding voltages are read from the system. In terms of voltage control, the phenomenon happens the other way around.

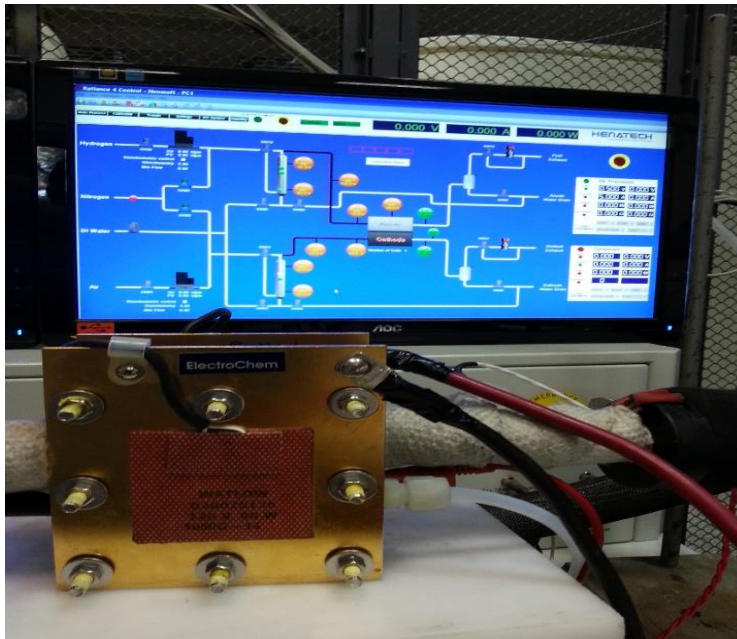


**Figure 26.** The view of single PEMFC (5 cm<sup>2</sup> active area) at METU Chemical Engineering Fuel Cell Laboratory

In this study, MEA0 Recasting Nafion, MEA1, MEA2, MEA3, MEA4 were performed at fully humidified (100 % RH) and totally dry (0 % RH) conditions at different temperatures which are 65, 70, 75 and 80°C. Therefore, two types of results are presented with regarding to under different relative humidity (RH) conditions which are 100 % RH and 0 % RH.

The test was performed with as the following reactant gases which have specific quality and flow rates;

- Hydrogen ( $H_2$ ); 0.10 slpm (standard liter per minute) and 2.00 at stoichiometry
  - % 99.995 Hydrogen /  $O_2 < 1$  vpm. / Humidity  $< 2$  vpm. /  $N_2 < 30$  vpm.
- Compressed Dry Air; 0.42 slpm and at 3.50 stoichiometry
  - % 20.9  $O_2$  / Humidity  $< 10$  vpm. / Bal.  $N_2$  (Balanced Nitrogen)

Moreover, nitrogen ( $N_2$ ) is also used for the inert gas to purge out the reactant gases as follows;

- Pure Nitrogen ( $N_2$ );
  - % 99.99  $N_2$  /  $O_2 < 50$  vpm. / Humidity  $< 30$  vpm.



## CHAPTER 5

### EXPERIMENTAL RESULTS AND DISCUSSIONS

In Chapter 5, the experimental results for novel nano-composite materials that can endure at low humidity levels and elevated temperatures are given. Optimization and determination of additive materials to polymer matrix are investigated and results are supported by characterization techniques. In this sense, the composite membranes with having SiO<sub>2</sub> contents ranging from 2.5 to 10 wt. % were prepared. Finally, they were performed at a PEMFC station. The composite membranes were compared with recasting Nafion. The morphology of prepared MEAs with help of their cross-sectional area was examined by SEM analyses to comprehend the distribution of SiO<sub>2</sub> particles in membrane and catalyst layers. From the point of ultrasonication, the main disadvantage of probe technique, solution in beaker was got hot immediately due to high frequency of power sources so that agglomeration risk for SiO<sub>2</sub> particles might be increased. To avoid heating effect of solution, an ice bath was used to stabilize temperature during ultrasonic probe mixing. However, it is realized that even with the ice bath, beaker was heated up. Moreover, one should take care of solution of composite membrane while pouring into the dishes before putting them into furnace. The furnace should be stable with respect to temperature which was adjusted around 80°C for 3 hours before operation. Otherwise, cracks were observed on the surface of membranes because of unstable temperature of the furnace. So then, it was almost impossible to skimming composite membranes from the surface of the dishes.

## 5.1. Water Uptake Capacity Results

The water uptake capacity has an important data in terms of water content in the polymer matrix, especially at elevated temperatures such as 80°C. The results were obtained for the membrane samples containing SiO<sub>2</sub> ranging from 2.5 wt. % to 10.0 wt. %.

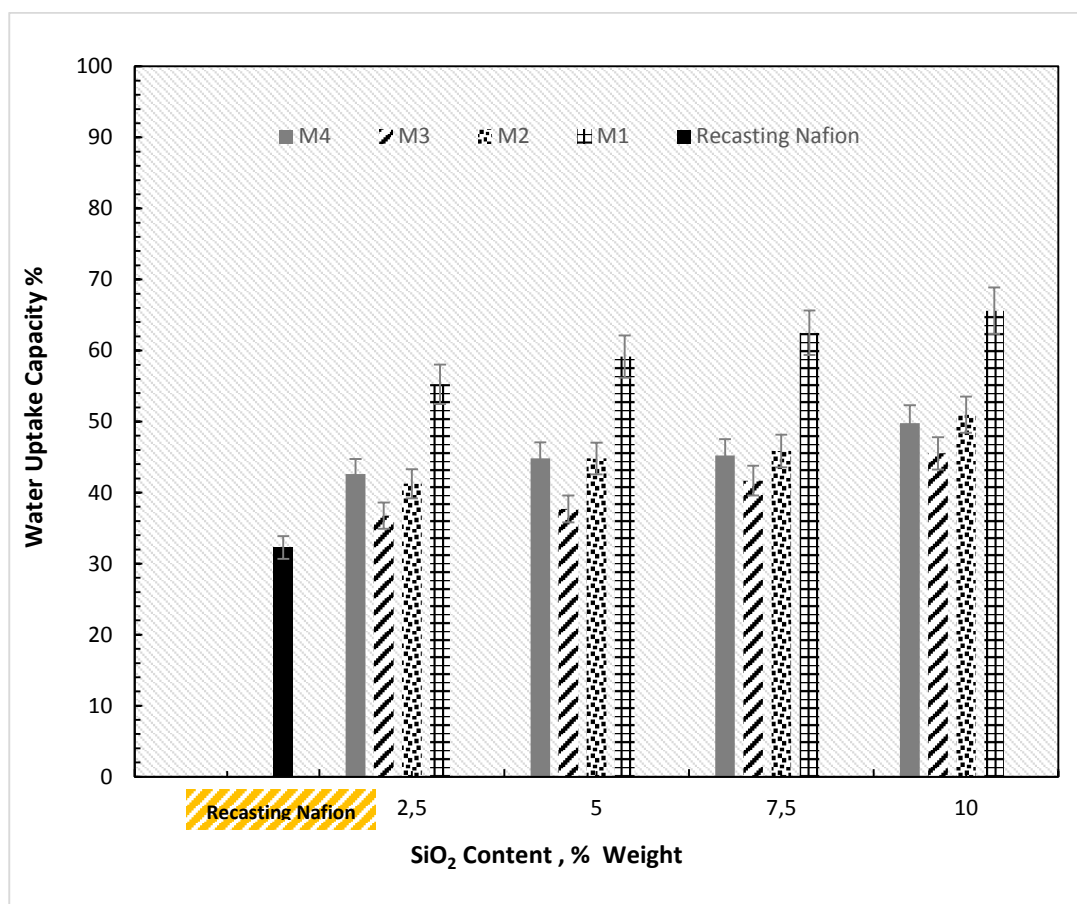


Figure 27. Water uptake capacity vs. SiO<sub>2</sub> content

- i. M1: Ranging from 2.5 wt. % to 10.0 wt. % SiO<sub>2</sub> with Pluronic-L64 (~2900 g/mole) were put in Nafion<sup>®</sup> with ultrasonic-probe technique.
- ii. M2: Ranging from 2.5 wt. % to 10.0 wt. % SiO<sub>2</sub> with PEG (~2000 g/mole) were put in Nafion<sup>®</sup> with ultrasonic-probe technique.
- iii. M3: Ranging from 2.5 wt. % to 10.0 wt. % SiO<sub>2</sub> were put in Nafion<sup>®</sup> with ultrasonic-probe technique.
- iv. M4: Ranging from 2.5 wt. % to 10.0 wt. % SiO<sub>2</sub> were put in Nafion<sup>®</sup> with ultrasonic-bath technique.
- v. Recasting Nafion: Recasting Nafion<sup>®</sup> were prepared with ultrasonic-probe technique.

The water uptake capacity plays a vital role in terms of self-humidifying property. It was shown that the composite membranes which contain copolymers such as PEG (2000 g/mole) and Pluronic L64 (2900 g/mole) (Poly (ethylene glycol)-block-poly (propylene glycol)-block-poly (ethylene glycol)) has more water retention capacity than the recasting Nafion. Figure (27) shows that the water uptake capacity of composite membranes (M1) containing Pluronic L64 was nearly two times higher than the Nafion membrane.

For the experiment, the 2.5 cm x 2.5 cm membranes were waited 24 hours at 100% relative humid conditions. The dry ( $W_{dry}$ ) and wet weights ( $W_{wet}$ ) were measured and the water uptake capacities were calculated using Equation (25). It has been observed that up to 10 wt. % of the SiO<sub>2</sub> the water uptake capacities showed growth trend.

The water uptake value is also one of the most significant key parameters due to the fact that to be able to maintain proton conductivity. In addition to this, as water uptake degree increases IEC increase as well. On the other hand, increasing of water uptake capacity brings along the swelling effect that is a problem for the PEMFC performance.

## 5.2. Tensile Mechanical Testing Results

The mechanical tensile tests were performed at METU Central Laboratory. The recasting Nafion was chosen as a reference sample. The thicknesses of the dog-bone shaped samples were measured by a micrometer. The stress and strain curves for the dog-bone shaped samples were obtained.

As the content of SiO<sub>2</sub> increases, the thickness of the membrane increases almost linearly. The average thicknesses were calculated by taking 5 measurements from different locations of the samples (M1, M2, M3, M4 and Recasting Nafion; from corners and the center of the sample), which are shown in Table (9).

**Table 9.** The thickness of the prepared samples

Samples	SiO <sub>2</sub> Content [wt. %]	Average Thickness [ $\mu\text{m}$ ]
M1	2.5	59.25
	5.0	81.70
	7.5	130.8
	10.0	225.5
M2	2.5	53.34
	5.0	78.74
	7.5	118.5
	10.0	212.9
M3	2.5	56.45
	5.0	101.9
	7.5	130.3
	10.0	223.4
M4	2.5	54.24
	5.0	100.8
	7.5	127.0
	10.0	218.4
Recasting Nafion	-	56.80

The prepared samples were dried at 60°C for 8 hours in the furnace and then conditioned for 24 hours at 45 % relative humidity and room temperature. The average mechanical properties (Ultimate Tensile Strength (UTS) and % elongation at break (EB)) of the samples were calculated only for M1, M4 and recasting Nafion since they were selected as possible candidates for self-humidifying PEMFC testing. The results were obtained as three measurements for each samples and summarized in Table (10).

**Table 10.** The mechanical properties of membranes

<b>Samples</b>	<b>SiO<sub>2</sub> Weight %</b>	<b>UTS [MPa]</b>	<b>Std. Dev. (UTS )</b>	<b>EB [%]</b>	<b>Std. Dev. (EB )</b>
<b>M1</b>	2.5	14,59	1.112	32.67	32.67
	5.0	4.51	0.090	49.79	49.79
	7.5	2.01	0.262	24.53	24.53
	10.0	0.86	0.007	14.93	14.93
<b>M4</b>	2.5	12.13	0.760	11.76	11.76
	5.0	5.89	2.152	9.29	9.29
	7.5	6.51	0,686	9.22	9.22
	10.0	4.40	0.792	5.28	5.28
<b>Recasting Nafion</b>	-	12.41	2.758	31.83	31.83

The stress – strain curves for all samples (M1, M2, M3, M4 and recasting Nafion) are given in Appendix C in detail.

### **5.2.1. Recasting Nafion**

The strain - stress plots of three samples of recasting Nafion samples demonstrated similar elongation at break values. However, the ultimate tensile strength (UTS) values of the samples were different from each other. The main reason of having tensile strengths which are deviates from each others could be taking specimens from different locations of recasting films which means that solution could be not distributed into the dishes homogenously.

Since it was quite hard to have a flat surface while casting the solution into the dishes, as a result, it was not possible to obtain the samples with homogeneous thickness.

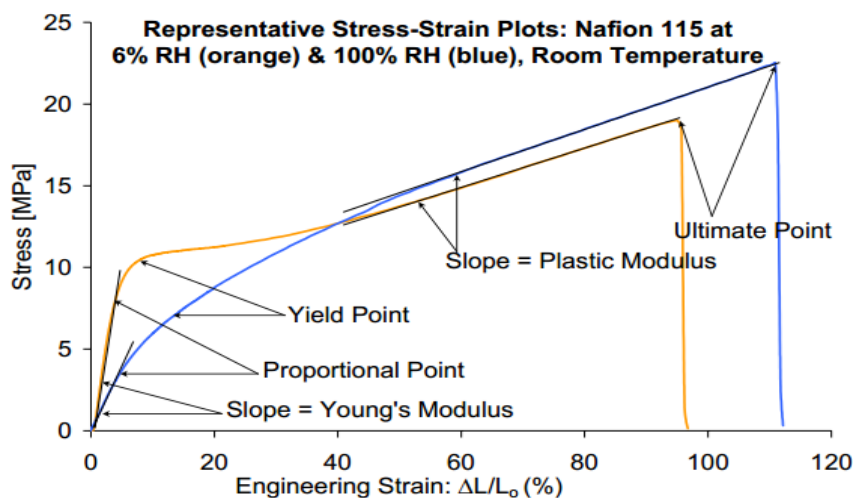


**Figure 28.** Sample analysis of stress-strain curves on Nafion 115 [44]

Figure (28) shows the tensile testing results for the Nafion conditioned at 6 % and 100 % RH. The Nafion samples conditioned at 6 % RH had higher young's modulus and yield point but less engineering strain compared to the ones conditioned at 100 % RH. These results for Nafion 115 can be used to compare the results for the membranes produced in this study.

### 5.2.2. M1: Pluronic L-64

The tensile test results for the membranes containing Pluronic (M1) is very similar to recasting Nafion suggesting that addition of 2.5 %  $\text{SiO}_2$  and Pluronic L64 do not influence the mechanical properties of the membranes M1. It is very important to keep the mechanical properties stable while enhancing water uptake capacity by adding  $\text{SiO}_2$  and Pluronic L64.

As the wt. % of SiO<sub>2</sub> increases in the polymer matrix, the tensile strength of the membranes became weaker. As can be seen from Table (10), the tensile strength of the M1 membranes decreases significantly from 14.6 MPa to 4.5 MPa when the SiO<sub>2</sub> content is increased from 2.5 wt. % to 5.0 wt. %.

The elongation at break values increases slightly for membranes when SiO<sub>2</sub> content increases from 2.5 wt. % to 5.0 wt. %.

When the SiO<sub>2</sub> content of the membranes is increased to 7.5 wt. %, the mechanical property of M1 reduces further. The membranes containing 5.0 wt. % of SiO<sub>2</sub> has lower the elongation at break values comparing with membranes containing 7.5 wt. % of SiO<sub>2</sub>.

When the SiO<sub>2</sub> content of the membranes is increased to 10.0 wt. %, the mechanical property of the membranes decreases further suggesting that the SiO<sub>2</sub> particles added to the membranes were not dispersed efficiently in the polymer matrix.

### **5.2.3. M4: Only SiO<sub>2</sub> (Ultrasonic Bath)**

There are no significant differences regarding tensile strength values of the samples containing 2.5wt. % of SiO<sub>2</sub> (M4). The elongation at break values of M1 containing 2.5 wt. % of SiO<sub>2</sub> couldn't exceed 14 %. This means that M4 (containing 2.5wt. % of SiO<sub>2</sub>) sample is more rigid comparing to M1 (containing 2.5 wt. % SiO<sub>2</sub>). In terms of tensile strength values, it is observed that there are no significant differences between M1 and M4 (containing 2.5 wt. % SiO<sub>2</sub>).

When SiO<sub>2</sub> content is increased from 2.5 wt. % to 5.0 wt. %, tensile strength of membranes decreases from 12.1 MPa (see Table 10) to 5.9 MPa. The tensile strength values of the membranes containing 5.0 wt. % of SiO<sub>2</sub> fluctuates between 4 and 8 MPa. The reason could be uneven distribution of SiO<sub>2</sub> particles into the polymer. In addition, as SiO<sub>2</sub> content increases, the elongation at break (strain) values of membranes decreases.

It is observed that the mechanical property dramatically decreases as the SiO<sub>2</sub> content is increased up to 7.5 wt. % and 10.0 wt. %.

Figure (29) shows the stress-strain curves for the membranes M1, M4, and recasting Nafion. When Pluronic L64 was added to the membrane (M1), the elongation at break values for these membranes were increased compared to recasting Nafion and the membranes only containing SiO<sub>2</sub> (M4).

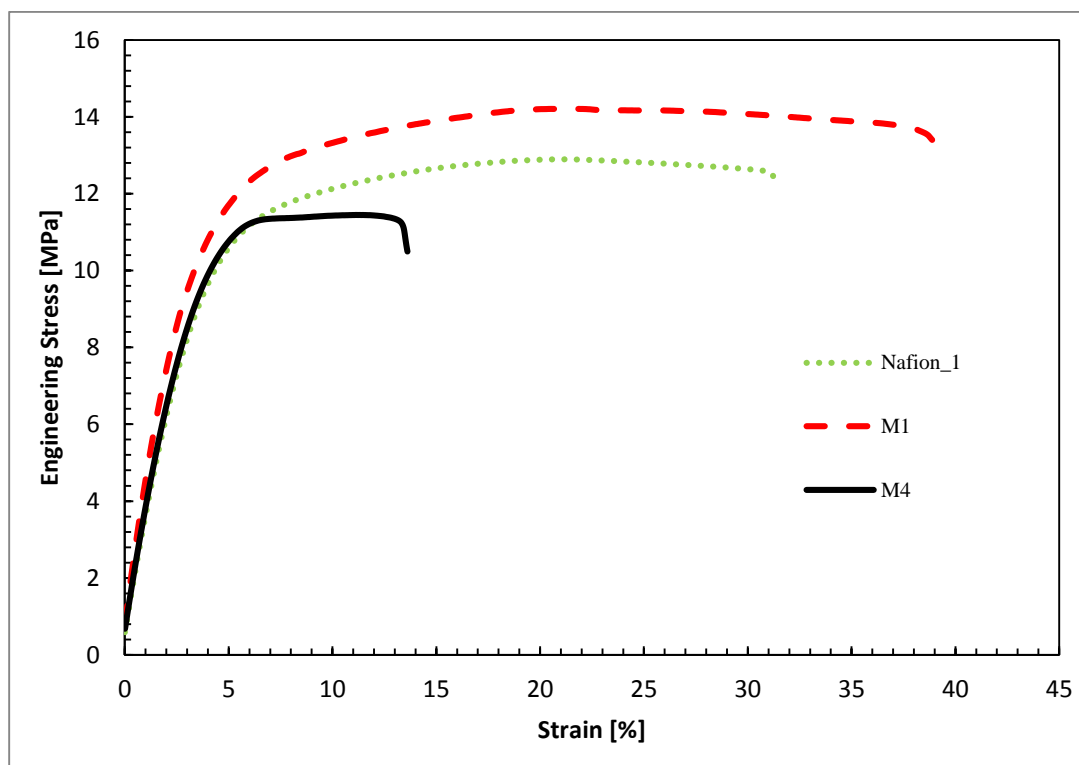


**Figure 29.** The mechanical tensile tests of 2.5 wt. % SiO<sub>2</sub> of M1, M4 and recasting Nafion

### 5.3. Thermo-Gravimetric Analyses-TGA Results

Thermogravimetric analysis results for the composite membranes are shown in Figure (30). The TGA tests were carried out from room temperature to 950°C with a heating rate of 10°C/min. Typically, three main stages were observed from the TGA curves. At the first stage which is between 80-120°C, dehydration stage is started. Then, around 290-370°C sulphonic groups  $-SO_3H$  are released and finally between 420-520°C main chain of polymer matrix is decomposed.

- M1 2.5 wt. %  $SiO_2$  with Pluronic® L64 (Ultrasonic probe)
- M2 2.5 wt. %  $SiO_2$  with PEG (Ultrasonic probe)
- M3 2.5 wt. %  $SiO_2$  (Ultrasonic probe)
- M4 2.5 wt. %  $SiO_2$  (Ultrasonic bath)
- Recasting Nafion (Ultrasonic probe)

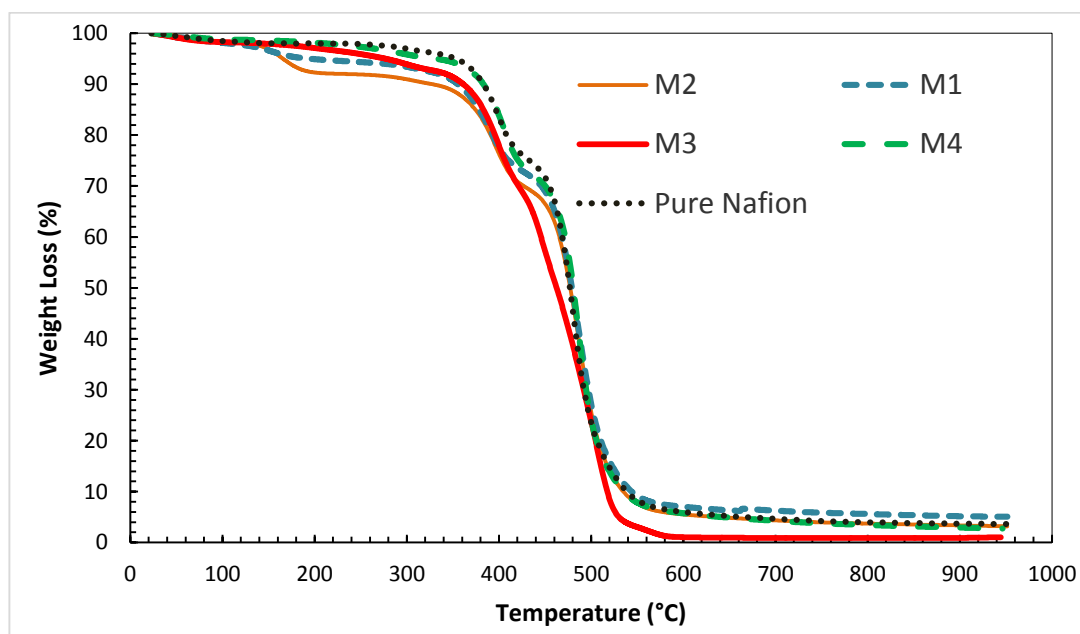


**Figure 30.** TGA plot of 4 different samples and recasting Nafion

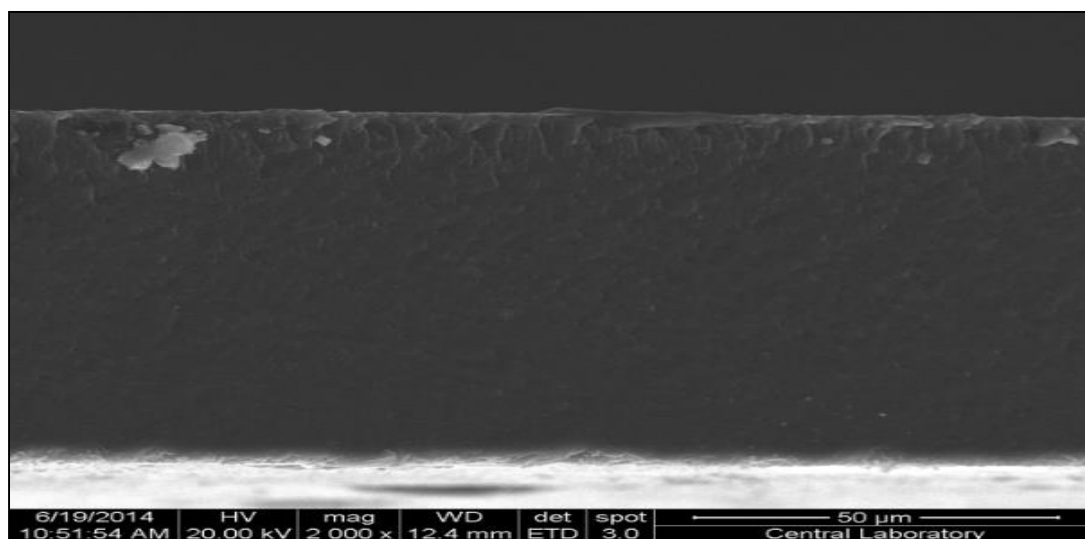
As can be seen from Figure (30), the TGA curves of these composite membranes were not significantly different from each other.

#### 5.4. SEM & EDXS Results

In order to realize the morphology of SiO<sub>2</sub> nanoparticles distribution in the polymer and the MEAs, SEM and EDXS analyses were carried out. The main idea of the taking SEM pictures is to show the influences of the additives (PEG and Pluronic-L64) and mixing techniques on the dispersion of SiO<sub>2</sub> particles in the polymer membrane matrix. EDXS images were taken for both agglomerate and non-agglomerate regions of samples.

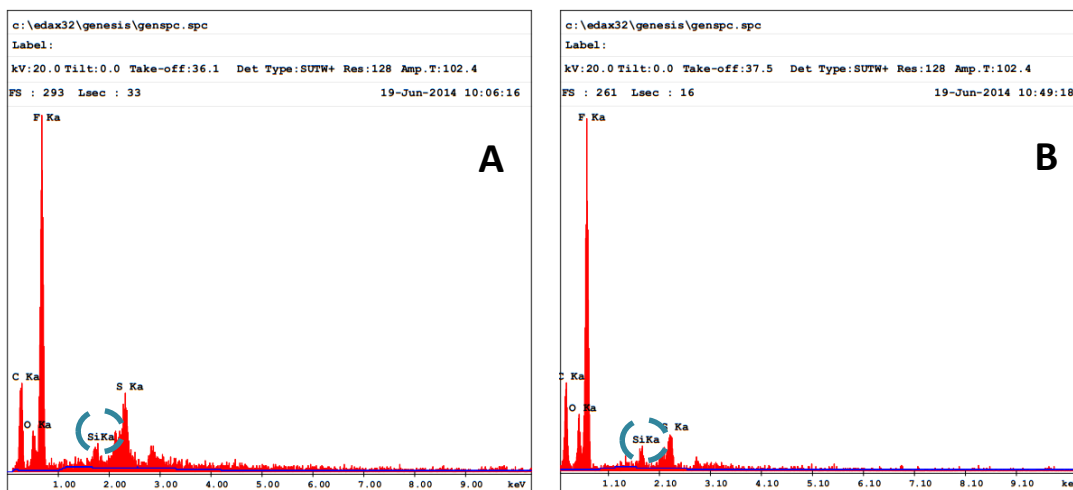
##### 5.4.1. SEM and EDXS Analyses of Composite Membranes

Figure (31) shows the SEM and EDXS results for the membrane M1, containing 2.5 wt. % SiO<sub>2</sub> and Plutonic L64 (3.0 wt. % of added SiO<sub>2</sub>) which is prepared with ultrasonic probe. As can be seen from Figure (31), the sample has no noticeably agglomeration regarding SiO<sub>2</sub> particles.



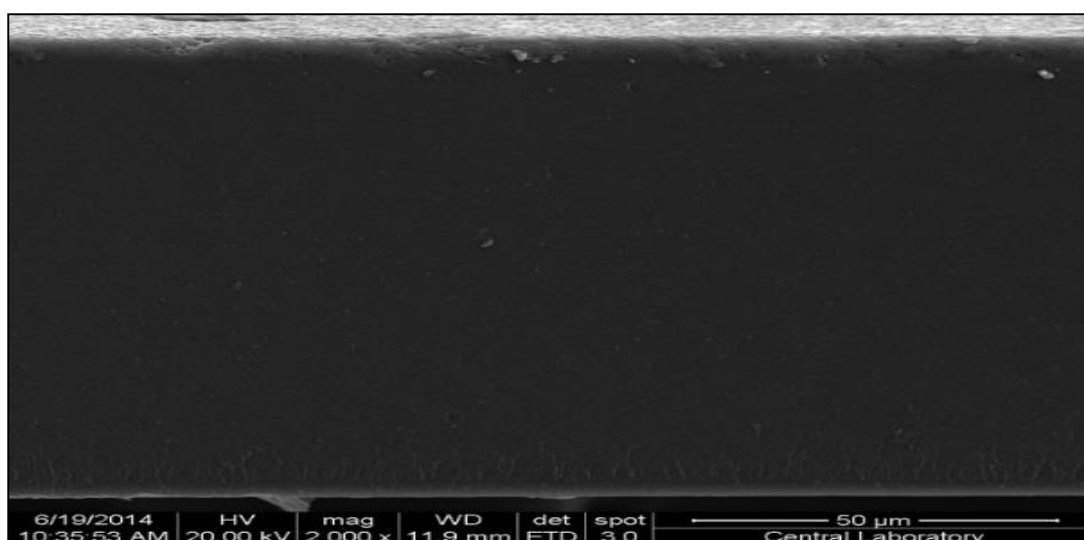
**Figure 31.** SEM image of M1 containing 2.5 wt. % SiO<sub>2</sub> and Plutonic L64 (3.0 wt. % of added SiO<sub>2</sub>) prepared via ultrasonic probe

Figure (32) demonstrates that SiO<sub>2</sub> peaks of two agglomerate and non-agglomerate regions have almost same intensity.



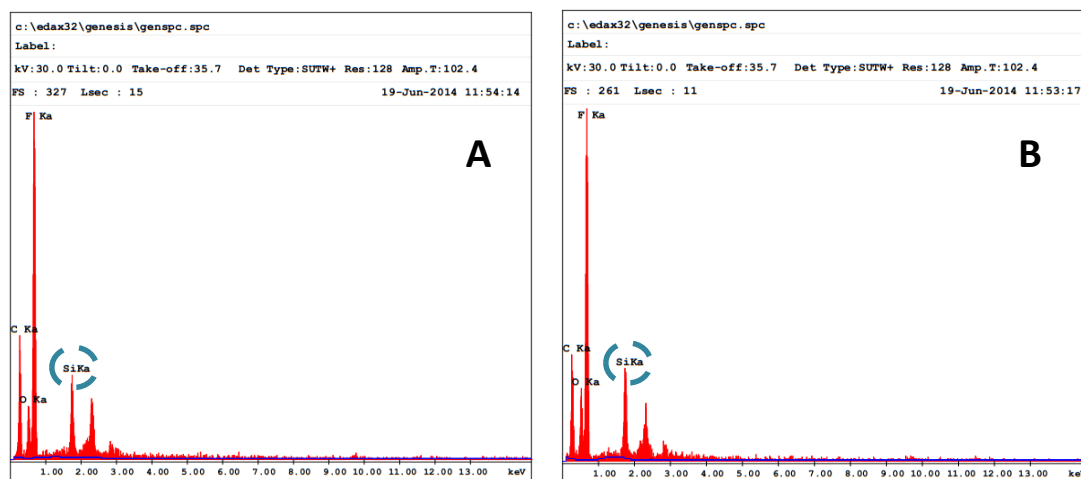
**Figure 32.** EDXS pattern for M1: 2, 5 wt. % of SiO<sub>2</sub> + Pluronic L64 prepared via ultrasonic probe, (A); EDXS pattern of non-agglomerate SiO<sub>2</sub> region, (B): EDXS pattern of agglomerate SiO<sub>2</sub> region

Figure (33) shows the SEM images for membrane M2, containing 2.5 wt. % SiO<sub>2</sub> and PEG (3.0 wt. of added SiO<sub>2</sub>) which is prepared with ultrasonic probe.



**Figure 33.** SEM image of M2 containing 2.5 wt. % SiO<sub>2</sub> + PEG prepared via ultrasonic probe

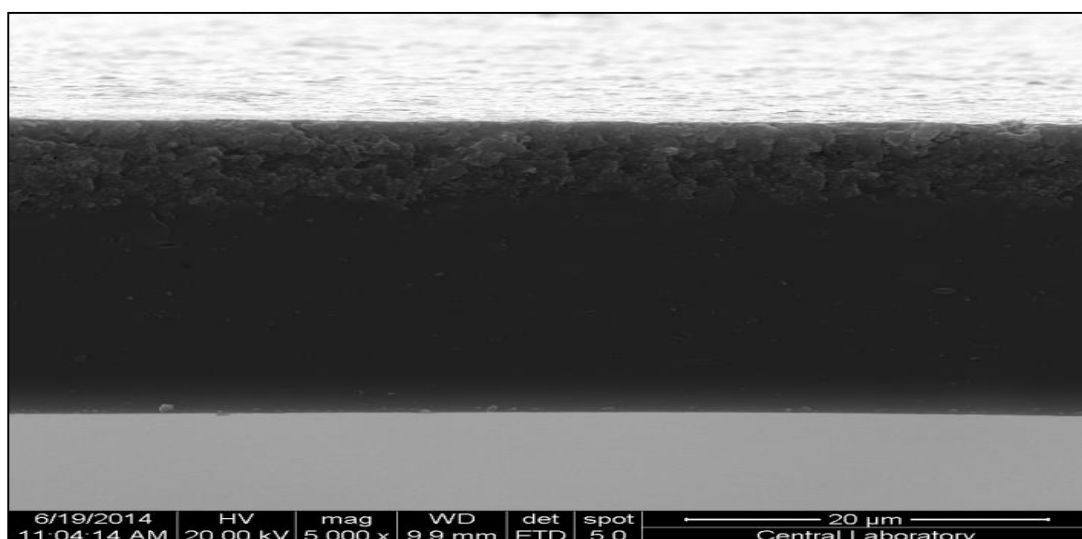
As can be seen from Figure (34), SiO<sub>2</sub> particles were well dispersed in polymer matrix since they have almost same intensity of SiO<sub>2</sub> peaks.



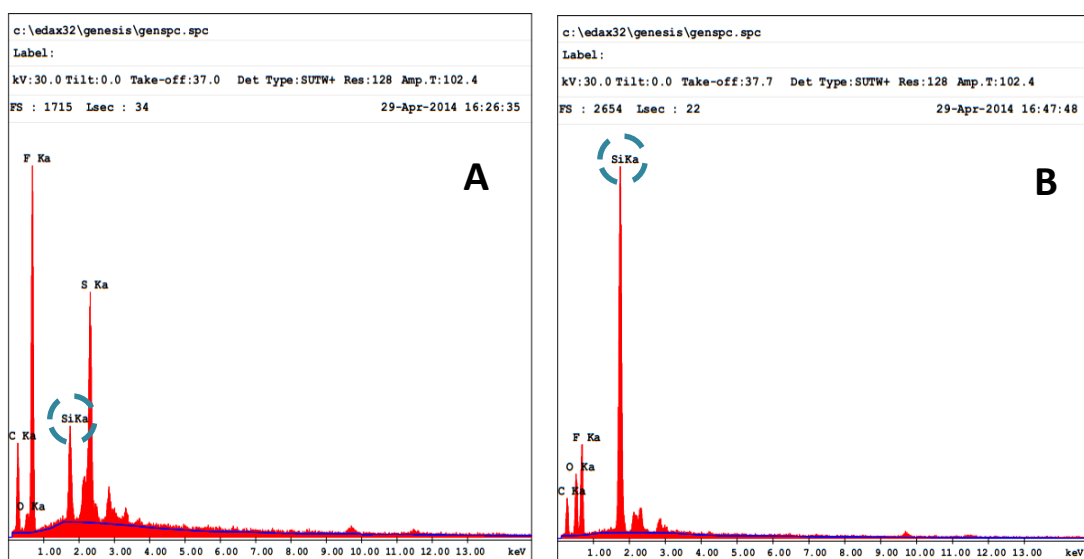
**Figure 34.** EDXS pattern for M2: 2, 5 wt. % of SiO<sub>2</sub> + PEG prepared via ultrasonic probe, (A); EDXS pattern of non-agglomerate SiO<sub>2</sub> region, (B): EDXS pattern of agglomerate SiO<sub>2</sub> region

From the SEM analyses shown in Figures (31) and (33), when Pluronic L64 and PEG were added to the polymer membrane containing 2.5 wt. % SiO<sub>2</sub>, the SiO<sub>2</sub> particles were successfully dispersed in the polymer matrix. However, when SiO<sub>2</sub> content was increased beyond 7.5 wt. %, the dispersion of the SiO<sub>2</sub> was not achieved.

Figure (35) shows the SEM and EDXS results for the membrane M3, containing 2.5 wt. % of SiO<sub>2</sub> which is prepared with ultrasonic probe. Based on the SEM picture for the sample M3, it is clearly seen that SiO<sub>2</sub> particles were segregated and concentrated at the bottom part of suspension cast membrane film suggesting that the dispersion of the SiO<sub>2</sub> particles may not be achieved when the dispersants (PEG and + Pluronic L64) were not used. In Figure (36, B), it is found by the EDXS pattern of M3 that the SiO<sub>2</sub> has significantly higher peak intensity at agglomerate region where SiO<sub>2</sub> is concentrated (B) at these region comparing to non-agglomerate region (A).



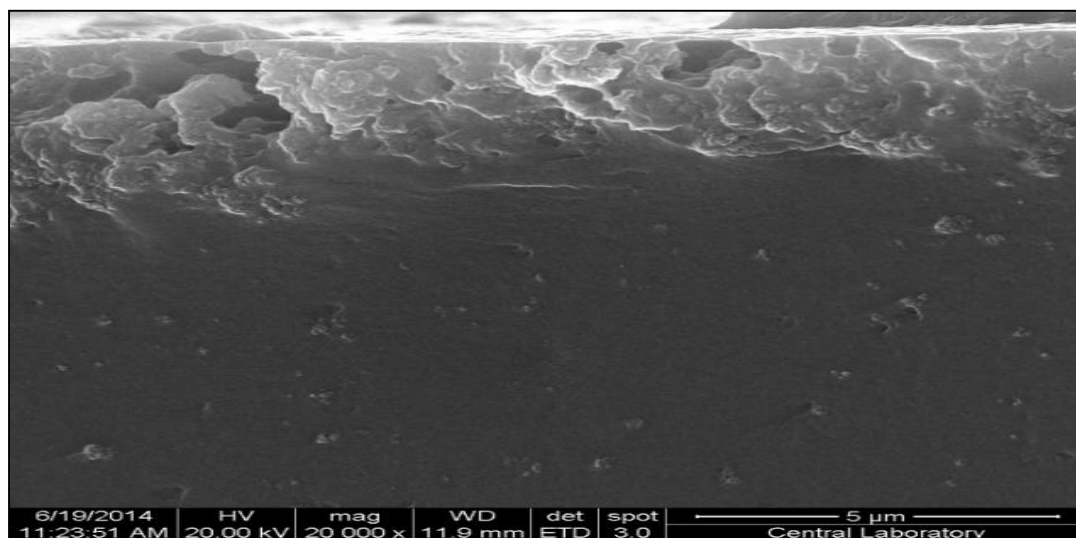
**Figure 35.** SEM image of M3 containing only 2.5 wt. %  $\text{SiO}_2$  prepared via ultrasonic probe



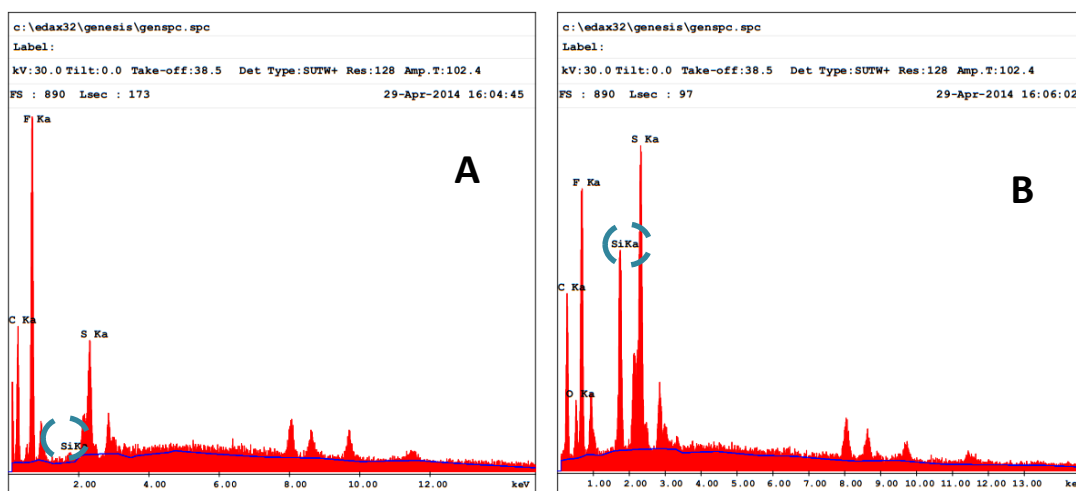
**Figure 36.** EDXS pattern for M3: 2, 5 wt. % of  $\text{SiO}_2$  + PEG prepared via ultrasonic probe M3, (A); EDXS pattern of non-agglomerate  $\text{SiO}_2$  region, (B): EDXS pattern of agglomerate  $\text{SiO}_2$  region

Figure (37) shows the SEM and EDXS results for the membrane M4. The segregation of the  $\text{SiO}_2$  particles observed for the both sample M3 and M4.

There is no difference between ultrasonic bath and probe techniques in terms of distribution of SiO<sub>2</sub> particles in Nafion polymer.



**Figure 37.** SEM image of M4 containing only 2.5 wt. % SiO<sub>2</sub> prepared via ultrasonic bath



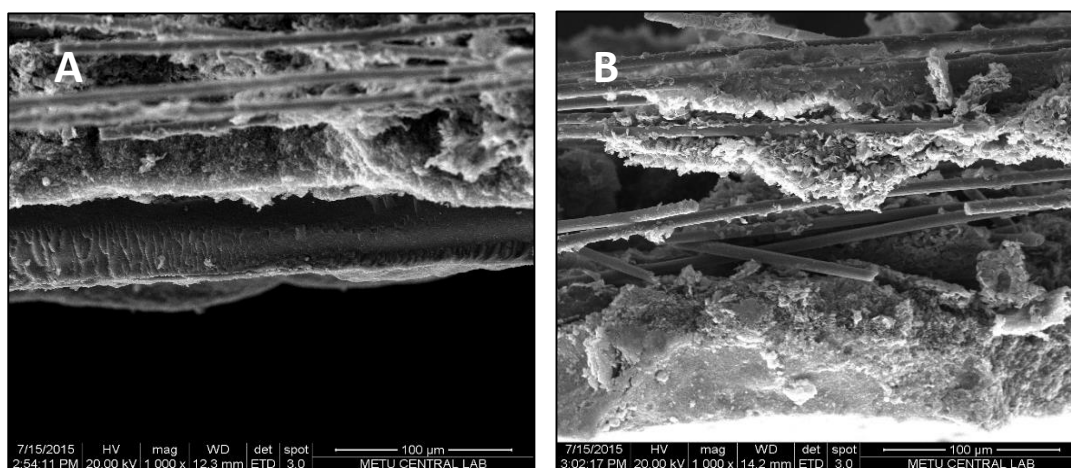
**Figure 38.** EDXS pattern for M4: 2, 5 wt. % of SiO<sub>2</sub> + PEG prepared via ultrasonic probe M4, (A); EDXS pattern of non-agglomerate SiO<sub>2</sub> region, (B): EDXS pattern of agglomerate SiO<sub>2</sub> region

## 5.4.2. SEM Analyses of the MEAs

The SiO<sub>2</sub> nanoparticles were also dispersed in the catalyst layer in order to comprehend the effect of inorganic filler at anode side. The groups of MEAs were analyzed. The MEAs, which were not subjected to the performance test in the PEMFC station, referred to as 'Non-Tested MEAs'. The MEAs, which were subjected to the performance test in the station, referred to as 'Tested MEAs'. The SEM analyses were only discussed for M1, M4 and recasting Nafion since their MEAs showed better cell performance.

### 5.4.2.1. SEM Analyses of Non-Tested MEAs

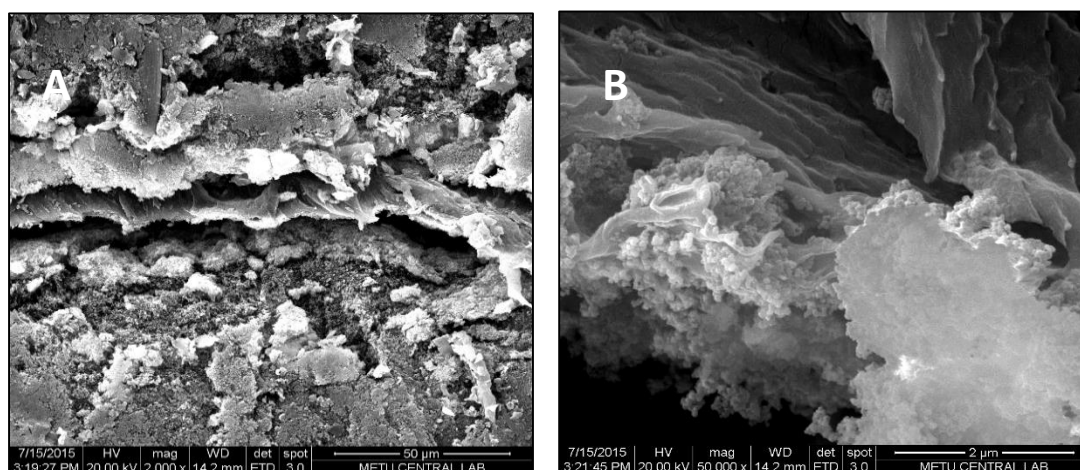
Figure (39) shows the SEM pictures for the Non-Tested MEA1 sample, 2.5 wt. % of SiO<sub>2</sub> and Pluronic L-64 (3.0 wt. % of added SiO<sub>2</sub>) which is prepared with ultra-sonic probe. The SEM pictures were taken from both anode and cathode sides of the membrane because of the fact that they were separated from each other during breaking the membrane into two pieces to reveal the cross sections of the membrane.



**Figure 39.** SEM images for MEA1: 2, 5 % Only SiO<sub>2</sub> (Ultrasonic Probe) Non-tested: 1.000 x magnified picture (A), 1.000 x magnified picture (B)

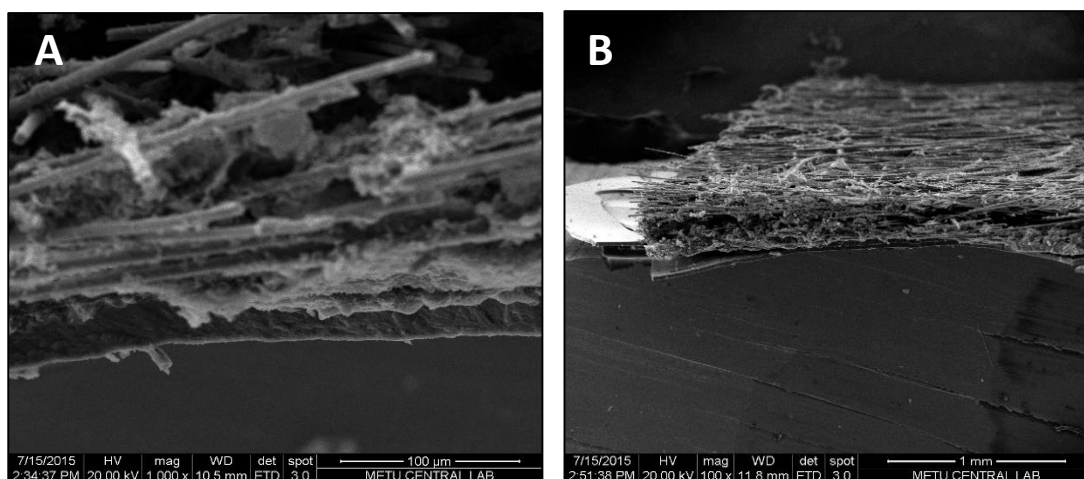
As can be seen from Figure (39), the rod type catalyst materials covered with SiO<sub>2</sub> particles. It appears that the SiO<sub>2</sub> particles were dispersed efficiently in the polymer matrix and there were good contacts between the catalyst layers and the polymer membrane.

Figure (40) shows the SEM pictures for the Non-Tested MEA4 sample, 2.5 wt. % SiO<sub>2</sub> which is performed with ultrasonic probe as well. There was a substantial gap between the catalyst and the membrane layers. Additionally, large SiO<sub>2</sub> agglomerates were observed in the structure (50.000 x magnified SEM picture - right hand side).



**Figure 40.** SEM images for MEA4: 2, 5 % Only SiO<sub>2</sub> (Ultrasonic Bath) Non-tested: 2.000 x magnified picture (A), 50.000 x magnified picture (B)

The gap might be occurred during immersion of composite membranes into liquid nitrogen. The liquid nitrogen was used to make membranes so brittle that the membrane could be broken easily without disturbing the microstructure of the membranes.



**Figure 41.** Recasting Nafion (Ultrasonic Probe) Non-tested MEA0: 1.000 x magnified picture (A), 100x magnified picture (B)

Figure (41) illustrates the SEM pictures for the Non-Tested Recasting Nafion and some small gaps are seen between the polymer matrix and the catalyst layer. The layered fiber/rod structures can be seen clearly. The SiO<sub>2</sub> particles were also agglomerated in this system.

### 5.5. Particle Size Test Results

The particle size analyses were performed for the suspensions which were prepared using ultrasonic bath and probe mixing techniques. The SiO<sub>2</sub> particles were added into the solvent (DMAc) containing Pluronic L64 (3.0 wt. % of the added silica) by using tubes. The weight percentage of SiO<sub>2</sub> in these suspensions ranged from 2.5 to 10 wt. %. The size of SiO<sub>2</sub> particles in these suspensions were calculated using Dynamic Light Scattering technique (DLS).

### 5.5.1. Optimization of Adding Organic Additive – Pluronic L 64

The optimum amount of the dispersant (Pluronic L 64) was studied in detail. The SiO<sub>2</sub> content of the suspension was kept at 2.5 wt. % and the dispersant content was varied between 1.0 – 10.0 wt. percent of SiO<sub>2</sub>. The sedimentation time of the SiO<sub>2</sub> particles in these suspensions was determined using visual examination. The sedimentation time as a function of Pluronic L64 content was illustrated in Figure (42).

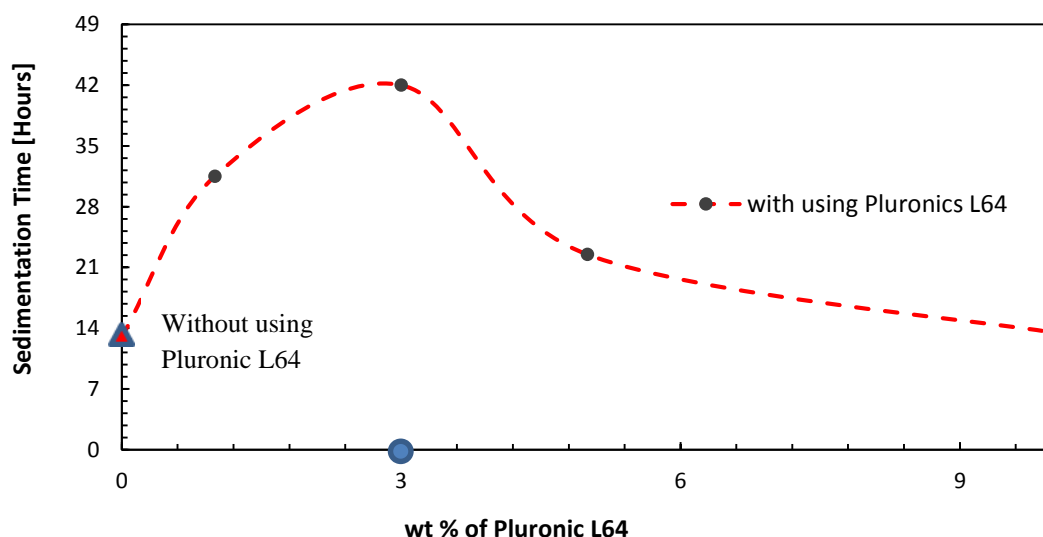


**Figure 42.** The sedimentation time of the suspensions containing various amount of Pluronic L64 (1 wt. %- 10 wt. % of the added SiO<sub>2</sub>)

Figure (42) suggests that the optimum amount of Pluronic L64 was found to be 3 wt. % of added SiO<sub>2</sub> and the samples containing optimum amount of Pluronic L64 were used in performance tests.

Considering Figure (42), the optimum amount of organic additive was found around 3 wt. % of SiO<sub>2</sub> ( ▲ ) at which the performance of samples were proved as well by the PEMFC test station. Moreover, sedimentation time for without using Pluronic L64 case ( ● ) were shown on Figure (42) which was around 14 hours.

Figure (43) shows the particle size distribution of the SiO<sub>2</sub> agglomerates since the primary particle size of the SiO<sub>2</sub> particles used in this study was about 20 nm. The particle size measurements for the same suspension were repeated 6 times.

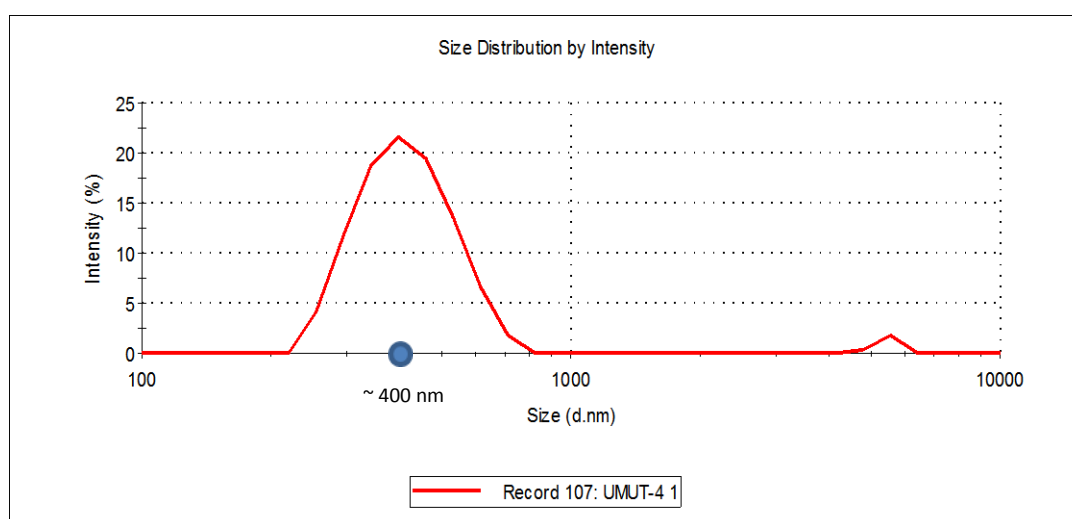


**Figure 43.** The particle size analysis of the suspension containing 2.5 wt. % of SiO<sub>2</sub> and 3.0 wt. % of Pluronic L64 based on the SiO<sub>2</sub> content

The z-average particle size of SiO<sub>2</sub> particles in these suspensions were approximately 480 nm, suggesting that the SiO<sub>2</sub> particles with a primary particle size of about 20 nm were significantly agglomerated.

**Table 11.** The particle size analysis results from the DLS technique for the suspension (M1) containing 2.5 wt. % of SiO<sub>2</sub> and 3.0 wt. % of Pluronic L64 based on the SiO<sub>2</sub> content

Set	T [°C]	Z-Ave [d.nm]	PdI
1	25.1	489.5	0.326
2	25	480.7	0.318
3	25	488.1	0.398
4	24.9	480.8	0.336
5	25.1	487.7	0.303
6	24.9	487.4	0.373
<b>Average</b>	25	485.7	0.342
<b>Std Deviation</b>	0.1	3.901	0.036

**Table 12.** Z-Average particle size of SiO<sub>2</sub> suspensions (M2, M3, and M4)

SiO <sub>2</sub> wt. %	Samples	Technique	Dispersant	T [°C]	Z-Ave [d.nm]
2.5	M2	U. sonic probe	Pluronic L64	25	489.5
2.5	M3	U. sonic probe	PEG	25	498.4
2.5	M4	U. sonic bath	-	25	500.1

As can be seen from Table (11) and Table (12), the z-average particle sizes of these suspensions were nearly the same. This observation suggests that the addition of dispersants (Pluronic L64 and PEG) is not so helpful to prevent agglomeration of SiO<sub>2</sub> particles.

## 5.6. Electro Impedance Spectrometry – EIS Results

The proton conductivity is one of the most important barrier properties in conjunction with water uptake. The EIS technique is used as ex-situ method and the resistivity values of the membranes were given in Table (13). According to Equation (28), as the resistivity decreases the proton conductivity increases. Firstly, the experiments were performed at stable humid and temperature conditions but the results fluctuated even a long-term conditioning was applied.

Then, 5 cm<sup>2</sup> (5 cm x 1 cm) the samples were totally immersed in the DI water. It is observed that as the humidification increases, the proton conductivity increases and more stable data were observed. The main reason of this observed phenomenon could be the different types of mechanism. Considering Figure (44), in order to have a continuous pathway for the H<sub>3</sub>O<sup>+</sup>, no gap must be present so that proton can move on through the cross-sectional direction of polymer or Nafion. However, within the comparison of the SEM images, SiO<sub>2</sub> particles in Pluronic L64 and PEG samples seemed to be well-distributed. Even so, the resistivity of them were obtained higher than the ultrasonic-bath and pure Nafion at 25°C which is performed at typical PEMFC operating temperature (60-80°C).



**Figure 44.** Representative view of proton transport in composite membrane including SiO<sub>2</sub> particles

The samples as the following;

- M1: Pluronic L64 + 2.5 wt. % SiO<sub>2</sub>; prepared with Ultrasonic probe
- M2: PEG + 2.5 wt. % SiO<sub>2</sub>; prepared with Ultrasonic probe
- M3: 2.5 wt. % SiO<sub>2</sub>; prepared with Ultrasonic probe
- M4: 2.5 wt. % SiO<sub>2</sub>; prepared with Ultrasonic bath
- Recasting Nafion: 0 wt. % SiO<sub>2</sub>; prepared with Ultrasonic probe

**Table 13.** Comparison of proton conductivity values of samples with only humid air (95 % RH)

Samples	$\sigma$ [ $\text{Scm}^{-1}$ ]	L [cm]	R [ $\Omega$ ]	A [ $\text{cm}^2$ ]
M1 [2.5 wt. SiO <sub>2</sub> %]	0.01793	0.011466	0.1279	5
M2 [2.5 wt. SiO <sub>2</sub> %]	0.01555	0.010067	0.1294	5
M3 [2.5 wt. SiO <sub>2</sub> %]	0.01844	0.010633	0.1153	5
M4 [2.5 wt. SiO <sub>2</sub> %]	0.01930	0.009200	0.0953	5
Recasting Nafion®	0.02649	0.009433	0.0712	5

The samples were chosen especially for 2.5 wt. % SiO<sub>2</sub> because of the fact that it was seen that as the SiO<sub>2</sub> content increase the proton conductivity is decreased. According to the Table (13), the presence of PEG and Pluronic L64 decrease proton conductivities. The reason of this might be the gap structures because of dispersing agents into the nano-composite membranes so that the performance shows downward trend comparing with other samples.

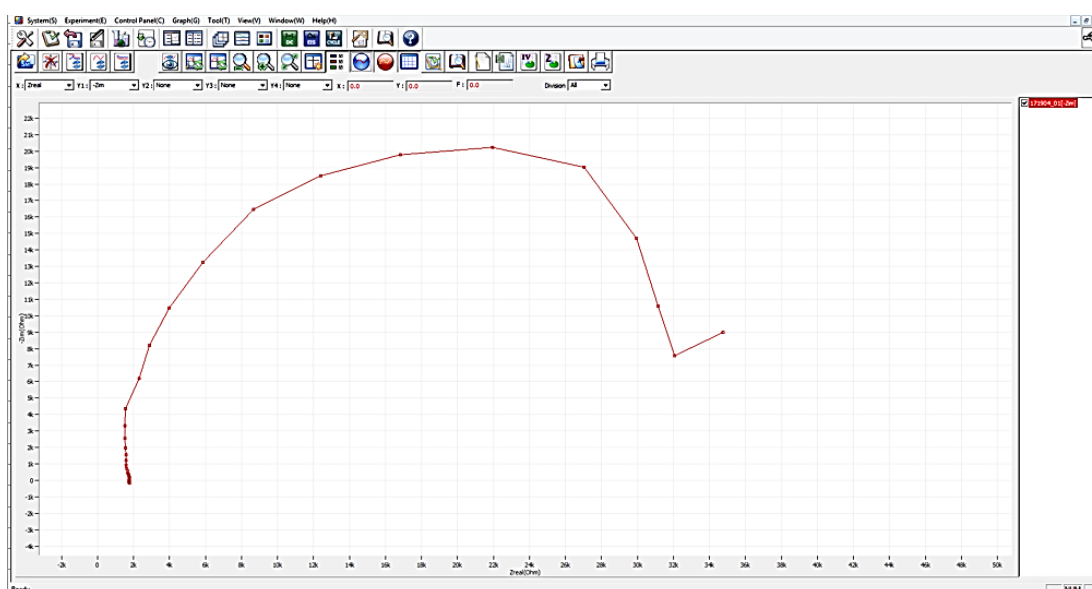


**Figure 45.** A representative Nyquist plot of recasting Nafion at 80°C

Basically, the real and imaginary resistivity can be read with the help of Nyquist plot which was shown in Figure (45). From software, the membrane resistivity were read and all other resistivity were tabulated as the following;

**Table 14.** The proton conductivity of the samples –totally immersed in DI water

Samples	A [ $cm^2$ ]	Proton Conductivity [ $Scm^{-1}$ ]		
		40°C	60°C	70°C
M1 [2.5 wt. SiO <sub>2</sub> %]	5	0.022	0.0452	0.0723
M2 [2.5 wt. SiO <sub>2</sub> %]	5	0.009	0.0411	0.0553
M3 [2.5 wt. SiO <sub>2</sub> %]	5	0.011	0.0362	0.0548
M4 [2.5 wt. SiO <sub>2</sub> %]	5	0.009	0.0232	0.0553
Recasting Nafion <sup>®</sup>	5	0.014	0.0462	0.0654

Moreover, it can be observed from the Table (14) that, when the samples were totally immersed into the DI water, the values were totally changed. The importance of temperature effect was also examined in this manner. In the DI water, the Nafion swells as shown in Figure (46) and then proton can be transported with the help of sulphonic acid groups [42].

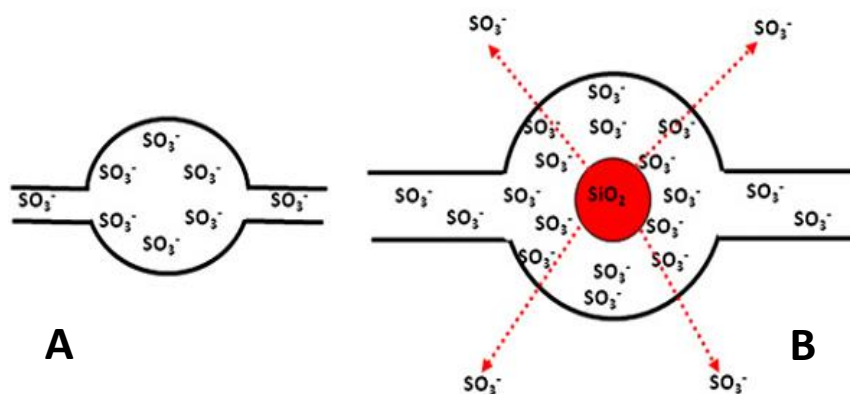


**Figure 46.** Pristine Nafion (A) and Nafion + SiO<sub>2</sub> composite ion cluster (B) [46]

As mentioned before, two types of proton transfer mechanism are available for the Nafion clusters. The Grotthuss mechanism is very effective at high amount of water presence or low temperature degree. It can be resulted as, for M1 sample at low degree temperature, Grotthuss mechanism works well. However, the performance of M2 and M4 samples are far behind of M1 and recasting Nafion.

### 5.7. PEMFC Testing Results and SEM Analyses

The single PEMFC performance tests for each sample were done three times in METU and Atılım University Fuel Cell Technology Laboratories. With the help of PEMFC station, the reactant gases were tested that required mass flow rates and different temperatures by sophisticated control systems which work with proportional integral derivative (PID).

Two types of humid conditions were considered for reactant gases which are totally humidification (with an external humidifier) 100 % RH and (with self-humidification) 0 % RH which is called as self-humidification. At external humidification case, the silica was not added in to the catalyst layer. However, in self-humidification case, the SiO<sub>2</sub> was added into anode side as 3 wt. % of catalyst solution. Fundamentally, at four different operational temperatures; 65 °C, 70 °C, 75 °C, 80 °C; pure hydrogen (% 99.995) at 0.10 slpm flow rate (2.00 stoichiometry), and compressed dry air at 0.42 slpm flow rate (3.50 stoichiometry) are fed to the cell. The current and voltage values were obtained from the station and transferred to the computer. All the samples were conditioned (~one day) and performed for three days and the results were gathered for V-I curves. To compare the results accurately, a commercial Nafion is also performed. Moreover, all samples have 5 cm<sup>2</sup> active area. Figure (47) shows the graphical user interface of HenaTech PEMFC test station in which an external humidifier is used to be able to humidify the reactant gases 100 %.



**Figure 47.** A representative PEMFC performance of M1 (2.5 wt. %) at 100 % RH of test station interface at METU Chemical Engineering Fuel Cell Laboratory (Anode: 0.1 slpm H<sub>2</sub> @ 100 % RH, Cathode: 0.42 slpm Compressed Dry Air @ 100 % RH)

### 5.7.1. With External Humidification (at 100 % RH)

- MEA0: Recasting Nafion (Ultra-sonic Probe Technique)

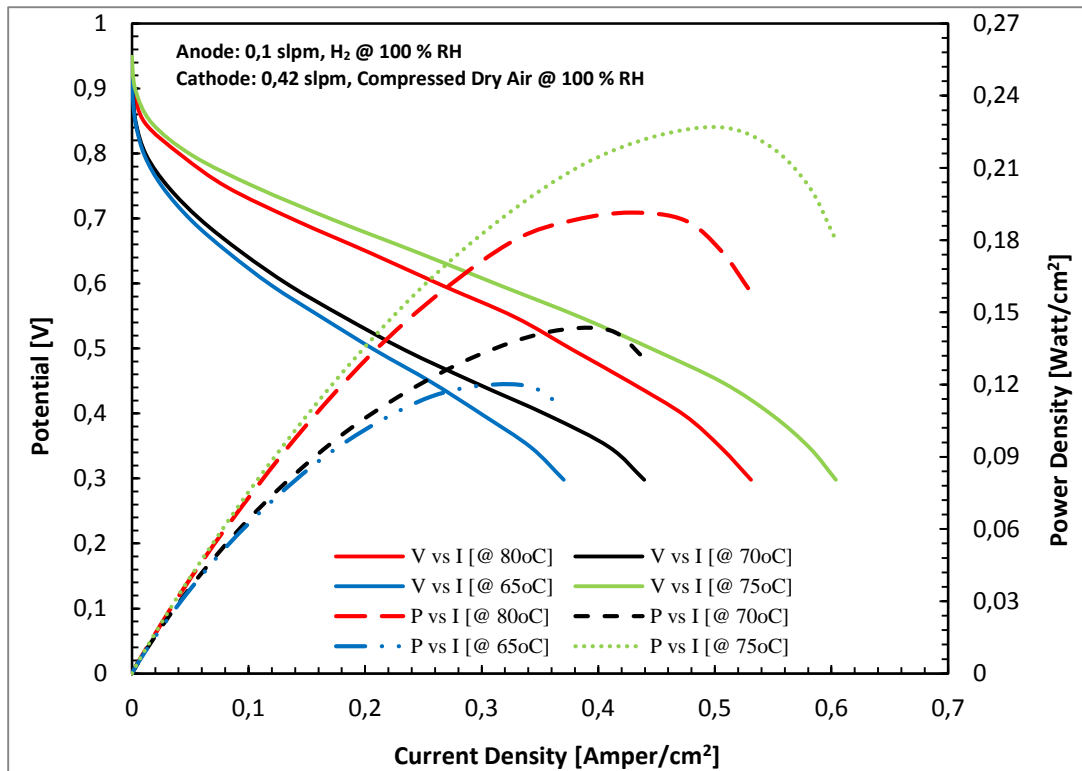


**Figure 48.** The PEMFC performance tests of recasting Nafion: MEA0, at 65°C, 70°C, 75°C, 80°C, Anode: 0,1 slpm, H<sub>2</sub> @ 100 % RH; Cathode: 0,42 slpm, Compressed Dry Air @ 100 % RH

Comparing to commercial Nafion, the recasting Nafion sample showed worse performance as plotted in Figure (48). In addition, after the 80°C which is a threshold temperature of Nafion, the voltage and current values started to decrease.

It is curiously enough that at 80°C, the recasting Nafion is not stable any longer which means the membrane has not enough water content in it for the proton transferring.

**Table 15.** Comparison of OCV and maximum power density values for recasting Nafion – MEA0

Temperature [°C]	OCV [Voltage- V]	Maximum Power Density [Watt / cm <sup>2</sup> ]
65	0,920	0,119
70	0,927	0,142
75	0,949	0,226
80	0,922	0,191

As can be comprehended from Table (15), up to 80°C, the PEMFC performance increases. However, at 80°C, a drastic decrement were seen at OCV values which are highly lower than the theoretical values (0.95 – 1.05 V). Regarding OCV values, it is seen that as temperature increases hydrogen crossover increases at 80 °C which is also closely related with thickness (56.80 μm, see Table (9)) of membrane so that permeability of hydrogen increases at that temperature and hence OCV drops. The reason could be that the polymer dried at that elevated temperature hereby it partially losses its ionomer properties. The membrane started to physically degrade at 80°C with losing its excellent mechanical, thermal and electro-chemical properties.

Moreover, at 80°C, the voltage loss caused by mixed potential could be decreased which is known as the one of the major factor on OCV drop. The OCV could be also dropped at 80°C because of the fact that partial pressure of fuels (H<sub>2</sub> and O<sub>2</sub>) decreases with temperature; whereas (H<sub>2</sub>O) increases with temperature (Equation (16)).

Thus, temperature increment could cause the above phenomenon which are expressed in detail so that OCV drops dramatically at 80°C.

As mentioned before at Chapter 1 (see section 1.4.2), three regions are available at PEMFC polarization curve which are activation, ohmic and concentration thereby one could comment on output (voltage, current and power) in a clear manner [7]. It is important to compare results in terms of the polarizations. At first region, it is seen that, due to sluggish kinetics, little amount of loss was observed which is called as ORR (oxygen reduction reaction). For this MEA, it is seen that due to lower kinetics at 80°C, OCV value decreases.

Furthermore, at second region, ohmic losses are observed which are caused by resistance to flow of ions in the membrane and resistance to flow of electrons through the electrodes. One may conclude that as the temperature increase, ohmic losses, and decreases till 80°C. Additionally, at third region which is known as concentration polarization, mass transport of reactant gases through GDL and CL dominates the polarization. It is found that, as temperature increase from 65 to 80°C, portion of concentration polarization increases.

One may also make an analogy between the PEMFC and proton conductivity (EIS) testing results. However, it is not so straightforward to have discussion on both of them since the EIS testing is substantially sensitive to temperature, humidity and even environmental factor such as mains electricity. Additionally, the proton conductivity of membranes was performed at ex-situ characterization meaning that the samples are exposed to external factors. However, the PEMFC performance is obtained for the samples which are put into PEMFC test station meaning that the samples are well-insulated to external factors. Differently from proton conductivity, the PEMFC samples are conditioned in PEMFC test station throughout one day.

▪ **MEA1: 2.5 % SiO<sub>2</sub> + Pluronic L64 (Ultra-sonic Probe)**

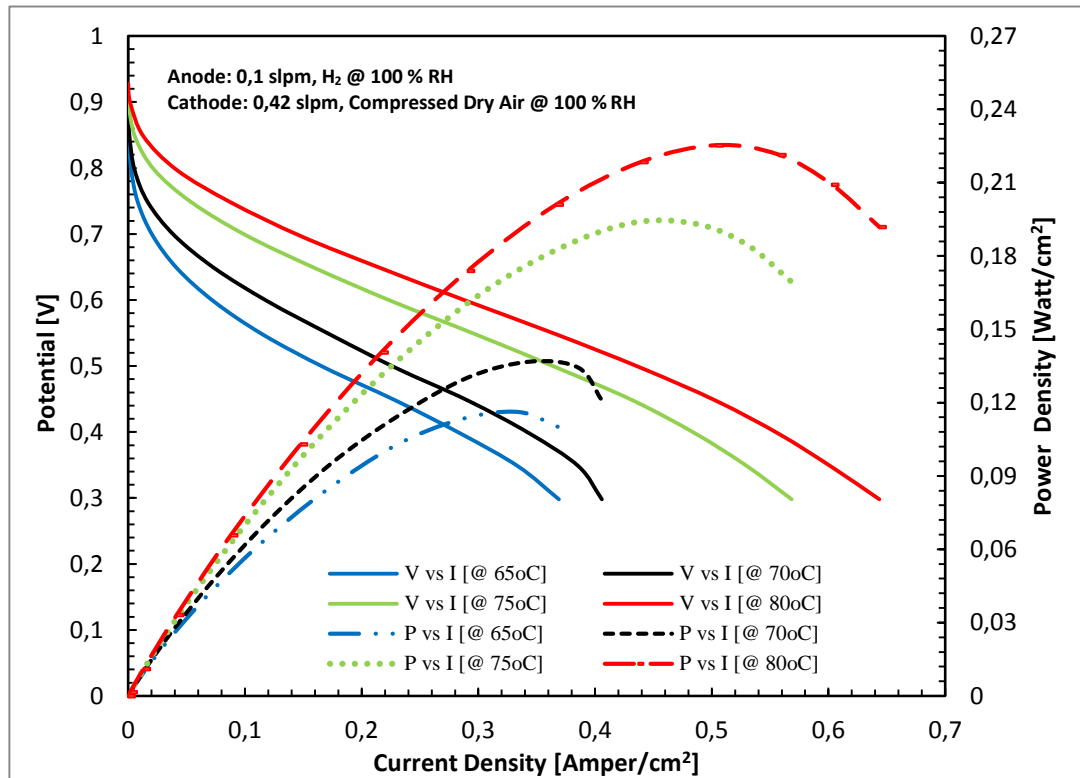


**Figure 49.** The PEMFC performance tests of 2,5 wt. % SiO<sub>2</sub> + Pluronic L64 via ultrasonic probe: MEA1, at 65°C, 70°C, 75°C, 80°C, Anode: 0,1 slpm, H<sub>2</sub> @ 100 % RH; Cathode: 0,42 slpm, Compressed Dry Air @ 100 % RH

This sample was expected to have more capabilities based upon proton conductivity tests. Although the performance is proportional with the temperature, MEA1 showed better performance, especially at 80°C comparing with recasting Nafion which is shown in Figure (49). Moreover, one may see the differences between four temperatures which were indeed separated after 70°C regarding the performance.

One may discuss the results because of the fact that with presence of Pluronic L64, the membrane might keep water content at a certain level which is at 80°C so that proton can be transferred as usual [28].

**Table 16.** Comparison of OCV and maximum power density values for MEA1 at 100 % RH

Temperature [°C]	OCV [Voltage- V]	Maximum Power Density [Watt / cm <sup>2</sup> ]
65	0,873	0,116
70	0,876	0,136
75	0,907	0,193
80	0,928	0,225

Based on OCV values in Table (16), as temperature increases, better OCV and power values were read from the PEMFC performance station meaning that reaction rate increases and thereby less ohmic and concentration losses were achieved by the help of Pluronic L64 dispersing agent. One may result that the thickness of membrane (59.25  $\mu\text{m}$ , see Table (9)) has an important effect on OCV drop. This membrane is slightly thicker than MEA0 because of adding  $\text{SiO}_2$  and Pluronic L64 which is associated with hydrogen crossover effect. It is possible that, hydrogen crossover effect could be prevented due to presence of  $\text{SiO}_2$  and Pluronic L64.

More importantly, the proton transfer mechanisms dominate the performance of the PEMFCs which were discussed as the Grotthuss and Vehicle mechanisms (see section 2.2.1.1.). One may deduce that the Grotthuss is more likely to happen at the condition in which the reactants are humidified 100 % because of the fact that water is available in the membrane since both  $\text{SiO}_2$  and Pluronic L64 have hygroscopic properties.

▪ MEA2: 2.5 % SiO<sub>2</sub> + PEG (Ultra-sonic Probe)

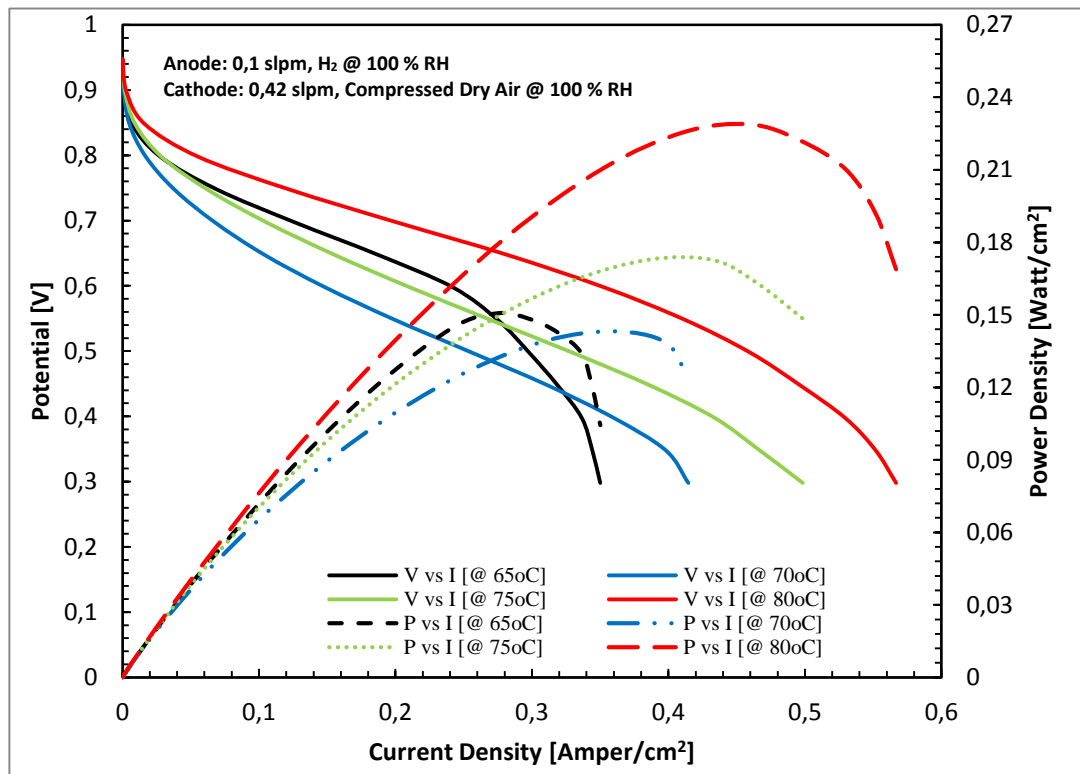


**Figure 50.** The PEMFC performance tests of 2,5 wt. % SiO<sub>2</sub> + PEG via ultrasonic probe: MEA2, at 65°C, 70°C, 75°C, 80°C, Anode: 0,1 slpm, H<sub>2</sub> @ 100 % RH; Cathode: 0,42 slpm, Compressed Dry Air @ 100 % RH

According to the Figure (50), the MEA2 showed a less PEMFC performance than MEA1 and considering operating voltage interval for PEMFC which is the between 0.5-0.6 V, the worst power output can be seen at 70°C. Therefore, it is seen that as temperature increases, higher performance possibly can be obtained but not necessarily.

In addition, a considerable extent of power loss was examined at 65°C. As it was touched on concentration polarization, the reactants might be not easily delivered fast enough to the active area so that sharp decrements were seen after roughly 0.25 current density (A/cm<sup>2</sup>).

**Table 17.** Comparison of OCV and maximum power density values for MEA2 at 100 % RH

Temperature [°C]	OCV [Voltage- V]	Maximum Power Density [Watt / cm <sup>2</sup> ]
65	0,920	0,143
70	0,900	0,150
75	0,930	0,172
80	0,940	0,228

According to Table (17), the OCV values are fluctuated with regard to operation temperatures; but maximum power values increases as the temperature increase. It is suspicious to comment on SiO<sub>2</sub> content at anode side catalyst layer whether helpful or not. However, comparing with MEA1, higher ohmic and concentration polarization are attained for MEA2 so that less performance was seen.

The OCV drop for MEA2 could be happened because of higher hydrogen crossover effect which is directly related with thickness of the membrane. Although the membrane thicknesses are quite similar to each other (especially at 2.5 wt. % of SiO<sub>2</sub>), the thinnest one (~53 μm) is belonged to MEA2 which could cause higher hydrogen crossover.

Similar to MEA1, the Grotthuss mechanism could work for proton transferring from anode to cathode side since water is expected to be kept in the membrane by PEG which has almost same chemical structure with Pluronic L64.

▪ **MEA3: 2.5 % Only SiO<sub>2</sub> (Ultra-sonic Probe)**

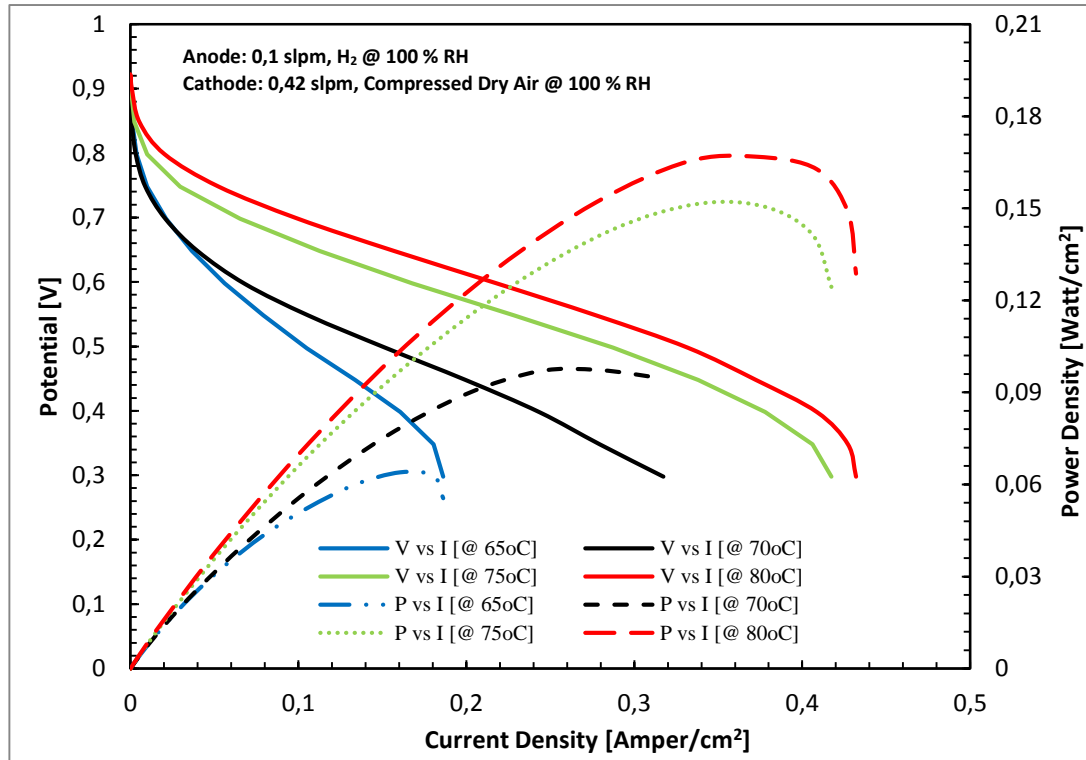


**Figure 51.** The PEMFC performance tests of only 2,5 wt. % SiO<sub>2</sub> via ultrasonic probe: MEA3, at 65°C, 70°C, 75°C, 80°C, Anode: 0,1 slpm, H<sub>2</sub> @ 100 % RH; Cathode: 0,42 slpm, Compressed Dry Air @ 100 % RH

Based on the plot, without using dispersing agents such as PEG or Pluronic L64, lower PEMFC performance was obtained. In contrast with MEA1 and MEA2, the PEMFC performance of MEA3 is very low.

As seen from Figure (51), the PEMFC performance of MEA3 increases as temperature increases. At 80°C, maximum power is obtained which is around 0.167 W/cm<sup>2</sup>.

**Table 18.** Comparison of OCV and maximum power density values for MEA3 at 100 % RH

Temperature [°C]	OCV [Voltage- V]	Maximum Power Density[Watt / cm <sup>2</sup> ]
65	0,904	0,063
70	0,886	0,097
75	0,897	0,151
80	0,911	0,168

Table (18) demonstrates that, less OCV and power density values were obtained in comparison with MEA0, MEA 1, and MEA2. Only difference between MEA1 and MEA2, MEA3 has same amount of SiO<sub>2</sub> content at polymer (2.5 wt. %). MEA3 is lack of any organic additive (Pluronic L64 and PEG) which shows that certain amount of dispersing agent is helpful to keep water inside of the cell so that as the temperature increases the performance would be higher.

The OCV values are far behind of MEA0, MEA1, and MEA2 PEMFC performance and the main reason could be higher hydrogen crossover effect. Absence of dispersing agents such as Pluronic L64 and PEG could cause water deficiency which has negative impact on proton transferring.

▪ MEA4: 2.5 % Only SiO<sub>2</sub> (Ultra-sonic Bath)

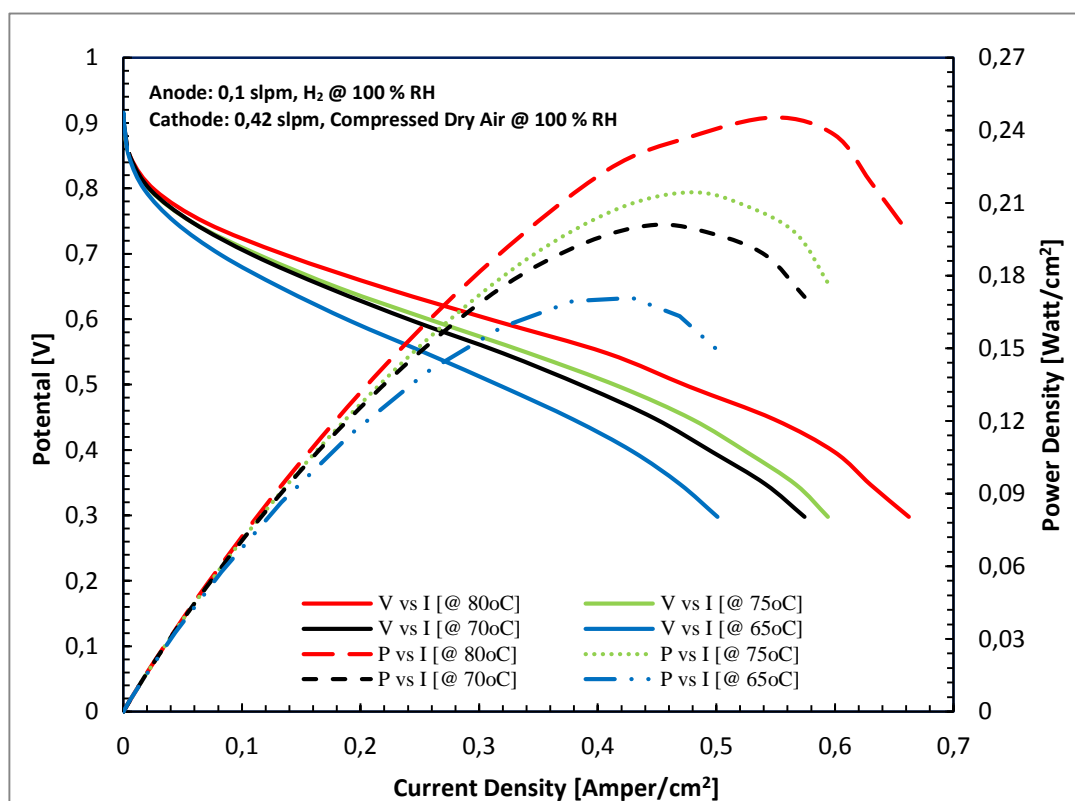


**Figure 52.** The PEMFC performance tests of only 2,5 wt. % SiO<sub>2</sub> via ultrasonic bath: MEA4, at 65°C, 70°C, 75°C, 80°C, Anode: 0,1 slpm, H<sub>2</sub> @ 100 % RH; Cathode: 0,42 slpm, Compressed Dry Air @ 100 % RH

The performance was obtained as the second highest performance after commercial Nafion. However, the difference between them is not by far. Indeed, the difference does not exceed 10 %.

Similarly the same affinity can be seen from the Figure (52) which is related with the directly proportionality of temperature increment with the cell performance. For instance, for 0.5 voltage value, the current density at 65°C is 0,325 V; whereas the current density at 80°C is around 0, 5 V.

**Table 19.** Comparison of OCV and maximum power density values for MEA4 at 100 % RH

Temperature [°C]	OCV [Voltage- V]	Maximum Power Density [Watt / cm <sup>2</sup> ]
65	0,920	0,170
70	0,927	0,200
75	0,949	0,214
80	0,922	0,245

Comparatively, the OCV and maximum power density of MEA4 are higher than all other MEAs which is shown in Table (19). The only difference between other MEAs is the sonication technique which is ultrasonic-bath. It is very interesting to have lower OCV values at 80°C but having higher power density. It is known that OCV drops mostly depends on mixed potential and hydrogen crossover which are strongly linked with temperature so that partial pressure of fuel and oxidants. Since mixed potential is dominantly depend on cathode side that is the function of partial pressure of oxygen, the only possibility left for OCV drop is hydrogen crossover. By means of hydrogen crossover, hydrogen reacts with oxygen and forms hydrogen peroxide (H<sub>2</sub>O<sub>2</sub>) radicals at cathode side thereby potential of cathode side drops. The H<sub>2</sub>O<sub>2</sub> attacks both electrolyte/membrane and ionomer in catalyst layer so that the phenomenon degrades both of them and OCV is decreased.

Having higher power density depends on voltage loss at first second and third region of polarization curve of PEMFC performance. It is seen that as the temperature increases sluggish kinetics are become less dominant in first region.

To sum up, all plots were examined at 70°C in between MEA0 (recasting Nafion), MEA1 and MEA4 since they showed better performance curves.

According to Figure (53), regarding with operational condition of a typical PEMFC, between 0.5 and 0.6 V, MEA4 had a significant difference. There is a considerable difference between MEA4 and MEA1, (Recasting Nafion) MEA0.

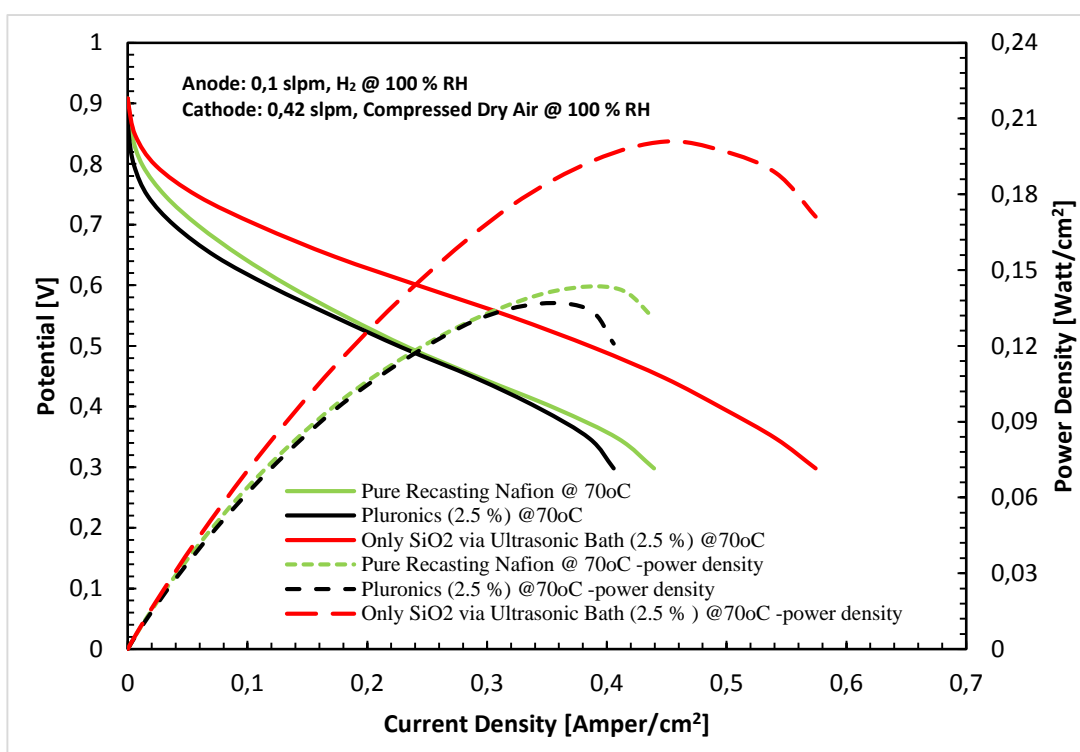


**Figure 53.** The comparison tests between MEA1, MEA4 and MEA0, at 65°C, 70°C, 75°C, 80°C, Anode: 0,1 slpm, H<sub>2</sub> @ 100 % RH; Cathode: 0,42 slpm, Compressed Dry Air @ 100 % RH

**Table 20.** Overall comparison of OCV and maximum power density values for MEA0, MEA1 and MEA4 at 100% RH condition

Samples	Temperature [°C]	OCV [ V]	Maximum Power Density [Watt / cm <sup>2</sup> ]
MEA0	70	0,927	0,142
MEA1	70	0,907	0,193
MEA4	70	0,927	0,200

Table (20) shows overall comparison that the ultrasonic bath technique has slightly priority on ultrasonic probe in terms of cell performance. The MEA4 has same OCV but have higher power density than MEA0, although MEA4 has SiO<sub>2</sub> content (2.5 wt. %) in polymer (Nafion).

### 5.7.2. With Self-Humidification (at 0 % RH)

Among the samples, because of the cell performances of MEA1 and MEA4, they were nominated as possible candidates to be performed without any humidification (0 % RH) at PEMFC test station. In this sense, it is examined that recasting Nafion (MEA0) showed hardly never performance at 0 % RH or self-humidification. This could be reason of absence SiO<sub>2</sub> (hygroscopic material) in recasting Nafion. Despite the fact that 3 wt. % of SiO<sub>2</sub> is available at anode layer of MEA1, MEA4 and recasting Nafion MEA0, since SiO<sub>2</sub> was not presented in recasting Nafion membrane, it was found that Nafion couldn't survive at self-humid condition. The curves are plotted as the following in Figure (54).

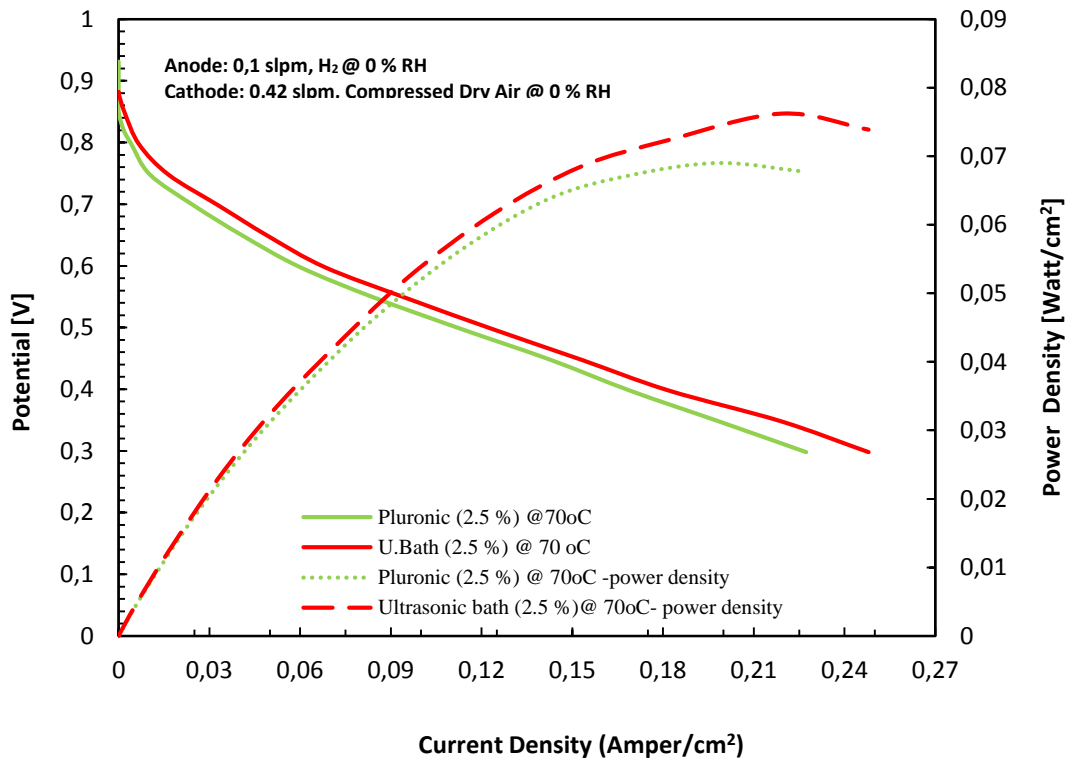


**Figure 54.** The comparison tests between MEA1, MEA4 at dry condition, at 70°C, Anode: 0,1 slpm, H<sub>2</sub> @ 0 % RH; Cathode: 0,42 slpm, Compressed Dry Air @ 0 % RH

To make it in a clear comparison between humid (100 % RH) and dry conditions (0 % RH), the current density decreased from 0.4 to 0.15 at 0.5 V. As, it was touched on in Figure (53) the curves deviate from each other which is available for humid condition.

However, in Figure (54), it seems that the curves are almost overlapped. This actually differs from the humid conditions. Therefore, MEA4 has as solid performance as MEA1.

Moreover, in Table (21) the OCV values are available for both MEAs. Despite the fact that MEA1 has higher OCV than MEA4, MEA1 has lower maximum power than MEA4.

**Table 21.** Overall comparison of OCV and maximum power density values for MEA1 and MEA4 at 0 % RH condition

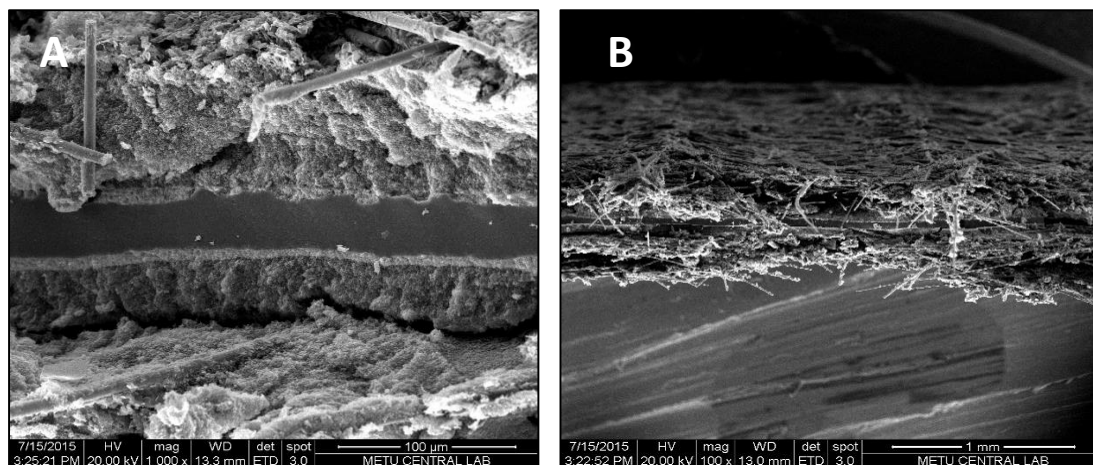
Samples	Temperature [°C]	OCV [ V]	Maximum Power [Watt / cm <sup>2</sup> ]
MEA1	70	0,931	0,069
MEA4	70	0,876	0,076

Besides, considerably ohmic losses might have an effect on the lower performance of the MEAs at 0 % RH condition. The phenomenon could be explained with Vehicle mechanism which is meaningful for protons are relocated with the help of diffusion by way of the electrolyte at high temperature and low humidity level.

### 5.7.2.1. SEM Analyses of Tested MEAs

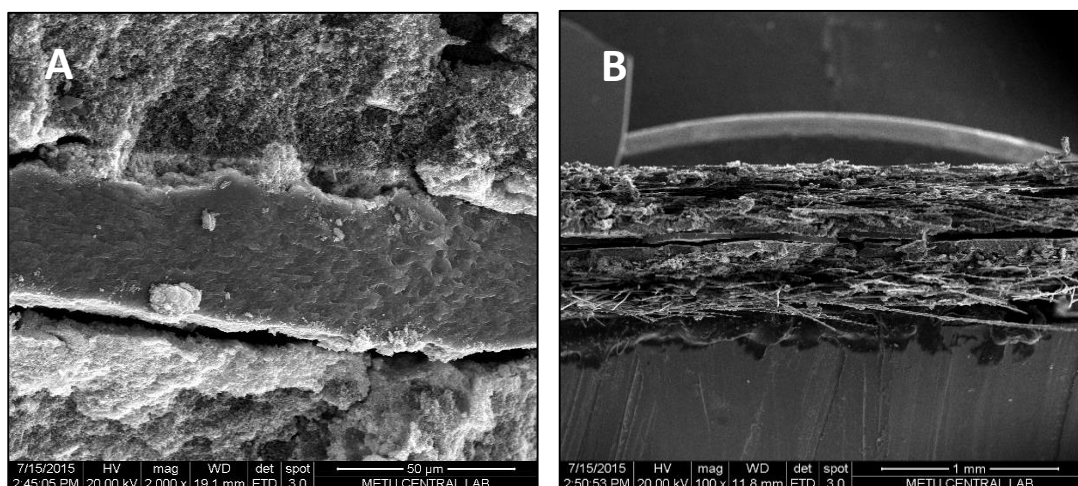
The SEM results for the MEAs tested at 70°C in single PEMFC station under humidification (100 % RH) of reactant gases are given in Figure (55) which shows the SEM pictures for the tested MEA1: 2.5 % SiO<sub>2</sub> + Pluronic L64 which is prepared with ultra-sonic probe. One may see that the catalyst layer and the membrane were well contacted with each other. The rod structure at the anode catalyst layer is seen to be encapsulated by the SiO<sub>2</sub> particles, Nafion and dispersing agent.

Furthermore, the agglomeration of SiO<sub>2</sub> particles in the polymer matrix was not observed suggesting that the ultrasonic-probe mixing technique was effective for dispersing SiO<sub>2</sub> particles when Pluronic L64 was used.



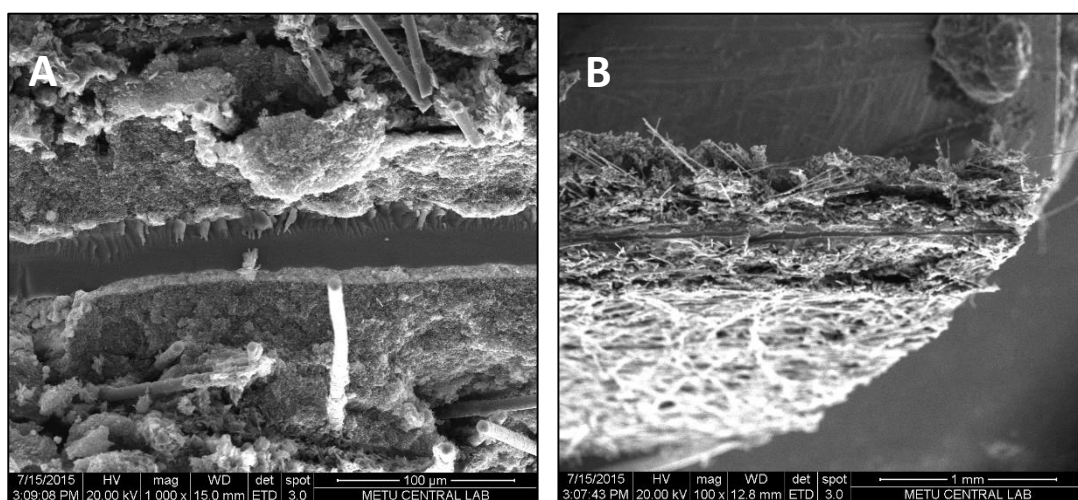
**Figure 55.** SEM pictures for MEA1 2, 5 % SiO<sub>2</sub> + Pluronic L64 Tested: 1000x magnified picture (A), 100x magnified picture (B)

Figure (56) shows the SEM pictures for the tested MEA4, 2.5 wt. % SiO<sub>2</sub> which is prepared with ultrasonic bath. As can be seen from the SEM image, some gaps are available between the polymer matrix and the catalyst layers. The reason of that might be weak force that is applied on during hot pressing. The SiO<sub>2</sub> particles in the membrane and catalyst layers were in agglomerated form.



**Figure 56.** SEM images for MEA4 2, 5 % Only SiO<sub>2</sub> (Ultrasonic Bath) Tested: 2.000 x magnified picture (A), 100 x magnified picture (B)

The SEM results for the Recasting Nafion Tested MEA0; which is prepared with ultrasonic probe are given in Figure (57). Comparing with the Non-Tested sample, in this tested sample, the contact between the polymer membrane and the catalyst layers were good since no gaps observed between them. Moreover, the rod structures in the catalyst layers could also be seen very easily, which are covered by agglomerated formation of SiO<sub>2</sub> and Nafion.



**Figure 57.** SEM images for Recasting Nafion MEA0 (Ultrasonic Probe) Tested: 1.000 x magnified picture (A), 100 x magnified picture (B)



## CHAPTER 6

### CONCLUSIONS

The conclusions regarding the main points for the development of novel membranes with using compatibility agents are summarized in this chapter.

#### 6.1. Characterization of the films and membranes

- **Water Uptake**

According to the results, one may conclude that the water uptake capacity of the membranes increases in the presence of organic additives such as Pluronic L64 and PEG. Moreover, the composite membranes including only SiO<sub>2</sub> particles are also have more water retention compared to the recasting Nafion.

To make comparison between the membranes, the trend for water uptake capacities is as follows; M1 > M2 > M4 > M3 > recasting Nafion.

#### ▪ SEM & EDXS Conclusions

First, the SEM and EDXS analyses were carried out for the composite membranes. Then, only SEM images for the MEA1 and MEA4 were examined due to their cell performance.

➤ For case of the composite membranes;

It was easily seen that for the samples such as M3 and M4 which were prepared without using any dispersing agent, the SiO<sub>2</sub> particles were segregated in the composite membranes. Therefore, the dispersing agent is very useful for the homogeneous distribution of the SiO<sub>2</sub> particles into the membrane. However, the agglomeration of the SiO<sub>2</sub> particles couldn't be prevented by the dispersants. In spite of the fact that the size of SiO<sub>2</sub> particles is 10-20 nm primarily, it is found that the SiO<sub>2</sub> particles agglomerated around 480 nm.

As can be seen from Figure (60) (see App. A.2.), the SiO<sub>2</sub> particles were better distributed in M1 (A) and M2 (B) than M3 (C) and M4 (D). For M3 (C) and M4 (D) samples, a clear difference in color is available which is an evident for non-homogeneity of silica distribution.

Based on the SEM picture of M3, it is clearly seen that the SiO<sub>2</sub> particles were segregated and concentrated at the bottom part of the suspension casting membrane film.

Therefore, one may suggest that the SiO<sub>2</sub> agglomerates may not be well distributed unless the dispersant (PEG and and/or Plutonic L64) are used.

There are two types of SEM data available for MEAs which were either *Tested* or *Non-Tested* in the cell station.

- For the case of Non-Tested MEAs;

It can be concluded that the rod-like structures were covered with SiO<sub>2</sub> particles. In addition, it is observed that there are gaps between the polymer and catalyst layers.

- For the case of Tested MEAs;

The catalyst layer and the membrane have better connection comparing with Non-Tested MEAs which have not SiO<sub>2</sub> at anode catalyst layer. It might be due to swelling of the membrane during PEMFC testing.

#### ▪ **EIS Conclusions**

Within 5 cm<sup>2</sup> membranes, the recasting Nafion showed lower resistance so that it has higher proton conductivity which was 0.02649. Then the proton conductivity of the membrane was ordered as M4 > M1 > M3 > M2. Since the test is an ex-situ technique, the results are not absolute. However, the results give some clue about the composite membrane performance. The test results were very sensitive to temperature, humidity. Moreover, the results were impacted by other environmental factors such as mains electricity which create an unexpected peak at 50 Hz.

#### ▪ **Tensile Testing Conclusions**

The tests were performed for the recasting Nafion, M1 (2.5, 5.0, 7.5, and 10 wt. %), and M4 (2.5, 5.0, 7.5, and 10 wt. %). It was found that, as the SiO<sub>2</sub> content increases, the mechanical strength of the membranes decreases. The membranes prepared with adding dispersing agents (M1) had the highest mechanical strength.

The stiffness of the membrane M4 was similar to that of the pure Nafion membrane, however, the elongation at break of the M4 was lower than that of the pure membrane suggesting that the M4 is more brittle than recasting Nafion membrane.

- **Particle Size Testing Conclusions**

Originally, the size of powder SiO<sub>2</sub> is stated by the supplier as 20 nm. According to results, even using dispersing agent the SiO<sub>2</sub> particles were not dispersed effectively and they were in the form of agglomerates with a size of approximately 480 nm. However, the dispersing agent or organic additive– Pluronic L64 assists the homogenous distribution of SiO<sub>2</sub> particles in the polymer matrix as confirmed by the SEM images.

- **PEMFC Testing Conclusions**

The PEMFC tests were carried out for two MEA groups. The first MEA group contains SiO<sub>2</sub> particles only within the membranes. However, the second one contains SiO<sub>2</sub> into both membrane (2.5 wt. %) and the catalyst layers (3 wt. % of catalyst solution). Therefore, in the second group, the reactant gases for the MEAs were not subjected to any external humidification.

- For the case of external humidification (at 100 % RH);

At these conditions, apart from the recasting Nafion - MEA0, all the samples showed better V-I curves as the temperature increases. Therefore, only recasting Nafion has the lower performance at 80°C. In terms of the cell performances, MEA4 sample showed slightly better V-I curve than both recasting Nafion and MEA1.

- For the case of self-humidification (at 0 % RH);

At self-humidifying condition of MEAs, the MEA1 and MEA4 samples were selected to be tested in PEMFC station. In this fashion, it was seen that the PEMFC performances of MEA1 and MEA4 at dry condition (0 % RH) was very similar to each other. Moreover, the Nafion presented very low performance.

Under humid conditions (100 % RH), the results shows that ultrasonic bath technique is more effective than ultrasonic-probe even some big aggregate structure were examined by SEM analysis.

## **6.2. Overall Conclusions**

The 2.5 wt. % of SiO<sub>2</sub> is found as the optimum amount to be added into the composite membranes in terms of mechanical stability, PEMFC performance, and proton conductivity. It was found that adding dispersants such as PEG and Pluronic is helpful to distribute SiO<sub>2</sub> particles in the polymer matrix.

Ultrasonic probe technique was found to be very effective mixing technique apart from heating effect during the mixing process. The primary particle size of the SiO<sub>2</sub> was between 10-20 nm as reported by the supplier, however, these small primary particles form larger agglomerates with a size of approximately 480 nm. Therefore, one may conclude that although the Pluronic L64 assists to distribute the SiO<sub>2</sub> (inorganic filler) into the polymer matrix uniformly, it was not useful to disperse the SiO<sub>2</sub> particles. It was observed that as the SiO<sub>2</sub> and dispersant content increase, the water uptake capacity increases. However, despite the fact that the water content and temperature are the main functions of the proton conductivity, it is examined that the samples containing PEG have lower performance comparing with those containing Pluronic L64 which is known as non-ionic surfactant [43].

The best cell performance is observed for the MEA4 which was produced with 2.5 wt. % of SiO<sub>2</sub> by ultrasonic bath. In case of using external humidifier, at 70°C which is a typical PEMFC temperature, MEA4 has remarkable performance with reference to MEA1 and recasting Nafion (MEA0). On the other hand, under the same conditions, MEA1 and MEA4 have almost similar performance at moisture-free (0 % RH) conditions. Indeed, MEA4 has higher performance than MEA1 but with a slight difference.

Mechanical durability of M1 is higher than recasting Nafion and M4. While M4 shows rigid or fragile fashion, M1 has a more flexible structure due to the nature of Pluronic L64. One may also conclude that adding 2.5 wt. % of SiO<sub>2</sub> into polymer either with or without dispersing agents contributes slight impact on mechanical stability.

MEA1 sample might be a potential candidate for PEMFCs which can be performed at dry conditions (0% RH) and it may unencumber from the cost and weight of external humidifier so that PEMFC could be commercialize especially on portable devices. However, the sample is needed to be test in long-term running period to be able to prove its durability.

## REFERENCES

- [1] V. Ramani, H. R. Kunz, and J. M. Fenton, "Metal dioxide supported heteropolyacid/Nafion® composite membranes for elevated temperature/low relative humidity PEFC operation," *J. Memb. Sci.*, vol. 279, no. 1–2, pp. 506–512, 2006.
- [2] B. Smitha, S. Sridhar, and A. A. Khan, "Solid polymer electrolyte membranes for fuel cell applications—a review," *Journal of Membrane Science*, vol. 259, no. 1–2, pp. 10–26, 2005.
- [3] J. Larminie and A. Dicks, *Fuel Cell Systems Explained*, vol. 93, no. 1–2, 2001.
- [4] W. Vielstich, A. Lamm, and H. A. Gaseiger, "Handbook of Fuel Cells—Fundamentals, Technology and Applications," *Handb. Fuel Cells—Fundamentals, Technol. Appl.*, vol. 3, p. 190, 2003.
- [5] V. Mehta and J. S. Cooper, "Review and analysis of PEM fuel cell design and manufacturing," *Journal of Power Sources*, vol. 114, no. 1, pp. 32–53, 2003.
- [6] A. Kirubakaran, S. Jain, and R. K. Nema, "A review on fuel cell technologies and power electronic interface," *Renewable and Sustainable Energy Reviews*, vol. 13, no. 9, pp. 2430–2440, 2009.
- [7] F. Barbir, "PEM Fuel Cells," in *Fuel Cell Technology*, 2006, pp. 27–51.
- [8] J. Zhang, H. Zhang, J. Wu, and J. Zhang, *Pem Fuel Cell Testing and Diagnosis*. Elsevier, 2013.
- [9] S. M. Haile, "Fuel cell materials and components," *Acta Mater.*, vol. 51, no. 19, pp. 5981–6000, 2003.
- [10] S. Litster and G. McLean, "PEM fuel cell electrodes," *Journal of Power Sources*, vol. 130, no. 1–2, pp. 61–76, 2004.
- [11] J. Zhang, *PEM fuel cell electrocatalysts and catalyst layers: Fundamentals and applications*. 2008.
- [12] G. Hoogers, *Fuel Cell Technology Handbook*, vol. 93, no. 1–2, 2003.

- [13] H. Pu, *Polymers for PEM Fuel Cells*. New Jersey: John Wiley & Sons, Inc, 2014.
- [14] J. A. Kerres, "Development of ionomer membranes for fuel cells," *Journal of Membrane Science*, vol. 185, no. 1. pp. 3–27, 2001.
- [15] P. Costamagna and S. Srinivasan, "Quantum jumps in the PEMFC science and technology from the 1960s to the year 2000: Part I. Fundamental scientific aspects," *J. Power Sources*, vol. 102, no. 1–2, pp. 242–252, 2001.
- [16] S. Motupally, A. J. Becker, and J. W. Weidner, "Diffusion of Water in Nafion 115 Membranes," *Journal of The Electrochemical Society*, vol. 147, no. 9. p. 3171, 2000.
- [17] R. Bouchet, S. Miller, M. Duclot, and J. L. Souquet, "A thermodynamic approach to proton conductivity in acid-doped polybenzimidazole," in *Solid State Ionics*, 2001, vol. 145, no. 1–4, pp. 69–78.
- [18] C. Yang, P. Costamagna, S. Srinivasan, J. Benziger, and A. B. Bocarsly, "Approaches and technical challenges to high temperature operation of proton exchange membrane fuel cells," *J. Power Sources*, vol. 103, no. 1, pp. 1–9, 2001.
- [19] A. S. Arico, V. Baglio, A. Di Blasi, P. Creti, P. L. Antonucci, and V. Antonucci, "Influence of the acid-base characteristics of inorganic fillers on the high temperature performance of composite membranes in direct methanol fuel cells," *Solid State Ionics*, vol. 161, no. 3–4, pp. 251–265, 2003.
- [20] S. Malhotra, "Membrane-Supported Nonvolatile Acidic Electrolytes Allow Higher Temperature Operation of Proton-Exchange Membrane Fuel Cells," *Journal of The Electrochemical Society*, vol. 144, no. 2. p. L23, 1997.
- [21] P. Jannasch, "Recent developments in high-temperature proton conducting polymer electrolyte membranes," *Current Opinion in Colloid & Interface Science*, vol. 8, no. 1. pp. 96–102, 2003.
- [22] A. Clearfield and A. Clearfield, "Role of ion exchange in solid-state chemistry," *Chem. Rev.*, vol. 88, no. 1, pp. 125–148, 1988.
- [23] S. J. Peighambardoust, S. Rowshanzamir, and M. Amjadi, "Review of the proton exchange membranes for fuel cell applications," *International Journal of Hydrogen Energy*, vol. 35, no. 17. pp. 9349–9384, 2010.
- [24] J. Fang, J. Qiao, D. P. Wilkinson, and J. Zhang, *Electrochemical Polymer Electrolyte Membranes*. Boca Raton, London, New York: CRC Press, Taylor & Francis Group, 2015.

- [25] T. A. Zawodzinski, J. Davey, J. Valerio, and S. Gottesfeld, "The Water-Content Dependence of Electroosmotic Drag in Proton-Conducting Polymer Electrolytes," *Electrochim. Acta*, vol. 40, no. 3, pp. 297–302, 1995.
- [26] C. Spiegel, *Designing and Building Fuel Cells*. Two Penn Plaza, New York: McGraw-Hill, 2007.
- [27] N. Sammes, *Fuel Cell Technology - Reaching Towards Commercialization*. Springer, 2006.
- [28] C. H. Lee, K. A. Min, H. B. Park, Y. T. Hong, B. O. Jung, and Y. M. Lee, "Sulfonated poly(arylene ether sulfone)-silica nanocomposite membrane for direct methanol fuel cell (DMFC)," *J. Memb. Sci.*, vol. 303, no. 1–2, pp. 258–266, 2007.
- [29] "Poly(ethylene glycol) methyl ether average Mn ~2,000, flakes | Sigma-Aldrich." [Online]. Available: <http://www.sigmaaldrich.com/catalog/product/aldrich/202509?lang=en&region=TR>. [Accessed: 19-Aug-2015].
- [30] "Poly(ethylene glycol)-block-poly(propylene glycol)-block-poly(ethylene glycol) average Mn ~2,900 | Sigma-Aldrich." [Online]. Available: [http://www.sigmaaldrich.com/catalog/product/aldrich/435449?lang=en&region=TR&gclid=Cj0KEQjw0tCuBRDIjJ\\_Mlb6zzpQBEiQAyjCoBs0VObPKCBnsWegC7GRJIAqdK-1p8w81XBhg5kwQa3gaAh6N8P8HAQ](http://www.sigmaaldrich.com/catalog/product/aldrich/435449?lang=en&region=TR&gclid=Cj0KEQjw0tCuBRDIjJ_Mlb6zzpQBEiQAyjCoBs0VObPKCBnsWegC7GRJIAqdK-1p8w81XBhg5kwQa3gaAh6N8P8HAQ). [Accessed: 19-Aug-2015].
- [31] M. Han, S. H. Chan, and S. P. Jiang, "Investigation of self-humidifying anode in polymer electrolyte fuel cells," *Int. J. Hydrogen Energy*, vol. 32, no. 3, pp. 385–391, 2007.
- [32] H. Su, L. Xu, H. Zhu, Y. Wu, L. Yang, S. Liao, H. Song, Z. Liang, and V. Birss, "Self-humidification of a PEM fuel cell using a novel Pt/SiO<sub>2</sub>/C anode catalyst," *Int. J. Hydrogen Energy*, vol. 35, no. 15, pp. 7874–7880, 2010.
- [33] V. Senthil Velan, G. Velayutham, N. Hebalkar, and K. S. Dhathathreyan, "Effect of SiO<sub>2</sub> additives on the PEM fuel cell electrode performance," *Int. J. Hydrogen Energy*, vol. 36, no. 22, pp. 14815–14822, 2011.
- [34] A. K. Mishra, S. Bose, T. Kuila, N. H. Kim, and J. H. Lee, "Silicate-based polymer-nanocomposite membranes for polymer electrolyte membrane fuel cells," *Progress in Polymer Science*, vol. 37, no. 6, pp. 842–869, 2012.
- [35] H. Liang, L. Zheng, and S. Liao, "Self-humidifying membrane electrode assembly prepared by adding PVA as hygroscopic agent in anode catalyst layer," *Int. J. Hydrogen Energy*, vol. 37, no. 17, pp. 12860–12867, 2012.

- [36] H. Liang, D. Dang, W. Xiong, H. Song, and S. Liao, "High-performance self-humidifying membrane electrode assembly prepared by simultaneously adding inorganic and organic hygroscopic materials to the anode catalyst layer," *J. Power Sources*, vol. 241, pp. 367–372, 2013.
- [37] Z. G. Shao, H. Xu, M. Li, and I. M. Hsing, "Hybrid Nafion-inorganic oxides membrane doped with heteropolyacids for high temperature operation of proton exchange membrane fuel cell," *Solid State Ionics*, vol. 177, no. 7–8, pp. 779–785, 2006.
- [38] D. Kurniawan, S. Morita, and K. Kitagawa, "Durability of Nafion-hydrophilic silica hybrid membrane against trace radical species in polymer electrolyte fuel cells," *Microchem. J.*, vol. 108, pp. 60–63, 2013.
- [39] W. Callister and D. Rethwisch, *Materials science and engineering: an introduction*, vol. 94. 2007.
- [40] T. Naya, "CONDUCTIVITY OF ION EXCHANGE MATERIALS," The Pennsylvania State University, 2010.
- [41] K. Kriangsak, S. Sangaraju, C. Suwanboonb, N. Chanunpanichb, and D. Leed, "Efficient water management of composite membranes operated in polymer electrolyte membrane fuel cells under low relative humidity," *J. Memb. Sci.*, vol. 493, pp. 295–298, 2015.
- [42] G. Gnana Kumar, A. R. Kim, K. Suk Nahm, and R. Elizabeth, "Nafion membranes modified with silica sulfuric acid for the elevated temperature and lower humidity operation of PEMFC," *Int. J. Hydrogen Energy*, vol. 34, no. 24, pp. 9788–9794, 2009.
- [43] L. Zheng, C. Guo, J. Wang, X. Liang, P. Bahadur, S. Chen, J. Ma, and H. Liu, "Micellization of Pluronic L64 in salt solution by FTIR spectroscopy," *Vib. Spectrosc.*, vol. 39, no. 2, pp. 157–162, 2005.

## APPENDICES

### A. ADDITIONAL CHARACTERIZATION DATA

#### A.1. SEM Pictures of Samples

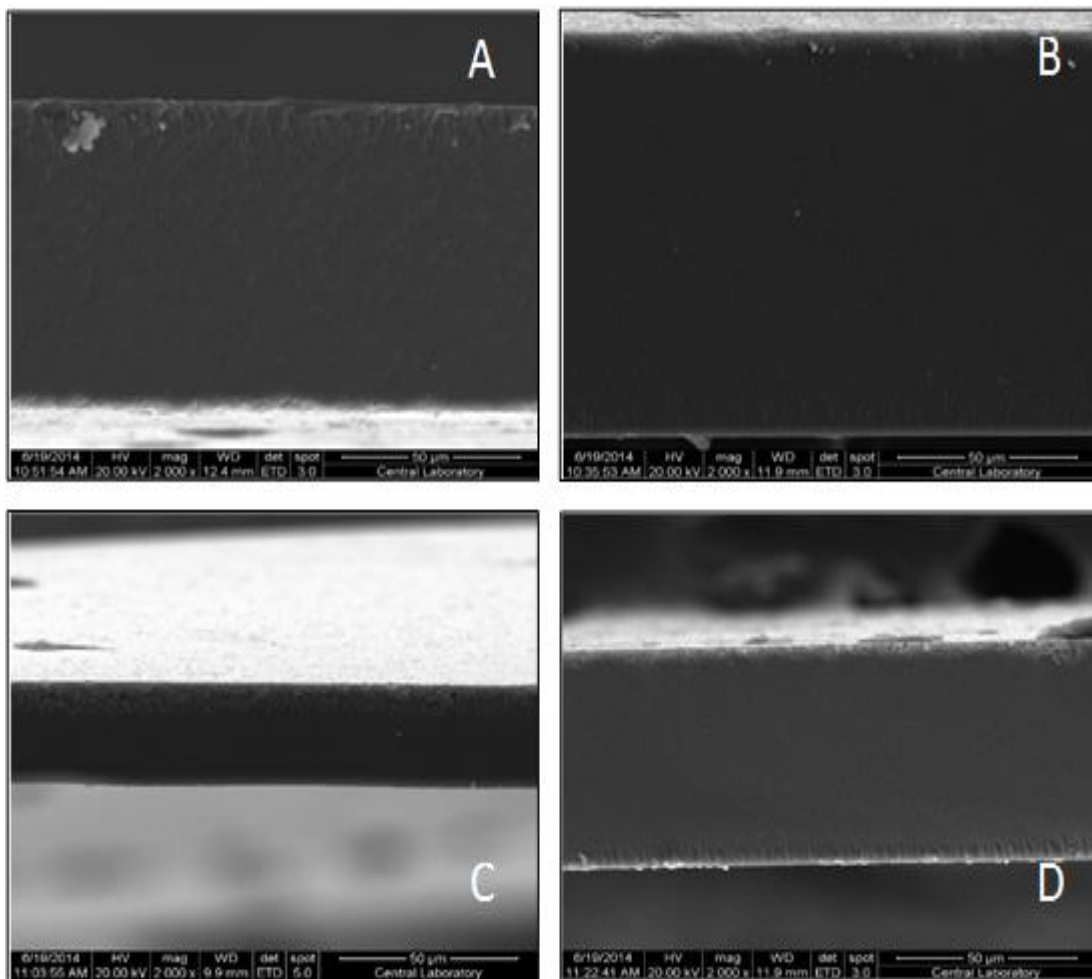


**Figure 58.** The SEM pictures of M1 (A), M2 (B), M3(C), and M4 (D) at 20.000 x magnified

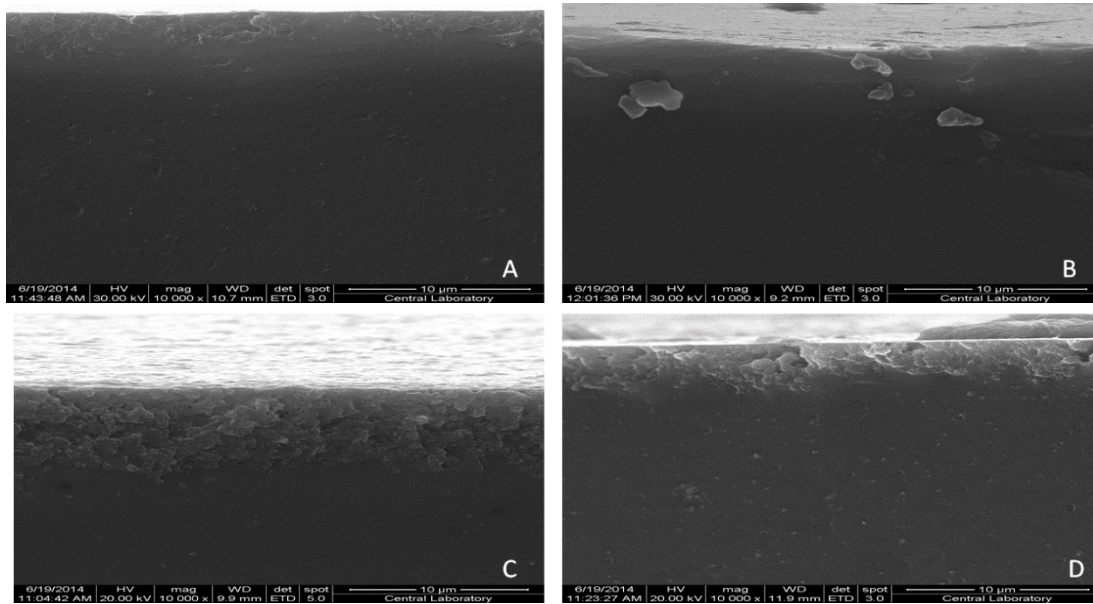


**Figure 59.** The SEM pictures of M1 (A), M2 (B), M3(C), and M4 (D) at 10.000 x magnified

#### A.2. Mapping Pictures of Sample

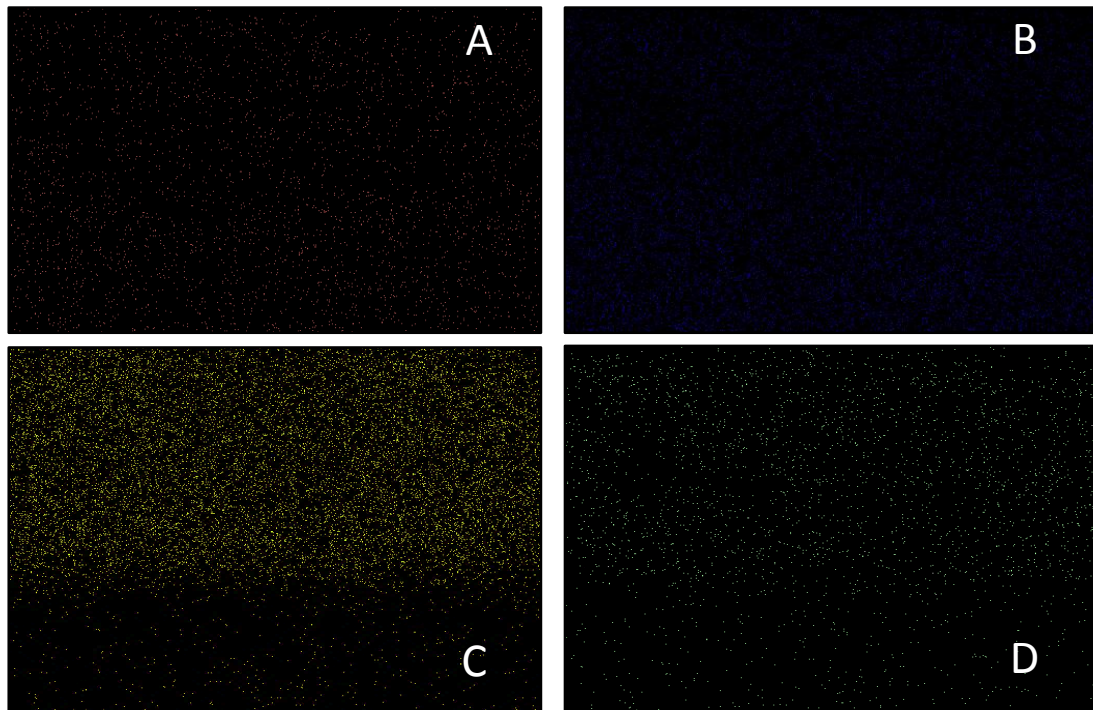


**Figure 60.** Mapping pictures of M1(A), M2 (B), M3 (C) and M4 (D) with adding 2,5 wt. % of SiO<sub>2</sub>

### A.3. EDXS Pattern of Samples

**Table 22.** EDXS pattern for M1: 2.5 wt. % of SiO<sub>2</sub> + Pluronic L64 prepared via ultrasonic probe, (A); EDXS pattern of non-agglomerate SiO<sub>2</sub> region, (B): EDXS pattern of agglomerate SiO<sub>2</sub> region

EDAX ZAF Quantification (Standardless)							A
Element Normalized							
SEC Table : Default							
Element	Wt %	At %	K-Ratio	Z	A	F	
C K	42.23	53.30	0.1429	1.0358	0.3264	1.0004	
O K	10.15	9.62	0.0209	1.0213	0.2013	1.0022	
F K	44.08	35.17	0.0983	0.9611	0.2320	1.0001	
SiK	3.54	1.91	0.0206	0.9859	0.5905	1.0000	
Total	100.00	100.00					
Element	Net Inte.	Bkgd Inte.	Inte. Error	P/B			
C K	30.85	0.77	4.68	40.00			
O K	15.04	0.39	6.70	39.00			
F K	102.13	0.77	2.53	132.42			
SiK	30.27	1.16	4.78	26.17			

EDAX ZAF Quantification (Standardless)							B
Element Normalized							
SEC Table : Default							
Element	Wt %	At %	K-Ratio	Z	A	F	
C K	39.79	50.71	0.1300	1.0364	0.3152	1.0004	
O K	12.03	11.51	0.0258	1.0219	0.2090	1.0022	
F K	44.17	35.59	0.0964	0.9617	0.2270	1.0001	
SiK	4.00	2.18	0.0231	0.9865	0.5851	1.0000	
Total	100.00	100.00					
Element	Net Inte.	Bkgd Inte.	Inte. Error	P/B			
C K	30.12	1.01	5.46	29.83			
O K	19.85	0.50	6.67	39.33			
F K	107.43	0.50	2.81	212.83			
SiK	36.43	1.60	5.01	22.79			

**Table 23.** EDXS pattern for M2: 2.5 wt. % of SiO<sub>2</sub> + PEG prepared via ultrasonic probe, (A); EDXS pattern of non-agglomerate SiO<sub>2</sub> region, (B): EDXS pattern of agglomerate SiO<sub>2</sub> region

EDAX ZAF Quantification (Standardless)							A
Element Normalized							
SEC Table : Default							
Element	Wt %	At %	K-Ratio	Z	A	F	
C K	44.51	57.71	0.0971	1.0361	0.2106	1.0003	
O K	4.13	4.02	0.0072	1.0216	0.1712	1.0020	
F K	39.08	32.04	0.0897	0.9614	0.2386	1.0003	
SiK	3.79	2.10	0.0239	0.9861	0.6358	1.0050	
S K	8.50	4.13	0.0681	0.9802	0.8169	1.0000	
Total	100.00	100.00					
Element	Net Inte.	Bkgd Inte.	Inte. Error	P/B			
C K	47.82	3.12	2.61	15.31			
O K	11.77	3.24	6.17	3.63			
F K	209.84	3.58	1.19	58.53			
SiK	78.00	16.65	2.30	4.68			
S K	208.79	17.64	1.27	11.84			

EDAX ZAF Quantification (Standardless)							B
Element Normalized							
SEC Table : Default							
Element	Wt %	At %	K-Ratio	Z	A	F	
C K	36.23	48.81	0.0689	1.0299	0.1845	1.0003	
O K	19.49	19.72	0.0374	1.0154	0.1889	1.0011	
F K	21.62	18.42	0.0375	0.9556	0.1815	1.0007	
SiK	22.66	13.05	0.1545	0.9801	0.6958	1.0000	
Total	100.00	100.00					
Element	Net Inte.	Bkgd Inte.	Inte. Error	P/B			
C K	49.30	4.53	3.27	10.88			
O K	88.12	4.80	2.36	18.37			
F K	126.89	5.42	1.95	23.42			
SiK	724.36	14.79	0.80	48.98			

**Table 24.** EDXS pattern for M3: 2.5 wt. % of SiO<sub>2</sub> + PEG prepared via ultrasonic probe M3, (A); EDXS pattern of non-agglomerate SiO<sub>2</sub> region, (B): EDXS pattern of agglomerate SiO<sub>2</sub> region

EDAX ZAF Quantification (Standardless)							<b>A</b>	EDAX ZAF Quantification (Standardless)							<b>B</b>
Element Normalized								Element Normalized							
SEC Table : Default								SEC Table : Default							
Element	Wt %	At %	K-Ratio	Z	A	F	Element	Wt %	At %	K-Ratio	Z	A	F		
C K	44.51	57.71	0.0971	1.0361	0.2106	1.0003	C K	36.23	48.81	0.0689	1.0299	0.1845	1.0003		
O K	4.13	4.02	0.0072	1.0216	0.1712	1.0020	O K	19.49	19.72	0.0374	1.0154	0.1889	1.0011		
F K	39.08	32.04	0.0897	0.9614	0.2386	1.0003	F K	21.62	18.42	0.0375	0.9556	0.1815	1.0007		
SiK	3.79	2.10	0.0239	0.9861	0.6358	1.0050	SiK	22.66	13.05	0.1545	0.9801	0.6958	1.0000		
S K	8.50	4.13	0.0681	0.9802	0.8169	1.0000	Total	100.00	100.00						
Total	100.00	100.00													
Element	Net Inte.	Bkqd Inte.	Inte. Error	P/B					Element	Net Inte.	Bkqd Inte.	Inte. Error	P/B		
C K	47.82	3.12	2.61	15.31	C K	49.30	4.53	3.27	10.88						
O K	11.77	3.24	6.17	3.63	O K	88.12	4.80	2.36	18.37						
F K	209.84	3.58	1.19	58.53	F K	126.89	5.42	1.95	23.42						
SiK	78.00	16.65	2.30	4.68	SiK	724.36	14.79	0.80	48.98						
S K	208.79	17.64	1.27	11.84											

**Table 25.** EDXS pattern for M4: only 2.5 wt. % of SiO<sub>2</sub> prepared via ultrasonic bath, (A); EDXS pattern of non-agglomerate SiO<sub>2</sub> region, (B): EDXS pattern of agglomerate SiO<sub>2</sub> region

EDAX ZAF Quantification (Standardless)							<b>A</b>	EDAX ZAF Quantification (Standardless)							<b>B</b>
Element Normalized								Element Normalized							
SEC Table : Default								SEC Table : Default							
Element	Wt %	At %	K-Ratio	Z	A	F	Element	Wt %	At %	K-Ratio	Z	A	F		
C K	53.94	65.96	0.1665	1.0329	0.2987	1.0003	C K	53.59	66.33	0.1238	1.0265	0.2251	1.0002		
F K	41.01	31.70	0.1014	0.9585	0.2581	1.0001	O K	7.97	7.41	0.0125	1.0121	0.1543	1.0012		
SiK	0.40	0.21	0.0025	0.9832	0.6456	1.0030	F K	25.36	19.85	0.0483	0.9525	0.2000	1.0003		
S K	4.65	2.13	0.0397	0.9773	0.8733	1.0000	SiK	5.32	2.82	0.0367	0.9770	0.7026	1.0049		
Total	100.00	100.00					S K	7.76	3.60	0.0633	0.9711	0.8402	1.0000		
							Total	100.00	100.00						
Element	Net Inte.	Bkqd Inte.	Inte. Error	P/B					Element	Net Inte.	Bkqd Inte.	Inte. Error	P/B		
C K	8.70	0.80	2.80	10.93	C K	19.24	1.76	2.51	10.91						
F K	24.87	0.86	1.57	28.93	O K	6.34	1.92	5.10	3.30						
SiK	0.86	1.21	16.01	0.71	F K	35.23	2.16	1.81	16.28						
S K	12.54	2.44	2.53	5.14	SiK	36.84	4.71	1.87	7.83						
					S K	59.48	5.54	1.43	10.74						

## B. MATERIAL DATA SPECIFICATIONS

### B1. Production Specifications of Pluronic L64, PEG, SiO<sub>2</sub>, Nafion 1100

The specification for the raw materials of composite membranes as the followings;

**SIGMA-ALDRICH**<sup>®</sup>

[sigma-aldrich.com](http://sigma-aldrich.com)

3050 Spruce Street, Saint Louis, MO 63103, USA

Website: [www.sigmaaldrich.com](http://www.sigmaaldrich.com)

Email USA: [techserv@sial.com](mailto:techserv@sial.com)

Outside USA: [eurtechserv@sial.com](mailto:eurtechserv@sial.com)

#### Product Specification

Product Name:  
Poly(ethylene glycol) methyl ether – average Mn ~2,000, flakes

Product Number:	202509
CAS Number:	9004-74-4
MDL:	MFCD00084416
Formula:	CH <sub>3</sub> (OCH <sub>2</sub> CH <sub>2</sub> ) <sub>n</sub> OH

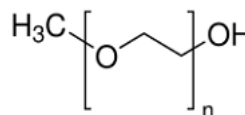


**Figure 61.** The production specification of Poly (ethylene glycol) methyl ether – average Mn ~ 2,000 g/mole, flakes

## Product Specification

Product Name:

Silicon dioxide - nanopowder, 10-20 nm particle size (BET), 99.5% trace metals basis

<b>Product Number:</b>	<b>637238</b>	SiO <sub>2</sub>
CAS Number:	7631-86-9	
MDL:	MFCD00011232	
Formula:	O <sub>2</sub> Si	
Formula Weight:	60.08 g/mol	

**Figure 62.** The production specification of SiO<sub>2</sub>-nano powder, 10-20 nm particle size (BET), 99.5 % trace metals basis

## Product Specification

Product Name:

Poly(ethylene glycol)-block-poly(propylene glycol)-block-poly(ethylene glycol) - average Mn ~2,900

<b>Product Number:</b>	<b>435449</b>
CAS Number:	9003-11-6
MDL:	MFCD00082049
Formula:	(C <sub>3</sub> H <sub>6</sub> O.C <sub>2</sub> H <sub>4</sub> O) <sub>x</sub>

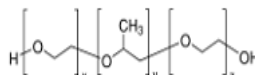


**Figure 63.** The production specification of Poly (ethylene glycol) – block – poly (propylene glycol) – block – poly (ethylene glycol) – average Mn ~ 2,000 g/mole

In this thesis, 3 x 125 ml of LIQUION® – 1115 were used for more than 60 composite membranes. As it is written in Figure (64), the curing time is required to evaporate the alcohol at 100-120°C more than half an hour.

<b>Physical Properties</b>		
<b>Solutions with a concentration of 15% weight NAFION®</b>		
<b>Product</b>	<b>LIQUION® LQ-1015</b>	<b>LIQUION® LQ-1115</b>
Composition	NAFION® 14.95-15.05%	NAFION® 14.95-15.05%
Alcohol	40% weight	40% weight
Density	1.0 gram/cm <sup>3</sup>	1.0 gram/cm <sup>3</sup>
Water	40% weight	40% weight
<b>Solutions with a concentration of 5% weight NAFION®</b>		
<b>Product</b>	<b>LIQUION® LQ-1005</b>	<b>LIQUION® LQ-1105</b>
Composition	NAFION® 4.95%-5.05%	NAFION® 4.95%-5.05%
Alcohol	75% weight	75% weight
Density	0.86 gram/cm <sup>3</sup>	0.86 gram/cm <sup>3</sup>
Water	20% weight	20% weight
Drying/curing procedure:		
Solvent should be removed at temperature less than 50°C for ½ hour or until dry, followed by a curing step at 100-120°C for 15 minutes as a minimum.		

**Figure 64.** Physical properties of Nafion – 1100 with the concentration of both 15 and 5 % weights (by LIQUION)



## C. TENSILE MECHANICAL TESTS

### C.1. M1: Pluronic L-64 prepared via Ultrasonic Probe (Testing at least two or three dog-bones for each membrane)

- 2.5 wt. % SiO<sub>2</sub> + Pluronic L-64 (Ultra-sonic Probe)

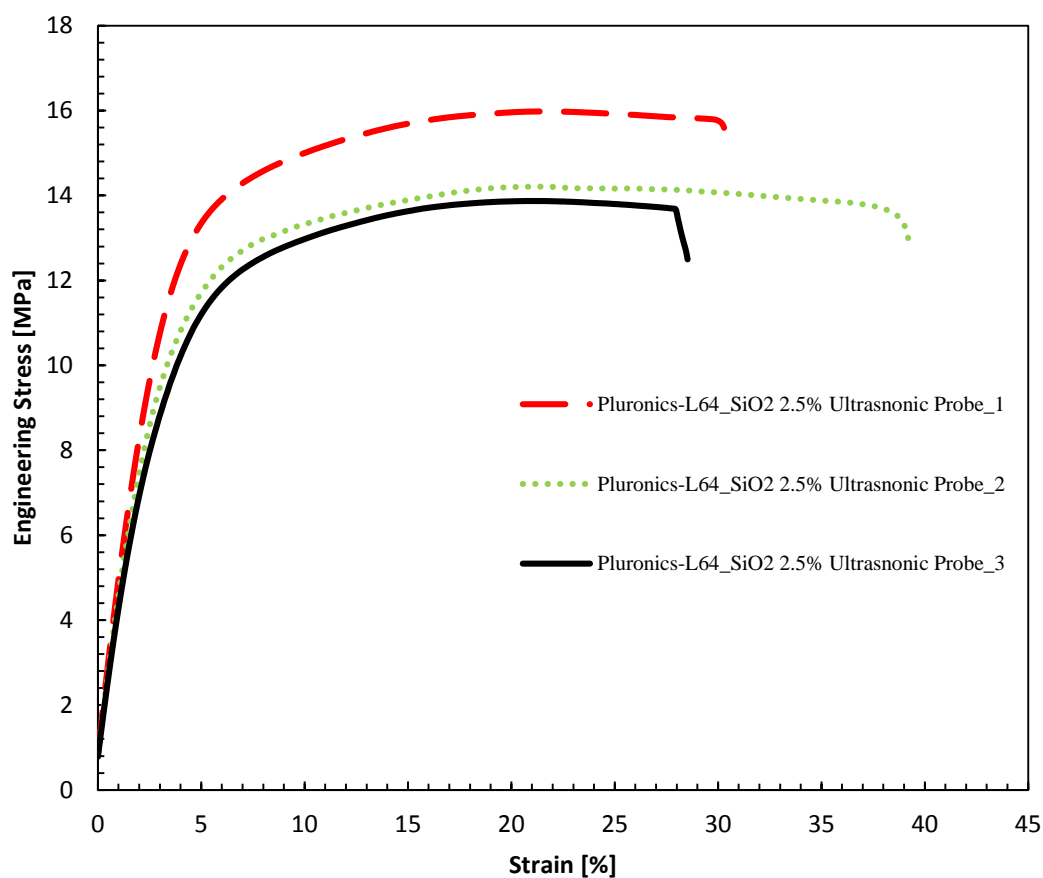


**Figure 65.** The mechanical tensile tests of (M1): Pluronic L64 2.5 wt. % SiO<sub>2</sub>

▪ 5.0 wt. % SiO<sub>2</sub> + Pluronic L-64 (Ultra-sonic Probe)

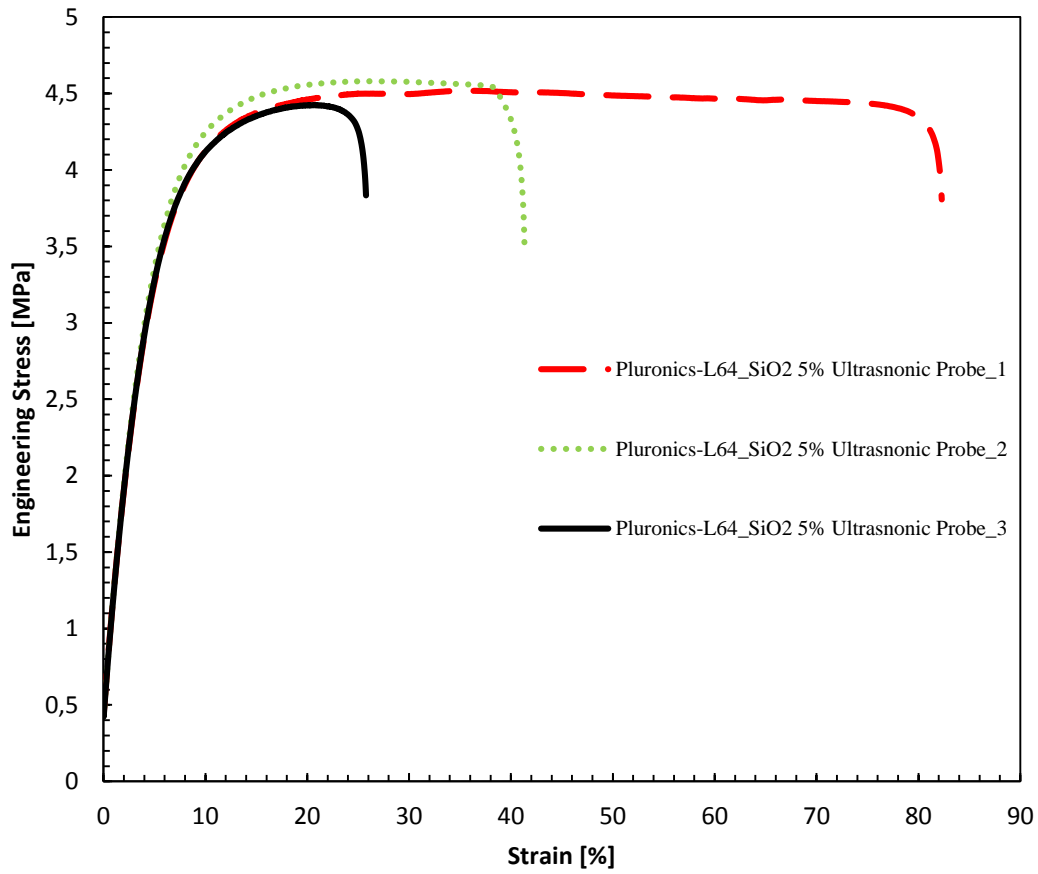


**Figure 66.** The mechanical tensile tests of (M1): Pluronic L64 5.0 wt. % SiO<sub>2</sub>

▪ 7.5 wt. % SiO<sub>2</sub> + Pluronic L-64 (Ultra-sonic Probe)

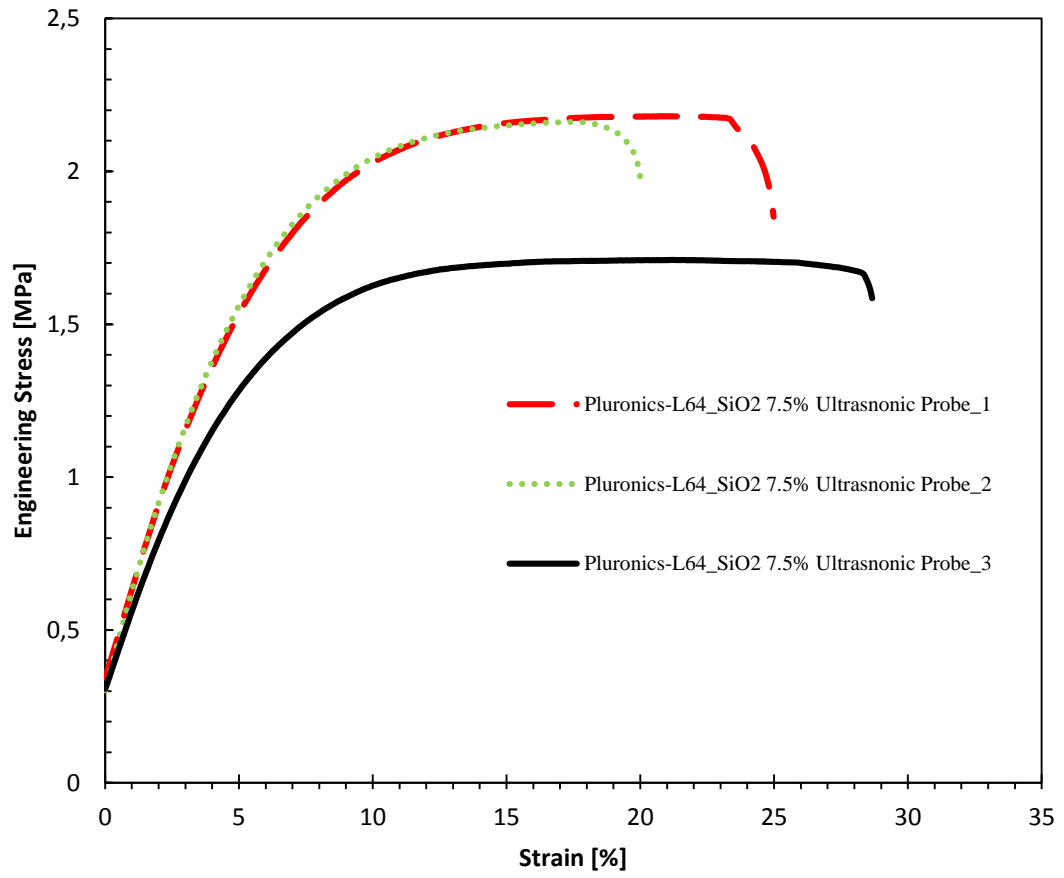


**Figure 67.** The mechanical tensile tests of (M1): Pluronic L64 7.5 wt. % SiO<sub>2</sub>

▪ **10.0 wt. % SiO<sub>2</sub> + Pluronic L-64 (Ultra-sonic Probe)**

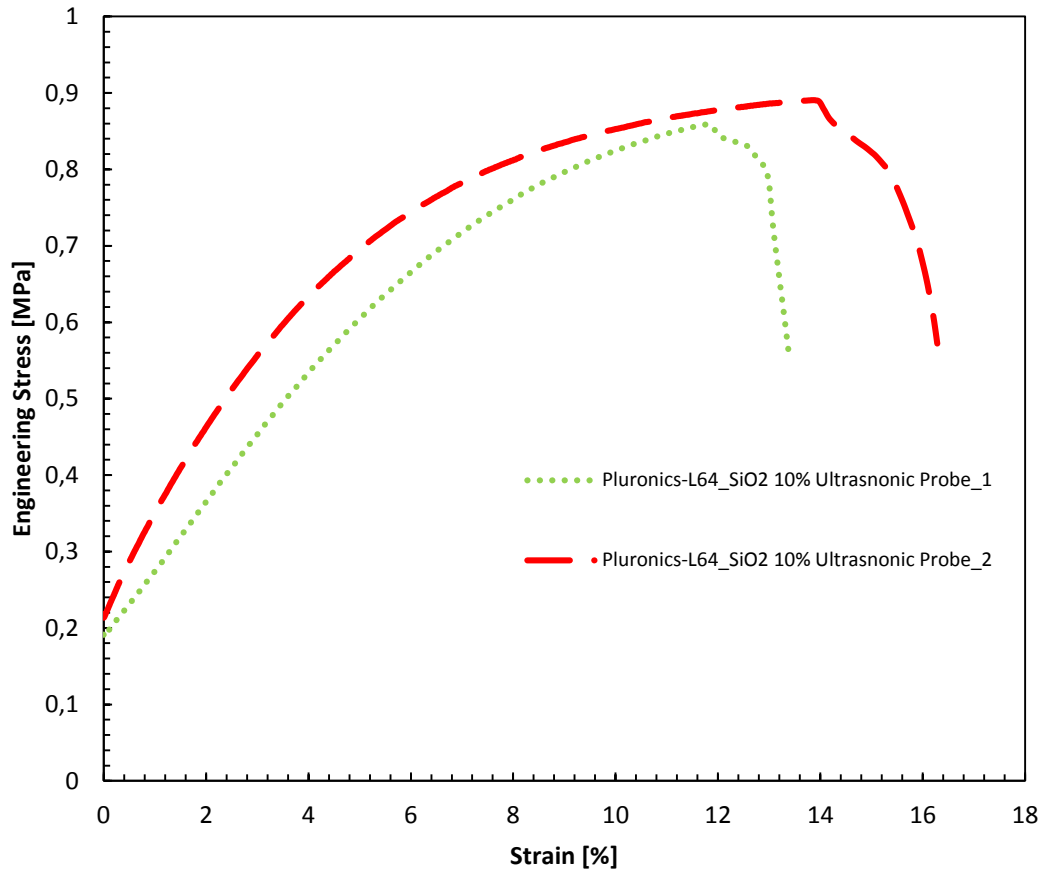


**Figure 68.** The mechanical tensile tests of (M1): Pluronic L64 10.0 wt. % SiO<sub>2</sub>

**C.2. M4: Only SiO<sub>2</sub> prepared via Ultrasonic Bath (Testing at least two or three dog-bones for each membrane)**

- **2.5 wt. % SiO<sub>2</sub>**

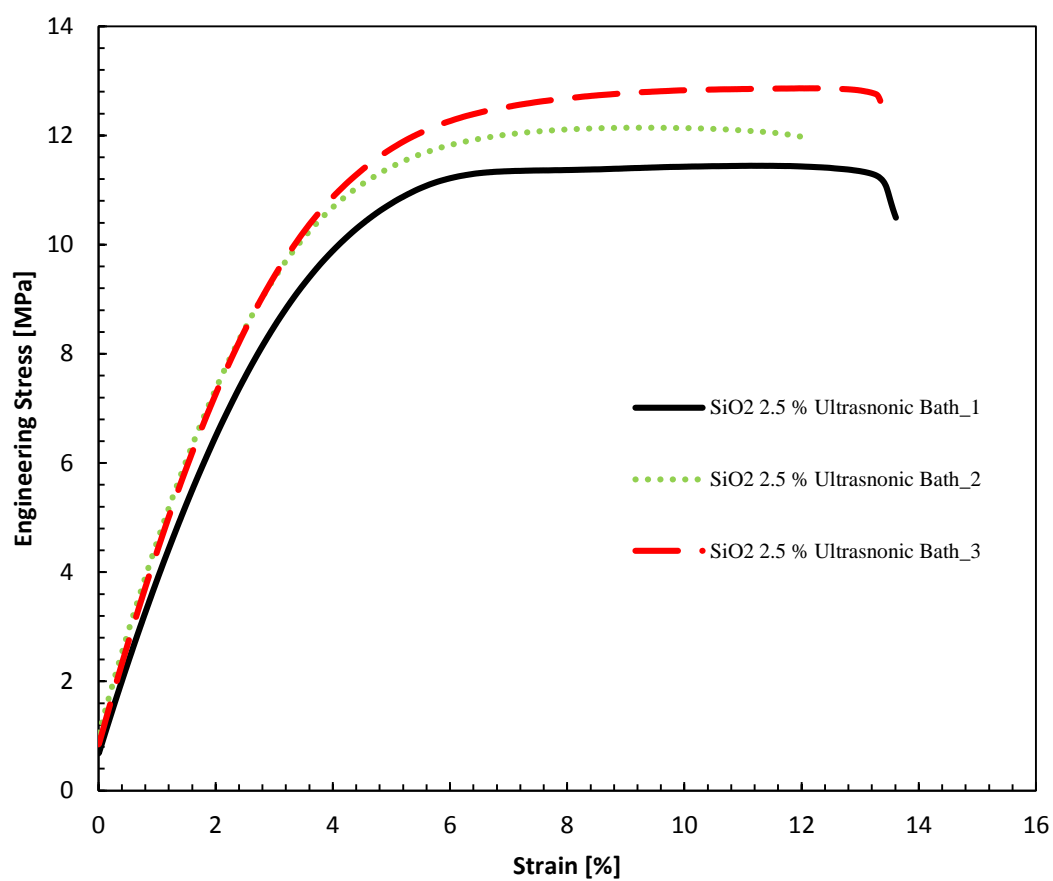


**Figure 69.** The mechanical tensile tests of (M4): only 2.5 wt. % SiO<sub>2</sub>

▪ 5.0 wt. % SiO<sub>2</sub>

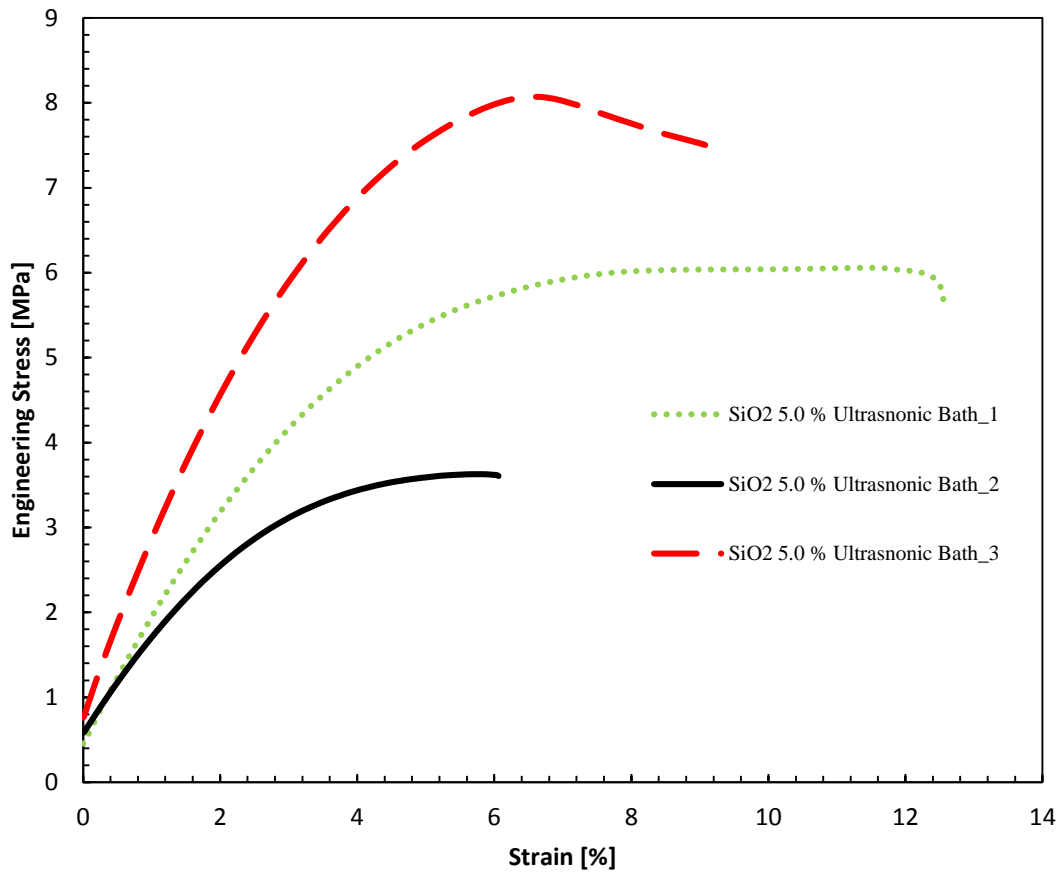


**Figure 70.** The mechanical tensile tests of (M4): only 5.0 wt. % SiO<sub>2</sub>

▪ 7.5 wt. % SiO<sub>2</sub>

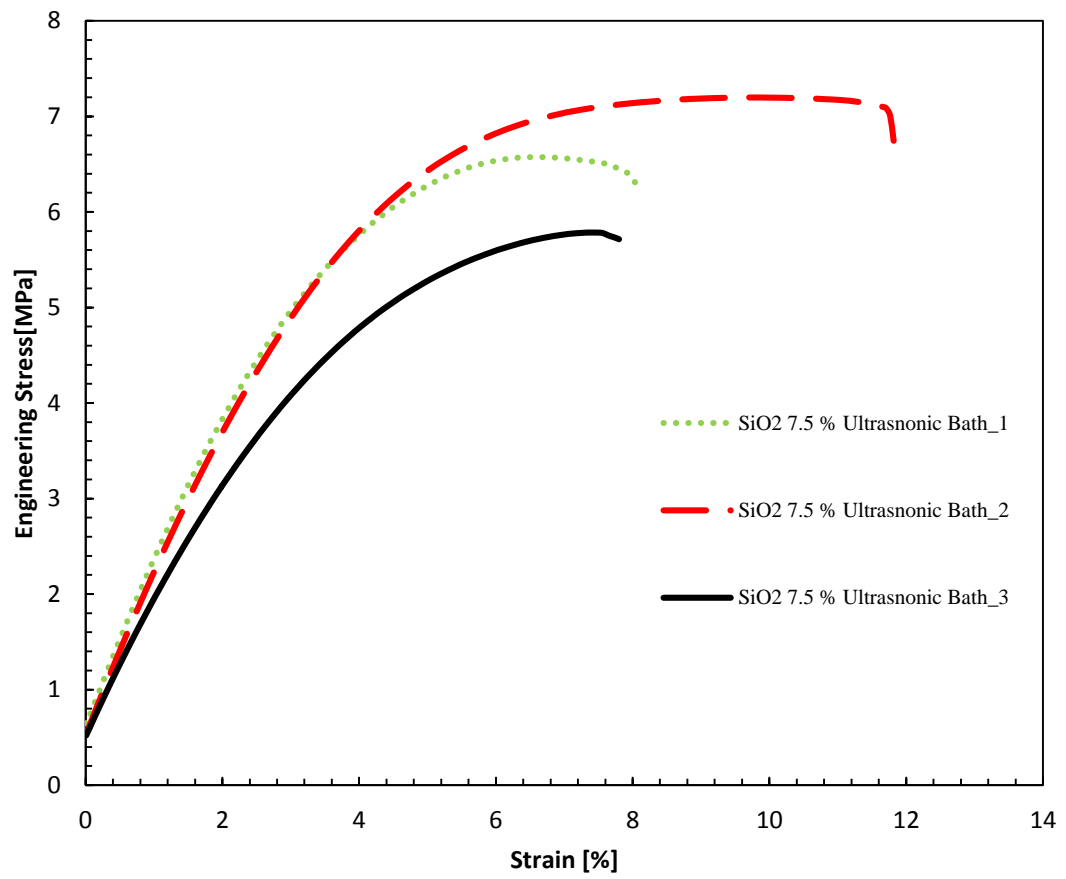


**Figure 71.** The mechanical tensile tests of (M4): only 7.5 wt. % SiO<sub>2</sub>

▪ 10.0 wt. % SiO<sub>2</sub>

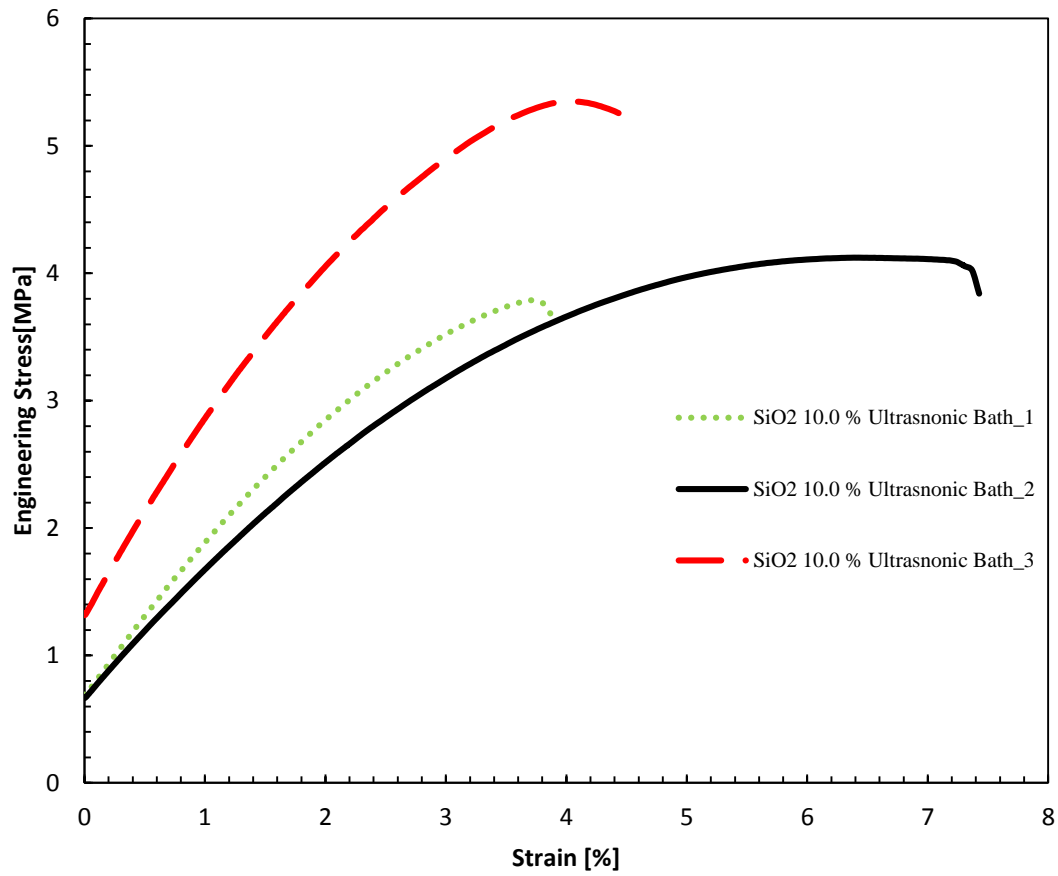


**Figure 72.** The mechanical tensile tests of (M4): only 10.0 wt. % SiO<sub>2</sub>